AN INVESTIGATION OF AGROCHEMICAL TRANSPORT MECHANISMS IN SOME CULTIVATED SOILS IN GHANA

By

DANIEL AMOAKO DARKO

(10071781)

THIS THESIS IS SUBMITTED TO THE UNIVERSITY OF GHANA, LEGON IN PARTIAL FULFILLMENT OF THE REQUIREMENT FOR THE AWARD OF PhD SOIL SCIENCE DEGREE

JULY, 2015

DEDICATION

I dedicate this work first to the glory of the almighty God, my beloved wife, Mrs Empi Adwoa Darko and my father Mr. KWADWO AMOAKO DARKO.

DECLARATION

I do hereby declare that, the thesis herein presented for a degree of PhD in Soil Science is the result of my own research. This thesis has neither in whole nor in part been presented for another degree elsewhere. All references to other authors' works as sources of information have been duly acknowledged.

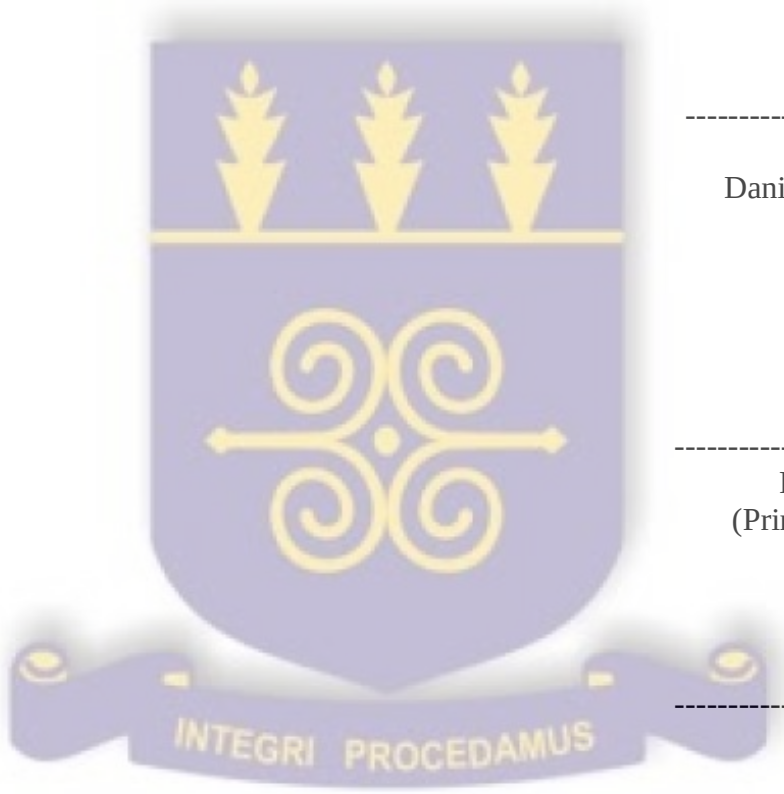

Daniel Amoako Darko
(PhD Candidate)

Prof. K. B. Laryea
(Principal Supervisor)

Dr. E. K. Nartey
(Co-Supervisor)

ACKNOWLEDGEMENT

I would like to wholeheartedly express my deepest thanks to the Almighty God for his blessing and guidance, without which this work would never have been possible. To him is the glory.

I am greatly indebted to Prof. K. B. Laryea for his immeasurable help, advice, valuable suggestions and guidance during the course of the production of this thesis. He acted like a father as well as a mentor throughout the production of this thesis. I would also like to register my sincerest gratitude to Dr Eric K. Nartey for his invaluable contribution in the production of this thesis.

My profound appreciation also goes to Prof. G. N. N. Dowuona for his guidance and to Dr Thomas Adjadeh, for his patience and encouragement during this research project. My special thanks also go to Prof. E. Owusu-Benoah, Prof. M. K. Abekoe, Dr. S. Assuming-Brempong, Prof. J. K. Amatekpor and all lecturers of the Department of Soil Science, University of Ghana, Legon for their suggestions and help towards the completion of this work.

I cannot forget the competent technical assistance and suggestions given to me by Mr. Julius N. Addo, Mr. Ben Anipa, Mr. Victor Adusei Okrah, Mr. M. K. Aggrey and especially, Messrs Edmund Anum, all of the Department of Soil Science during the laboratory investigations. To all other members of staff I say 'thank you'.

Finally, I would like to say thank you to my dad, KWADWO AMOAKO DARKO, brothers EMMANUEL K. BANDOH, KINGSLEY K. AMOAKO, OLIVER O. AMOAKO my sisters' in-law Mrs. MONICA AMOAKO and Mrs. BETTY AMOAKO, my brother in-law Mr. PETER PEPRAH and all friends who contributed to the success of this work. I really do appreciate your individual and collective efforts.

ABSTRACT

The study basically examined the movement of agrochemical compounds in soil. Four different soil samples made up of three sandy loams and a sandy clay were used in the study. Potassium chloride solution and chlorpyrifos were used as infiltration solutions in a horizontal infiltration study under laboratory conditions. At the end of each experiment, the infiltration column was sectioned and the moisture content as well as the solution concentration of the agrochemical compound (Cl^-, K^+, and chlorpyrifos) contents determined. The water content, Cl^-, K^+ and chlorpyrifos contents profiles preserved similarity with regards to the variable $\lambda = xt^{-1/2}$. Moisture diffusivity and dispersion coefficients were therefore considered to be dependent on water content only. The moisture diffusivity function and the dispersion coefficients of the solutes were derived using the θ(λ) and c(λ) data together with the Continuous System Modeling Program (CSMP) computer program. The moisture diffusivity values obtained showed that the sandy loams due to their large pore sizes permitted higher infiltration of water than the sandy clay. With the exception of the Xanthic Ferrasol and Ferric Lixisol, which are sandy loam, the chloride profiles moved ahead of the profiles of water and the other solutes. The chloride concentration front measured in the Ferrasol and Lixisol lagged behind that of the water, thus suggesting chloride mobility was retarded during the infiltration experiment. Differences in the notional planes of chloride and water used as influent solutions in the infiltration experiments also suggests the existence of immobile water content in the sandy clay and one of the sandy loams. Estimation of the dispersion coefficient of chloride in the two soils in which immobile water content was established suggests that chloride dispersion was low when immobile water content was accounted for in the estimation of the dispersion coefficient.

TABLE OF CONTENT

LIST OF TABLES

LIST OF FIGURES

LIST OF PLATES

CHAPTER ONE

INTRODUCTION

1.1 Background

Agrochemicals (fertilizers, pesticides and herbicides) are very important but often controversial component of modern agriculture. It is generally acknowledged that the use of agrochemicals for crop protection and animal health has immense benefits for agricultural production. Agrochemical use has become a major factor in improving the efficiency in modern agriculture. The use of agrochemicals in agriculture has increased tremendously over the years and largely account for the increase in food production world-wide (Sattler *et al.*, 2006; Cooper and Dobson 2007).Fertilizers directly supply nutrients to crops while pesticides have the adverse impact on pests. It is argued that ceasation of agrochemical application could lead to significant crop loss and a drastic reduction in food supply (Oerke, 2006; Cooper and Dobson 2007).

Notwithstanding their beneficial effects, the growing use of agrochemicals is dramatically affecting both ecosystem and public health. In most cases, during and after their application, a substantial amount ends up in the air and the soil, which eventually are transported into surface and ground water sources. The presence of agrochemicals in these domains may constitute considerable negative effects to ecosystems and human health. In particular, one of the greatest potential for unintended negative effects on the environment is through contamination of the soil, the hydrologic system and human health (Calamari and Naeve, 1994; Barbash, and Resek, 1996; Eddleston *et al*., 2002; Wesseling *et al.*, 2005; Ntow, 2007). In the particular case of pesticides, large quantities of pesticides applied to control pests on agricultural fields, most often, do not reach the target species thereby leaving a large portion to migrate off-site (Pimentel, 1995;

Gebremariam *et al*., 2012). This usually results in residues o the pesticides contaminating soils and water, remaining in the crops, entering the food chain, and finally being ingested by humans with foodstuffs and water. In general, the over or mis-use of agrochemicals are implicated in the loss of biodiversity and the deterioration of natural habitats in areas where they are persistently used (Sattler *et al.*, 2006). Globally, this is a major issue of concern to both agriculturists and environmentalist as attempts are made to minimise the impact on the environment, and remediation efforts are often very expensive (Huber*et al*., 2000; Kidd *et al*., 2001; Cerejeira *et al*., 2003).

The application of different kinds of agrochemical varies depending on the region where users are located. For instance, herbicides are applied in large quantities to control weeds in the developed economies of North America and Western Europe due to the high cost of labour. In Latin America and Asia on the other hand, farmers use lesser amounts of herbicides and rather rely on human labour because it is a cheaper option (Carvalho, 2006). In most tropical regions fertilizers and pesticides application is low. Nitrogen fertilizer application in Ghana for instance is about 15 kg N per ha, but a large proportion is lost by runoff and leaching (MOFA, 2014). To offset the losses, farmers tend to increase the application. Also, pesticide usage in Ghana is considered to be generally low, although excessive and intensive usage occurs in most areas where they are applied. In Ghana, the need to address weeding and labour demands as well as the incidence of pests and diseases on farms have led to a rapid increase and more frequent applications of agro-chemicals by most farmers.

1.2 Problem statement

Available evidence indicates that in Ghana, over 80 % of farmers now use agrochemicals for agricultural production. Total fertilizer imports for instance, averaged 458, 241 metric tonnes in the year 2013. In the case of pesticides, it is on record that about 2,283,210 metric tonnes were imported into Ghana in 2011 with insecticides constituting over 42 % and the remaining being herbicides (MOFA, 2014). The Afram plains of Ghana which has become a major vegetable production zone for instance, has seen a tremendous increase in the application of agrochemicals. The large flood plains of the Volta River, which are suitable soils for agricultural production suggests an increased agrochemical loading of the river with time. Also, the Ankasa series of the western region of Ghana as well as the Vertisols of the Volta basin have become agricultural zones where large quantities of agrochemicals are applied.

Once applied to soil, the agrochemical is subjected to a number of processes. It may be taken up by plants or ingested by insects, worms or microorganisms in the soil. It may also move downward in the soil and either be adsorbed to soil particles or dissolve in soil solution. Pesticide may vaporize and enter the atmosphere, degrade via solar energy or break down in soil via microbial and chemical pathways into other less toxic compounds. Those that are not subjected to adsorption or any form of degradation may leach out of the root zone or wash off the surface of land by rain or irrigation water, and eventually end up in river sediments or groundwater (Funda *et al*., 2014).

Thus, the soil has a major influence on the fate and behavior of agrochemicals. Whether or not an agrochemical would be adsorbed and hence persist in the soil or leach out depends on the chemical properties and the physico-chemical properties of the soil. For coarse textured soils with organic matter content less than 5 %, adsorption of agrochemicals is due to a combination of soil organic matter and the clay fraction of the soil (Laabs and Amelung, 2005; Đurović *et al.*,

2009; Funda *et al*., 2014). Therefore, it is expected that the texture as well as the structure of the soil can play a significant role in the transport processes of agrochemicals in soil (Tabarzad *et al.*, 2011). In this regard, soils that are very sandy (such as those of the Afram plains) are more likely to allow rapid movement of water and agrochemical leaching. Conversely, soils that are high in clay (such as Akuse series) and organic matter would slow the movement of water and result in agrochemical accumulation and persistence.

It is important to note that whereas these mechanisms have been widely researched in temperate soils and environmental conditions, the peculiarities of tropical soils and the implications of agrochemical transport are not well documented. For example, many tropical soils are well aggregated, exhibiting a 2-phase pore system, namely inter-aggregate and intra-aggregate pores (Brand and Philipson, 1985; Blonquist, et al., 2006). This implies that during transport, part of the chemical will be retained within the aggregates and later diffuse gradually into the macro pores. Agrochemical loading to the soil may be higher than would be predicted by simple loading models. Furthermore, most tropical soils contain appreciable quantities of sesquioxides or oxides and hydroxides of Fe and Al (Sanchez and Logan, 1992). The lingering question is how agrochemicals interact with sesquioxides and how do these interactions affect solute transport.

Understanding the transport of agrochemicals in soils is important to many management problems in agriculture and the environment (Lal and Shukla, 2002). Most importantly, it can help in the development of strategies for effective use of these compounds within the root zone whiles minimizing the risks associated with their movement into groundwater sources. Additionally, it is important to understand the processes of redistribution and leaching in the vadose zone to aid in the development of strategies to minimize the contamination of soil and

water sources (Lal and Shukla, 2002). It is also necessary for the development and validation of computer simulation models for use as predictive tools in the assessment of the fate of agrochemicals in the Ghanaian environment.

Currently, the fate of most of these agrochemicals in Ghanaian soils is not known. For instance, very little information is available on the mobility, persistence or otherwise of agrochemicals in most Ghanaian soils. Studies have mainly focused on the extent of agrochemical use by farmers Fianko *et al*., (2011), and their impact on health via vegetable production and the level of pesticide residue in some parts of the Volta River (Ntow, 2007). However, there seem to be little information on the fate and transport of agrochemicals in Ghanaian soils.

1.3 Hypothesis

This research study is based on the null hypothesis that the pattern of agrochemical transport will be the same in all the soil samples used in the study.

1.4 Thesis Objectives

The overall objective of this study is to understand the transport mechanisms of agrochemicals in four agricultural soils in order to facilitate the development of strategies for their use. Specifically, the study objectives are to;

a. Determine the sorption dynamics of the agrochemicals 'potassium chloride' (KCl) and 'chlorpyrifos' in the selected soils.
b. Use horizontal infiltration experiments to obtain concentration fronts of some of these chemicals.
c. Investigate the influence of soil physical and chemical properties on the patterns of movement of these chemicals in soil.

1.5 Outline of the Thesis

The thesis is organized into 6 chapters. Chapters 1 and 2 provide an introduction and review of relevant scientific literature respectively. Chapter 3 presents the theory that forms the basis for the determination of the transport parameters in the laboratory experiments undertaken in this study. In chapter 4, the methodology of the study is provided in detail. Chapter 5 takes a look at the results and the discussion of the findings. Chapter 6 provides the conclusion and recommendations for future research.

CHAPTER TWO

LITERATURE REVIEW

2.1 Agrochemical use in Agriculture

2.1.1 Fertilizer use in Ghana

In most regions over the world, increase in agricultural production has been associated with a sharp increase in the use of chemical fertilizers. In Ghana, fertilizers of various forms are applied by most farmers. The low fertility status, resulting from the highly weathered nature and the limited nutrients reserves of most Ghanaian soils makes it practically difficult to produce crop without nutrient amendments (Singh and Steinnes, 1994). Although fertilizer use in Ghana is considered as very low, the trend shows a steady increase in fertilizer imports over the years. Fertilizer imports into Ghana have increased steadily over the past decade and reached a total of about 670, 000 metric tonnes in 2012 (MOFA, 2014).

The most common fertilizers imported include the compound fertilizer (Nitrogen-Phosphorus-Potassium), Sulphate of Ammonia, Urea, Muriate of Potash, Phosphates, Nitrates and Cocoa fertilizer. Of the total fertilizer imports in 2012, NPK, Sulphate of Ammonia, Urea and Muriate of Potash accounted for about 60 %.

2.1.2 Pesticide use in Ghana

Pesticides have become integral parts of the current agricultural production systems in Ghana. For most farmers in Ghana, the use of pesticides has become critically important in increasing and sustaining crop yields. Significant amounts of pesticide are applied by most farmers in the

cocoa, oil palm, cereals, vegetables and fruits sectors of the economy.There has been a continuous growth in pesticide usage in Ghana over the years, both in variety and quantity due to the expansion of acreages under cultivation for food and cash crops as well as livestock production (MOFA, 2003).

According to Dinham (2003), about 87% of farmers in Ghana now apply pesticides to control pests and diseases on vegetables and fruits. A study by Ntow (2007) indicates that of the proportion of pesticides applied by vegetable farmers in Ghana, 44 % are herbicides, 33 % insecticides with fungicides forming 23 %. A report by the Statistics Research and Information Directorate (SRID) of the Ministry of Food and Agriculture and the Ghana Statistical services indicates that a total of 13,690 metric tonnes of pesticides were imported into Ghana in 2010. Analysis of the trend of pesticide imports over the years indicate a steady increase with 2011 recording over 2.2 million metric tonnes of commercial products and of which insecticides constituted more than 36 % (MOFA, 2014).

2.2 Fate of Agrochemicals in soils

2.2.1 Fertilizers

Agrochemicals are chemical compounds with varying levels of complexity. Some fertilizers may consist of two simple elements, for example, Muriate of potash (KCl). Others such as Sulphate of Ammonia and Urea may have more complex formulation. The essential aspects of fertilizers is that when applied to soils, they are soluble in soil water and hence can be taken up by plants via the roots. In most parts of Ghana In this study, the focal fertilizer is Potassium Chloride (KCl), which will dissociate as:

$$KCl \rightarrow K^+ + Cl^- \quad [2.1]$$

The dissolved ions may interact with the soil colloids depending on the charge characteristics of the soil colloids. Soil colloids are generally negatively charged and hence would attract K^+ and repel Cl^-. However, beyond the simple exchange reaction, the attraction reaction could become so strong that K^+ is actually adsorbed i.e. because the binding forces between K^+ and the clay surfaces are greater than the hydration forces between individual K^+ ions Sparks and Huang(1987), and hence cannot be easily removed by leaching water.

Depending on the chemical stability or reactivity, solutes are broadly classified into two main categories. Lal and Shukla, (2002) broadly, classified solutes as either conservative or non-conservative. Conservative solutes remain physically and chemically unchanged and do not undergo irreversible reactions during transport through soil. Typical examples of conservative solutes include chloride (Cl) and Bromide (Br). The other category are the non-conservative solutes, which undergo irreversible reactions and change their physical and chemical phase (Lal and Shukla, 2002). These can further be divided into labile and reactive solutes. The labile solutes can undergo reversible or irreversible physiochemical, biological or microbiological reactions and can change their physical or chemical phase with time. Nitrates, sulphates and ammonia are typical examples of labile solutes. Some categories of pesticides are also labile and their half-life is used to quantify the extent to which they are labile (White *et al.*, 1998). Reactive solutes on the other hand undergo reversible and irreversible reactions with soil constituents in the form of adsorption, precipitation or dissolution. Examples of reactive solutes include the adsorption of Ca^{2+} *and* Mg^{2+} on clay particles and the precipitation of calcium as calcium sulphates and calcium carbonates.

Sorption is a major process influencing the transport of solutes in soils. Majority of solutes that enter the soil environment are removed through sorption (Braids, 1981). It is a surface phenomenon which may be either absorption or adsorption, or a combination of the two (Morrill, *et al.*, 1982). Adsorption within the soil environment could be referred to as the association of a compound onto the surface of a material usually in a liquid-solid or vapor-solid system. Absorption on the other hand involves the redistribution of a compound from the aqueous phase into a volume of material. The term sorption is often used when the specific mechanism is not known (Site, 2001).

It is believed that several mechanisms may operate during the interaction between a given agrochemical compound and soil particles, depending on nature of the organo-mineral association (Konda *et al.*, 2002). Generally, positively charged ions in the soil solution are attracted to the negatively charged sites on the soil particles. Because most soils have negatively charged colloidal surfaces cation exchange is a major sorption mechanism for inorganic compounds in soils. Cation exchange refers to a process where cations in the soil solution that come into the vicinity of another cation on the exchange site are possibly able to replace that cation.

Usually, cations in the soil solution are in equilibrium with the cations on the exchange sites (Site, 2001). Whether a cation is exchanged or not depends on the charge density of both cations involved. In general, cations of higher valence are held more tightly to the exchange sites. Additionally, the size of the cation may affect the sorption affinity (the degree to which the cation is held tightly to the exchange site). Consequently, cations that are smaller in size like Na^+ (which is normally highly hydrated in soil) will be held at the exchange site with a lower force of attraction and can be exchanged rather easily.

Also, the ionic strength (which is a measure of the concentration of ions in a solution) relating to a given ion in solution affects the sorption affinity. Therefore, if a sufficiently strong solution of an ion like K^+ is introduced into a soil solution, the K^+ may be able to replace most of the cations at the exchange site including ions with a higher sorption affinity.

Regardless of the mechanism for replacing cations in the soil solution, the maximum concentration of a particular cation in solution is dependent on its solubility product. If the solubility product of the cation in the soil solution is exceeded, the cation can combine with negatively charged species and precipitate as insoluble salts. In this regard, the exchange sites and precipitated salts become reserve supplies of cations to replenish the soil solution. In most cases ions that are not very mobile in soils tend to be positively charged and relatively insoluble.

Many factors influence the tendency of cations to be adsorbed to soil. Notable among them are soil type, pH, presence of other ions that compete for exchange sites and the presence of other compounds that tend to form complex molecules with the cation (Moldrup *et al.*, 1994.). Cation exchange at negatively charged sites on soil surfaces is a major retention mechanism for agrochemicals and other pollutants in soils.

Soil sorption is characterized by a partition constant or coefficient, usually referred to as the distribution coefficient and conventionally written as (K_d). The distribution coefficient is defined as the ratio of the quantity of molecules adsorbed to the quantity of molecules in solution at equilibrium. For direct measurement of the distribution coefficient (*Kd*), the batch equilibration method is generally used (OECD, 1997). In some cases, dynamic partition coefficient is also used.

As with all mass transfer or exchange processes between phases, the description of the sorption and desorption processes require information about the equilibrium reached between the various phases and the speed at which this equilibrium is attained. The equilibrium sorption of both ionic and non-ionic pollutants is commonly described by adsorption isotherms. Adsorption isotherms describe the equilibrium relationship between the activity of solute or compound in solution and the amount or quantity adsorbed on the soil or solid exchange sites at constant temperature. For maximum precision in adsorption experiments, it is preferable to adjust the adsorbent concentration so that between 20%–80% of the pollutant is removed or adsorbed from solution. Furthermore the soil/solution ratio should be as wide as possible in the range between 1:5 and 1:20 (Site, 2001).

Sorption tests require an accurate preparation of the soil/sediment sample before the onset of the experiment in order to have reliable and reproducible data (Site, 2001). These processes may include sieving, homogenization and sterilization (in instances where microbial degradation of the chemical under investigation is to be prevented). Sorption isotherm is a plot of the equilibrium concentration of the chemical sorbed on a material as a function of its equilibrium concentration in solution at a given temperature. The experimental data generated are then fit by an isotherm expression to determine whether the experimental system satisfies the assumptions of the isotherm derivation or not.

Sorption isotherms have been classified into general types with each isotherm interpreted by a specific model (Abdul and Gibson, 1986; Moldrup *et al.*, 1994). For purposes of this review three main sorption isotherms are described namely (i) linear (ii) Langmuir (iii) Freundlich

The linear sorption isotherm is the most common and simplest of all the isotherms. This is described by only one model parameter, which is the distribution coefficient (K_d). Linear

adsorption generally occurs at very low solute concentrations as well as low loading of the sorbent. The isotherm assumes a constant fractional distribution between dissolved and sorbed chemical and in principle implies an infinite sorption capacity that is only limited by the water solubility of the pollutant. Therefore, it describes the phenomenon that the amount of a solute that is sorbed is directly proportional to its concentration in solution. The linear adsorption isotherm is described by the equation

$$Q_s = K_d \,.\, C_l \qquad [2.2]$$

where,

Q_s ($ug\ g^{-1}$) is the amount of pollutant sorbed

K_d (L g^{-1}) is the linear distribution coefficient and

C_l (ug L^{-1}) is the equilibrium concentration in solution.

For a given chemical in a given soil environment, high K_d values indicate a relatively large tendency towards sorption whereas low values are interpreted as a low tendency towards sorption.

The Langmuir model is based on the assumption that there are only a certain number of sorption sites available on the soil. It further assumes that these sorption sites are situated in one layer and have the same affinity towards sorption. In other words, the same sorption energy is associated with each site. The principle applied in this instance is that, adsorption sequentially fills surface sites of the material until all sorption sites are occupied to the extent that a further increase in liquid concentration will not increase the amount of chemical adsorbed. This isotherm is described by a two parameter model. In this model, the mass of pollutant sorbed per unit mass of soil material initially increases linearly with increasing solute concentration at low surface

coverage but, declines later and approaches an asymptotic value when the adsorption sites approach saturation. The equation for the Langmuir isotherm is usually given as

$$Q_s = Q_{max} \frac{K_L.C_l}{1+ K_L.C_l} \quad [2.3]$$

where

Q_s ($ug\ g^{-1}$) is the amount of pollutant sorbed,

Q_{max} ($ug\ g^{-1}$) is the maximum sorption capacity of the soil material,

K_L(L g^{-1}) is the Langmuir distribution coefficient, and

C_l (ug L^{-1}) is the equilibrium concentration in solution.

The Freundlich isotherm is non-linear in the entire concentration range and does not exhibit a maximum sorption capacity. It is the most often used non-linear sorption isotherm in experiments to describe solute-soil interactions. This may be due to the fact that the isotherm allows for a heterogeneous surface that is more often seen in natural systems. The Freundlich isotherm is described by the equation,

$$Q_s = K_F.C_l^n \quad [2.4]$$

where

Q_s ($ug\ g^{-1}$) is the amount of pollutant sorbed,

K_F (L g^{-1}) is the Freundlich distribution coefficient,

C_l (ug L^{-1}) is the equilibrium concentration in solution, and

n (-) is an empirical parameter assuming values between 0 and 1.

2.2.2 Pesticides

Application of pesticides comes in various forms. Some pesticides are applied directly to the soil to kill weeds and insects. Pesticides may also get to the soils in drips from plants during

application, as seed treatments, as sprays which does not get to the target organism and in the tissues of plants and insects which have been killed. Once in the soil, three major factors may control the fate of the pesticide (Wild, 2006). These include adsorption by the solid phase, volatilization and decomposition. Usually, the portion of pesticides that are not adsorbed or decomposed may (depending on the solubility) dissolve into the soil solution. Depending on climatic conditions, precipitating water percolates and transport the pesticide (or the residue) with the soil solution beyond plant root zone and into ground water and other water sources (Lal and Shukla, 2002).

Pesticide in surface and groundwater sources has become an issue of great concern to both agriculturalists and environmentalist in Ghana. A study by Ntow (2007) found residues of pesticides in water and sediments in the Volta Lake that were high enough to be of concern to both environmentalists and health officials. In the cocoa growing areas of the Ashanti and Eastern regions of Ghana, high levels of the pesticides lindane and endosulfan have been detected in water samples from rivers (Acquaah, 1997). In the vegetable growing areas of Akumadan in the Ashanti region, very high levels of pesticide residues were detected in samples of both water and sediments (Ntow, 1998; Yeboah, *et al.*, 2004; Fianko, 2011). Residues of pesticides have also been detected in fruits and vegetables, milk, fish and other food samples at different intervals within the country. For example, analysis of food samples sold by street vendors in the major Ghanaian cities of Accra and Kumasi between 1999 and 2002 revealed disturbing levels of pesticides and heavy metals (Armah *et al.*, 1999; Ntow, 2001; Darko and Acquaah, 2008; Essumang, *et al.*, 2009). It is evident from the above that pesticide residues in river sediments, water and food sources have reached limits that have become major concerns to

both consumers and health officials and the easiest pathway for these pesticides are through overland flow of water and leaching.

Pesticides also undergo sorption when applied to soils. However, unlike inorganic compounds, the mechanism by which most organic pollutants such as pesticides are retained by soils is quite different. The sorption of non-polar organic compounds is primarily driven by hydrophobic interactions (Moldrup *et al.*, 1994). When hydrophobic molecules associate with soil organic matter, there is no competition with water. Rather, the contact surfaces between water and the non-polar compounds are minimized due to the collection of the non-polar compounds in lumps (Chiou *et al.*, 1988). The interactions resemble a dissolution reaction into an organic solvent and require much less energy.

Besides the physico-chemical properties of the chemical itself, the sorption of an organic chemical or compound on a natural solid is a very complicated process that involves many properties of the sorbent (Site, 2001). Among the various soil properties, organic matter plays a very significant role in the adsorption of organic compounds in the soil environment. According to Chen *et al*. (2004), adsorption of hydrophobic pollutants on soils is described by two stage kinetics. The vacant sites are filled in a rapid initial stage while diffusion of the hydrophobic pollutants into soil organic matter is a slow rate-limited process (Chiou *et al*., 1983; Weber *et al*., 1991).

Since soil organic matter is generally less polar than water, it provides a more favorable environment because its polarity with that of the organic compound is similar. Therefore, soil organic matter is the predominant sorbent for non-polar compounds in soil. However since the bonding between soil organic matter and the non-polar compound is not due to actual attraction

between the components and no binding energy is created, this type of sorption is a very weak one. The persistence of organic pollutants in soils, their migration to groundwater and the evaluation of the degree of contamination expected in a groundwater system are problems that require the knowledge of the sorption characteristics of the pollutants to be investigated as well as the knowledge of the type of soil and of its characteristics (Schwarzenbach and Westall, 1981; McCarthy and Jiminez, 1985). This is due to the fact that the transport of reactive and non-reactive solutes through soil is affected relative to the movement of water (Nielson *et al*,. 1986).

2.2.3 Agrochemical use and contamination of the environment

Modern agriculture depends heavily on the use of agrochemicals to sustain optimum yields. In agricultural ecosystems, agrochemicals may be categorized on the basis of their function. Therefore, agrochemicals could be nutrients like fertilizers, pesticides like insecticides, herbicides and fungicides, organic chemicals or microbial materials like biological pesticides (Lal and Shukla, 2002). Along with chemical fertilizers, synthetic pesticides have enabled dramatic increases in agricultural productivity and quality of produce without the need to increase farmland and labour (Cooper and Dobson 2007). The use of pesticides by farmers reduces drastically, the impact of pests on agricultural productivity. Some researchers have argued that the cessation of pesticide use could lead to significant crop loss and eventually result in increased food prices worldwide (Oerke, E. C. 2006;Cooper and Dobson 2007). Farmers therefore depend on the use of pesticides to obtain optimum yields in agriculture and it could be argued that together with fertilizer they form the backbone of modern agriculture.

In the humid tropics, pesticides are applied on crops throughout the growing season to control pests and diseases all year round. In some instances, pesticides are also applied to control soil-dwelling pests after harvesting. These practices are common in the humid tropics due to climatic

conditions which are very conducive for proliferation of pests and diseases. The growing indiscriminate use of pesticides however has become a cause of serious concern due to its adverse effect on both ecosystem and public health. Most often, only a small amount of an applied pesticide reaches the target species, (Pimentel, 1995). Thus, a large portion of applied pesticides migrate off-site and affect non-target species and degrade the environment. Concerns over such occurrences have led to considerable investigations into the various processes that mediate pesticide transport in soil and water and consequently its impact on the environment.

2.2.3.1 Leaching and Transport

The transport of agrochemicals and solutes (in general) in soils has perhaps attracted the most extensive study in chemical transport phenomena. Studies on the subject dates as far back as 1961 (Nielsen and Biggar, 1961). It is generally agreed that chemical transport in soils is due to two main processes:

i) Convective flux (or mass flow) where the bulk dissolved chemical moves with the soil water (solvent) and
ii) Diffusion (and dispersion) whereby the chemical moves along a concentration gradient within the solvent.

Additionally, the chemical front becomes dispersed due to the non-uniformity of soil pore size, with the larger pores transmitting water faster than the smaller ones. This process leads to the mixing of the incoming solute with the antecedent water. The combination of these three mechanisms results in the well-known general convective-dispersive equation.

$$J = \left[\bar{v}\,\theta C - \theta \wp_C (\theta\,\bar{v})\frac{\partial C}{\partial x}\right] \qquad [2.5]$$

where,

J = total mass of solute transported across a unit cross-sectional area of soil per unit time

$(mol\ m_b^{-2} s^{-1})$,

$\bar{v}$ = average flux velocity (m_b/s),

θ = moisture content (m_w^3/m_b^3),

C = concentration of solute (mol/m_w^3),

$\wp_C$ = hydrodynamic dispersion coefficient (m_b^2/s), and

$\frac{\partial C}{\partial x}$ = solute concentration gradient

The transport process is often analyzed in terms of Breakthrough curves (BTC), described by the solution to equation [2.5], given as:

$$\frac{C}{C_o}(L,t) = {}^1/_2\, erfc\ \frac{(L-vt)}{(4D^* t)^{1/2}} \qquad \text{(Carslaw and Jaeger, 1959)} \qquad [2.6]$$

where

C = output concentration (mol/m_w^3),

C_o = input concentration (mol/m_w^3),

t = time (s)

L = length of soil column (cm)

V = pore water velocity (q/θ)

D^* = apparent dispersion coefficient (m_b^2/s)

erfc = complimentary error function

Equation [2.6] has been used to successfully predict the transport of many chemicals, especially the conservative types (Cl^-, NO_3^-, Br^-, etc) that do not interact with the soil colloids. Examples of

such studies can be found in Nielsen and Biggar (1961); Nielsen *et al.*(1962); Biggar and Nielsen (1962); Addiscott and Wagenet (1985).

For Ghanaian soils, solute transport studies are limited and confined to laboratory situations. Laryea (1979) studied the hydrodynamic dispersion of KCl through Akuse series (Vertisol). Adiku (1982) studied soil and water transport near crystalline NaCl in Akuse series (Vertisol) and Sumosie series (Acrisol) under unsaturated conditions. It was observed that a great more quantity of water vapour condensed near the salt for the Sumosie series than the Akuse series. Also, soil aggregation affected the flow process. Subsequently, the movement of dissolved NaCl into the soil was also greater for the Sumosie series than the Akuse series. Recently, Arthur (2010) studied the simultaneous movement of ammonium and potassium during unsaturated transient water flow in Akuse series (vertisols) and Toje series (Alfisol) under laboratory conditions. Observations made from this study indicated that soil moisture diffusivity and dispersion coefficients were considered to be dependent on moisture content only. It was also observed that the dispersion coefficient for Cl^- in the alfisol was about three times that of the vertisols. The dispersion coefficients of K^+ and NH_4^+ followed similar patterns to that of the Cl^- in both soils. Beyond these studies carried out essentially on disturbed repacked soil samples, actual field studies or studies on undisturbed monoliths are lacking.

Whereas the validity of equation [2.6] has been observed for the limited Ghanaian studies, it would require expansion to deal with the situations of non-conservative solutes such as K^+ and especially, the organic chemicals such as pesticides. Further, the influence of soil structure on transport must be considered, if field scale transport is to be described. The general approach to incorporating the soil-solute interaction for non-conservative solute is to define a retardation factor R, given by:

$$R = \left(1 + \frac{\rho_b K_d}{f}\right) \quad [2.8]$$

where

ρ_b = soil bulk density (g/cm^3)

K_d = partition coefficient (L/g)

f = porosity

For those chemical ions (e.g. K^+, pesticides) that are adsorbed by the soil matrix, the retardation factor (R) is used to adjust the pore water velocity:

$$V^* = \frac{V}{R} \quad [2.9]$$

where

V^* = apparent pore water velocity

V and R, are previously defined.

Equation [2.9] suggests that the movement of a non-conservative chemical will be slower than that of a conservative one. Thus, the shape of the BTC of a conservative chemical may differ from that of a non-conservative one. Further, the issue of soil structure has to be included in the transport equation. This is essentially an issue of aggregation and two-phase porosity (macro and micro). The general approach in the literature, is to partition soil water into (i) mobile and (ii) immobile water fractions (Coats and Smith, 1964). The assumption is that the water-filled pore space is partitioned into two distinct domains:

1. A mobile domain (θ_m), which occupies the centre of saturated pores and subject to steady-state flow. Thus, movement of water within the soil is assumed to occur only in the mobile region where solute transport is due to convection and dispersion.

2. An immobile domain (θ_{im}) that is considered representative of stagnant water existing as thin films on soil particles, water trapped in small unsaturated pores and water within dead-end pores (vanGenuchten and Wierenga, 1976; Robin *et al*., 1983). Within this domain, solute movement is only by diffusion (vanGenuchten and Wierenga, 1976). By accounting for immobile water fraction for solute movement in soil, total water content θ (L^3L^{-3}) is defined as $\theta = \theta_m + \theta_{im}$.

2.2.4 Chlopyrifos-Soil interactions

Unlike most fertilizers that are inorganic, most pesticides are organic compounds of complex composition. The particular pesticide of interest in this study in 'Chlopyrifos', an insecticide sold under the trade name Dursban, Pyrinex or Pyrinex Quick in Ghana. Chlorpyrifos, (*O*,*O*-Diethyl-*O*-(3,5,6-trichloro-2-pyridyl) phosphorothioate (C9H11Cl3NO3PS), is an organophosphate insecticide, and one of the most-widely used active ingredients for pest control products worldwide (Nair and Pradeep, 2007; Gebremariam *et al*., 2012). It is also one of the most intensively used insecticides in agriculture and is described as a chlorinated organophosphate (Larson *et al*., 1995; USEPA, 2006). Between 2002 and 2006 the annual average global use of chlorpyrifos was estimated at 25 million kg active ingredient, of which 98.5% was used for agricultural purposes (Eaton *et al*. 2008; Gebremariam *et al*., 2012).

Chlorpyrifos is one of several compounds designed to replace persistent and ecologically toxic organo-chlorine pesticides that were banished in the 1970s (USEPA 1986). The compound kills target organisms upon contact by affecting the normal function of the nervous system (USEPA, 1999). The insecticidal action of chlorpyrifos is due to the inhibition of the enzyme acetylcholinesterase, resulting in the accumulation of the neurotransmitter, acetylcholine, at nerve endings of target organisms. When insects are exposed, chlorpyrifos binds to the active site of the cholinesterase enzyme, which prevents breakdown of acetylcholine in the synaptic cleft

(Karanth and Pope, 2000). The resulting accumulation of acetylcholine in the synaptic cleft causes overstimulation of the neuronal cells, which leads to neurotoxicity and eventually death (USDHHS, 1997; Karanth and Pope, 2000).

Chlorpyrifos is a colorless to white crystalline solid with a mild mercaptan odor that is similar to the smell of sulfur compounds found in rotten eggs, onions and garlic (Lewis, 1998; Tomlin, 2006; USEPA, 2006). It has a molecular weight of 350.6 g mol^{-1}, and a solubility in water of 2.0 mg L^{-1} at 25 ^{o}C (USEPA, 2006; Tomlin, 2006). The compound has a melting point of 42 °C and boils at approximately 100 ^{o}C at 100 kPa. Chlorpyrifos has a specific gravity of 1.03 g m^{-1} at 20 ^{o}C and a vapour pressure of 2.49 × 10-3 Pa at 25 °C.

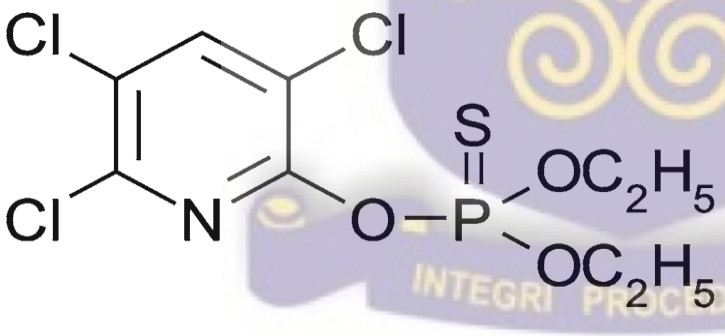

Fig 2.1 Chemical structure of chlopyrifos

Chlorpyrifos exhibits a moderate level of hydrophobicity and a strong tendency to sorb to organic matter and soil (Gebremariam *et al*., 2012). Its soil sorption coefficient (K_{oc}) is between 360 to 31,000 depending on soil type and environmental conditions (Smegal, 2000).

Chlorpyrifos is registered for the control of soil and foliar insects on a wide range of crops including fruits and vegetables (Kidd and James, 1991). Chlorpyrifos is made in different formulations for agricultural use. In Ghana, the compound is widely used by many small and large scale farmers, mostly as emulsifiable concentrates, for the control of pests in agricultural production. Chlorpyrifos has been described as moderately to extremely toxic to humans and wild life and chronic exposure has been linked to neurological effects, developmental disorders, and autoimmune disorders (Thrasher *et al.*, 2002; Merrington *et al.*, 2002).

2.2.4.1 Chlopyrifos persistence and toxicity

Persistence and mobility are among the very important properties that could influence the fate and transport of the insecticide in the soil. Persistence refers to how well the pesticide can resist breakdown and is usually measured by the half-life. The half-life of a chemical is described as the period of time it takes for half of the amount of pesticide in soil to be degraded or transformed. Thus, each half-life that passes reduces the amount of pesticide in soil by one half. The half-life of a pesticide can vary due to factors including microbial population, soil moisture and soil temperature. Pesticides with half-lives of 30 days or less are classified as non-persistent, those with half-lives between 30 and 100 days are classified as moderately persistent with persistent pesticides having half-lives of more than 100 days (Gebremariam *et al*., 2012).

Most pesticides have half-lives ranging from a few days to months although some highly persistent pesticides may have half-lives as long at 500 days (Gebremariam *et al*., 2012). Racke *et al*, (1994) studied the degradation and fate of chloropyrifos in agricultural and urban environments and found that nearly 70 % of the initial residue remained in soil 18 months after application. Subsequent laboratory investigation revealed a half-life of between 116 – 1576 days. However, the half-life of the compound is dependent on the application rate, the ecosystem type

and environmental factors. For instance, Racke (1993) and Dabrowski *et al*. (2002) studied the degradation of chlorpyrifos in soil and concluded that environmental dissipation half-lives of the compound ranged from a few days to more than 4 years, depending on application rate, ecosystem type, and pertinent environmental factors. They concluded that higher application rates, such as termiticidal applications, resulted in considerable increase in persistence of the compound (Racke *et al*., 1994; Murray *et al*. 2001; Gebremariam *et al*., 2012). Persistence of the compound in soil may therefore depend on the formulation, application rate, soil type and climatic conditions (Roberts and Hutson, 1999).

Although the level of toxicity of chlorpyrifos is variable across organisms of different species and orders, it generally arises from its inhibition of the neuroenzyme acetylcholinesterase in exposed organisms. For most sensitive organisms acute toxic concentrations of chlorpyrifos range from as low as 1×10^{-10} g/L for insect larvae to 1×10^{-3}g/L for freshwater crustaceans. In field soils with nematodes, laboratory studies and with stocked fish in ponds, chlorpyrifos displayed acute toxicity at doses equivalent to recommended agricultural application rates ranging 480 and 960 g/ha (Davey *et al*. 1976; Roh and Choi, 2008). In aquatic environments, chlorpyrifos was reported to have changed the composition of the plankton community at a concentration of 100×10^{-10} g/L in sea water (Tagatz *et al*. 1982; Gebremariam *et al*., 2012). Additionally, Schimmel *et al*., (1983) reported in a study that the compound had an acute toxicity against mysid shrimp at 35×10^{-10} g/L. Chlorpyrifos is known to be highly toxic to freshwater fish, aquatic invertebrates and estuarine and marine organisms (Gebremariam *et al*., 2012).

In humans, excessive exposure to chlorpyrifos may cause nausea, vomiting, diarrhea, abdominal cramps, headaches and dizziness. Additional symptoms of excessive exposure to the compound may include eye pain, blurred vision, dilation of the pupils of the eye, salivation and sweating.

Severe cases of poisoning may affect the central nervous system and could result in incoordination, slurred speech, loss of reflexes, weakness and involuntary muscle contractions, tremors of the tongue and eventual paralysis of the respiratory muscles (Davey *et al*. 1976; Roh and Choi, 2008; Gebremariam *et al*., 2012).

2.2.4.2 Chlopyrifos degradation

Chlorpyrifos degradation in the natural environment is the result of abiotic and biotic processes that often work in tandem. A key process that has been observed to mediate in the degradation of the compound involves the enzymatic or clay-/metal-catalyzed hydrolysis. This leads to the cleavage of the phosphorothioate ester bond to form the by-product 3,5,6-trichloro-2-pyridinol, which is further broken down to organo-chlorine compounds and carbon dioxide (Racke, 1993; FAO/WHO, 2000).Chlorpyrifos is also known to undergo photolytic degradation in sunlight, resulting in the partial dechlorination of the pyridine ring and the demethylation of the phosphorothioate ester (Attila and Diana 2009). Additionally, pH and temperature are known to exert an influence of the degradation of chlorpyrifos. Chapman and Cole (1982a) and Getzin (1985) reported that increasing pH and temperature respectively resulted in a rapid increase in the rate of hydrolysis of the compound. Although chlorpyrifos can be completely mineralized in soil, the process is a very slow one. In an incubation study in soils, Racke *et al*. (1994) found that only 5% of the compound was mineralized to CO_2 after 13-months of incubation. In another study, Gebremariam and Beutel (2010) realized that only 2.5% was mineralized when the compound was incubated for almost 2 months in wetland sediments.

Applied chlorpyrifos may be exposed to photodegradative conditions in the soil. For instance, the compound may directly absorb sunlight mostly in the ultraviolet region of the spectrum or

may react with secondary reagents (such as soil humic and inorganic substances that absorb sunlight) and lead to degradation (Zepp and Schlotzhauer, 1983).

Quantitatively, pesticide degradation could be described by a decay function of the form;

$P_t = P_o(1 - e^{kt})$ (Chapman and Cole, 1982b; Wang, and Hoffman, 1991) [2.10]

where

P_t = the pesticide concentration in the soil at time t (g/L)

P_o = the initial pesticide concentration applied to the soil (g/L)

k = decay constant

t = time (s)

Thus in determining the fate of applied pesticide to soil, the natural decay must be accounted for if study periods are long.

CHAPTER THREE

THEORY

3.1 Water flow in soil columns

Dissolved solutes move with water in soils under both saturated and unsaturated conditions. Saturated conditions often occur below the water table where water movement is assumed to be predominantly horizontal with little flow in the vertical direction. The driving force of flow under both saturated and unsaturated conditions is the hydraulic potential gradient, with flow occurring in the direction of decreasing hydraulic potential. Under such conditions, the flux density of water is proportional to the hydraulic potential gradient and the hydraulic conductivity.

Unsaturated flow conditions usually predominate above the water table (Radcliffe and Rasmussen, 2002). Although soil water movement in the unsaturated zone is generally thought to be vertical, some lateral movement may also occur (Radcliffe and Rasmussen, 2002).

Water and solutes (principally agrochemicals) transport in soils could be considered either under steady or transient flow conditions. In steady flow systems, the flux, gradient and water content are constant in time whereas under transient flow conditions they vary. Generally, transport of solutes in soil depends on the water flow velocity, the soil moisture content, soil characteristics, solute species and their reactions with the soil matrix (Radcliffe and Rasmussen, 2002). Understanding the mechanisms of the simultaneous movement and interactions of water and agrochemicals in soil will help in the modeling of their transport in soils. In this study, water with an agrochemical as its solute load was therefore examined under horizontal flow conditions in columns of repacked soil and steady state vertical infiltration conditions in "undisturbed" soil columns.

To describe mathematically water and agrochemical transport in soil, we would combine the flux (Darcy's law) and the continuity equations pertaining to either water or the agrochemical under consideration. According to Darcys' law, water flow occurs in the direction of hydraulic potential energy gradient. The flux density of water (i.e. quantity of water per unit area per time) is thus proportional to the hydraulic potential energy gradient ($^{\partial \psi_h}/_{\partial n}$). Thus;

$$v = -K \frac{\partial \psi_h}{\partial n} \qquad [3.1a]$$

In equation 3.1a, K = hydraulic conductivity of water and it is a function of water content and soil matric potential ψ_m. The hydraulic potential $\psi_h = (\psi_m + \psi_p + \psi_z + \psi_s)$ where the

subscripts m, p, z and s indicate the matric, pressure, gravitational and osmotic potentials respectively. The coordinate n, will be represented as x in the horizontal and z in the vertical domains. Consequently, for horizontal water flow, equation [3.1a]

is written as $v = -K(\theta)\frac{\partial \psi_h}{\partial x}$ [3.1b]

and

$v = -K(\theta)\frac{\partial \psi_h}{\partial z}$ for vertical flow [3.1c]

3.1.1 Horizontal water flow in soil columns

For horizontal unsaturated flow under transient conditions, $\psi_h = \psi_m$

$$because, \psi_z = 0, \psi_p = 0 \; and \; \psi_s = 0.$$

Therefore, $v = -K(\theta)\frac{\partial \psi_m}{\partial x}$ [3.2]

In using the Darcy's equation to describe water flow in soils in the form as in equation 3.2, it is assumed that;

1. There is no change in state of water during flow.
2. The soil pores are continuously connected throughout the flow region.
3. Roots in the soil system are absent and therefore sources and sinks are zero.
4. Conditions in the soil are isothermal and
5. The soil is homogenous.

Assuming that the soil moisture characteristics, $[\psi_m(\theta)]$ is unique (i.e. ignoring hysteresis), the chain rule of differentiation may be used to re-write equation [3.2] as:

$v = -K(\theta)\frac{\partial \psi_m}{\partial \theta}.\frac{\partial \theta}{\partial x}$ which then becomes;

$$v = -D(\theta)\frac{\partial \theta}{\partial x} \quad [3.3]$$

where, the soil water diffusivity, $D(\theta) = K(\theta)\frac{\partial \psi_m}{\partial \theta}$

The assumption inherent in this derivation is that the moisture characteristic $\psi_m(\theta)$ is unique and that isothermal conditions prevail.

The continuity equation for water flow states that, in the absence of any sources or sinks of water, the time rate change of water content of a volume element of a conducting porous medium (soil in this case) must be equal to the change of flux density of water with distance. For one dimensional water flow in soil, this conservation of mass can be stated mathematically as;

$$\frac{\partial \theta}{\partial t} = -\frac{\partial v}{\partial x} \quad [3.4]$$

Substituting equation 3.3 into equation 3.4 gives:

$$\frac{\partial \theta}{\partial t} = \frac{\partial}{\partial x}\left[D(\theta)\frac{\partial \theta}{\partial x}\right] \quad [3.5]$$

In this study, the set-up for the horizontal flow experiment was such that water movement was through a narrow horizontal semi-infinite air dry soil column, which is uniformly packed initially at moisture content θ_n. The arrangement was made to ensure that the gravitational potential was negligible. A source of water was introduced instantaneously and maintained at θ_0 at the inlet of the horizontal tube at time t > 0 where $x = 0$. This ensured the following initial and boundary conditions:

$$\theta = \theta_n, x \geq 0, t = 0 \quad [3.6a]$$

$$\theta = \theta_0, x = 0, t \geq 0 \quad [3.6b]$$

Assuming that the soil moisture diffusivity (D), is a function of water content (θ) only, equation (3.5), may be transformed into an ordinary differential equation using Boltzmann's transformation $\lambda = xt^{-1/2}$ to obtain,

$$-\frac{\lambda}{2}\frac{d\theta}{d\lambda} = \frac{d}{d\lambda}\left[D(\theta)\frac{d\theta}{d\lambda}\right] \quad [3.7]$$

Equations [3.6a] and [3.6b] may also be transformed using Boltzman's equation to obtain,

$$\lambda = \infty, \theta = \theta_n \quad [3.8a]$$

$$\lambda = 0, \theta = \theta_0 \quad [3.8b]$$

The solution of equation [3.7] for $D(\theta)$ subject to equations (3.8a) and (3.8b) is;

(see Appendix A1);

$$D(\theta) = -\frac{1}{2}\frac{d\lambda}{d\theta}\int_{\theta_n}^{\theta} \lambda d\theta \quad [3.9]$$

Equation (3.9) was used to calculate the soil moisture diffusivity, $D(\theta)$ function from the horizontal infiltration experiments and subsequently used in derivation and calculation for solute dispersion coefficient.

3.2 Solute movement during horizontal infiltration of water into soil

Solutes move with and within soil water in response to concentration gradient. Within the soil solution, solutes react with themselves and may interact with the soil solids. These reactions and interactions are strongly influenced by the composition and concentration of the soil solution as

well as the physico-chemical properties of the soil. An understanding of the movement and interactions of water and solutes in soil is important in the management of the environment especially, surface and groundwater resources. To adequately describe the movement of solutes in soils, the flux equation is required.

3.2.1 The solute flux equation

Formulation of the flow equation for solute in soils requires both the flux and the continuity equations. The flux equation takes into account the three mechanisms of solute movement in soils namely, convection, molecular diffusion and hydrodynamic dispersion. The combined solute flux is therefore represented as:

$$\begin{bmatrix} Combined \\ Solute \\ Flux \end{bmatrix} = \begin{bmatrix} Convective \\ Flux \end{bmatrix} + \begin{bmatrix} Flux\ due \\ to\ diffusion \end{bmatrix} + \begin{bmatrix} Flux\ due\ to \\ hydrodynamic \\ dispersion \end{bmatrix}$$

The solute flux in this study was the combination of the convective, diffusive and hydrodynamic dispersion fluxes of either the Cl^{-} and K^{+} ions in the case where KCl solution was used and chloropyrifos where the insecticide was used. Mathematically, this may be represented as;

$$J^{Cl} = \left[\bar{v}\,\theta C^{Cl} - \theta \wp_{Cl}(\theta\,\bar{v})\frac{\partial C^{Cl}}{\partial x}\right] \quad [3.20a]$$

$$J^{K} = \left[\bar{v}\,\theta C^{K} - \theta \wp_{K}(\theta\,\bar{v})\frac{\partial C^{K}}{\partial x}\right] \quad [3.20b]$$

for the Cl^{-} and K^{+} respectively, and

$$J^{Cf} = \left[\bar{v}\,\theta C^{Cf} - \theta \wp_{Cf}(\theta\,\bar{v})\frac{\partial C^{Cf}}{\partial x}\right] \quad [3.20c]$$

for the chlorpyrifos.

Here, J^{Cl}, J^{K}, and J^{Cf} are the total mass of solute (either Cl^-, K^+ or chlorpyrifos) transported across a unit cross-sectional area of soil per unit time $mol\, m_b^{-1}\, s^{-1}$; $\bar{v}$ is the average flux velocity (m_b/s), θ is moisture content (m_w^3/m_b^3), C^{Cl}, is the concentration of chloride, (mol/m_w^3), $\wp_{Cl}$the hydrodynamic dispersion coefficient (m_b^2/s) and ($\frac{\partial C^{Cl}}{\partial x}$), ($\frac{\partial C^{K}}{\partial x}$), ($\frac{\partial C^{Cf}}{\partial x}$) are the gradients of Cl^-, K^+ and chlopyrifos respectively. It must also be indicated that x is the horizontal coordinate (m_b) and the subscripts b, and w denote bulk and water respectively (Hillel, 2004). Also, C^{Cl}, C^{K} and C^{Cf} denote the concentration of chloride, potassium and chlopyrifos in solution. It must be indicated that Smiles and Philip (1978) and Smiles *et al.*, (1978) have demonstrated that during absorption of water by soil (in horizontal infiltration) in laboratory columns, the volume flux densities ($\bar{v}$) of the water in the soil are so small for the duration of the experiment that the apparent longitudinal dispersion coefficient of a non-reactive solute may be considered independent of $\bar{v}$. Equations 3.20a, 3.20b and 3.20c may therefore be written as:

$$J_{Cl} = \left[\bar{v}\,\theta C^{Cl} - \theta \wp_{Cl}(\theta)\frac{\partial C^{Cl}}{\partial x}\right] \qquad [3.21a]$$

$$J_{K} = \left[\bar{v}\,\theta C^{K} - \theta \wp_{K}(\theta)\frac{\partial C^{K}}{\partial x}\right] \qquad [3.21b]$$

$$J_{Cf} = \left[\bar{v}\,\theta C^{Cf} - \theta \wp_{Cf}(\theta)\frac{\partial C^{Cf}}{\partial x}\right] \qquad [3.21c]$$

Equation (3.21a, 3.21b and 3.21c) can only describe the one-dimensional steady state for the solutes (i.e. the respective Cl^-, K^+ and chlorpyrifos) that is moving with water in a horizontal porous medium (Hillel, 2004). Moreover, its use is limited on the assumption that the solutes are neither subject to adsorption by soil solids nor subject to chemical or biological reactions. Additionally, the parameters, $\wp_{Cl}$, $\wp_{K}$ and $\wp_{Cf}, \theta, Cl, K$ and Cf can only be defined in

macroscopic terms as gross spatial averages. Hence, equations 3.21a, 3.21b and 3.21c are only approximations of the processes they are meant to depict (Hillel, 2004).

To transform the equations into the transient state form, in which fluxes and concentrations of the solutes can vary in both space and in time, each equation (3.21a, 3.21b and 3.21c) was combined with its respective continuity equation.

3.2.2 The continuity equation

The continuity equation states that, the rate of change of solute mass per bulk volume of soil is equal to the difference between the incoming and outgoing fluxes of the solute, provided there are no gains or losses of the solute by any mechanisms operating within the soil volume (Hillel, 2004). In other words, no solute is lost. In essence, the equation indicates that the rate of change of solute per bulk volume of soil is equal to the gradient of the flux density of the solute. In one-dimension, this may be represented mathematically as;

$$\frac{\partial M}{\partial t} = -\frac{\partial J}{\partial x} \qquad [3.22]$$

where,

M is the total quantity of solutes (Cl^-, K^+ or chlorpyrifos) per unit volume of soil (mol/m_w^3), t is time (s), J is the flux density of solute and x is the horizontal coordinate (m_b). In practice, most solutes that move in soil may either be interactive or non-interactive. It must therefore be indicated that equation (3.22) may represent the continuity equation for either non-interacting or interacting solutes.

For Cl^-: $M = \theta C^{cl}$ [3.23a]

For K^+: $M = \theta C^K + \rho S^K$ [3.23b]

For Chlorpyrifos: $M = \theta C^{Cf} + \rho S^{Cf}$ [3.23c]

where,

ρ is the bulk density of the soil $(\mathrm{kg\ m_b^{-3}})$; S^K and S^{Cf} are quantities of the K^+ and chlorpyrifos respectively, associated with the soil matrix per unit mass of soil ($mol_c\ kg^{-1}$) while θ is the volumetric water content $(\mathrm{m_w^3\ m_b^{-3}})$.

During the horizontal infiltration process, it was assumed that any interaction between the soil and the insecticide would be instantaneous. Earlier studies by Smiles *et al.* (1978) also assumed that for the horizontal flow, the dispersion coefficient ($\wp$) should be considered as a function of moisture content (θ) only.

If these assumptions are considered, then equations 3.21a, 3.21b and 3.21c may be combined with 3.22 and 3.23a, 3.23b and 3.23c to obtain the following equations which describe the flow of the respective ionic and solute species respectively in soil:

$$\frac{\partial}{\partial t}(\theta C^{cl}) = \frac{\partial}{\partial x}\left[\theta \wp_{Cl}(\theta)\frac{\partial C^{Cl}}{\partial x}\right] - \frac{\partial}{\partial x}(\bar{v}\, C^{Cl}) \quad [3.24a]$$

$$\frac{\partial}{\partial t}(\theta C^{K}) + \frac{\partial}{\partial t}(\rho S^{K}) = \frac{\partial}{\partial x}\left[\theta \wp_{K}(\theta)\frac{\partial C^{K}}{\partial x}\right] - \frac{\partial}{\partial x}(\bar{v}\, C^{K}) \quad [3.24b]$$

$$\frac{\partial}{\partial t}(\theta C^{Cf}) + \frac{\partial}{\partial t}(\rho S^{Cf}) = \frac{\partial}{\partial x}\left[\theta \wp_{Cf}(\theta)\frac{\partial C^{Cf}}{\partial x}\right] - \frac{\partial}{\partial x}(\bar{v}\, C^{Cf}) \quad [3.24c]$$

In the horizontal infiltration experiment, packing of the soil in the column was done in such a way as to ensure a constant bulk density along the length of the column with time. As a

consequence, the second term on the left hand side of the equations 3.24b and 3.24c involving bulk density (ρ) then becomes$\rho\frac{\partial S^K}{\partial t}$ and $\rho\frac{\partial S^{Cf}}{\partial t}$ respectively. Also, the continuity equation [3.4] for the horizontal flow of water (with its solute load) into a soil column allows equations 3.24a, 3.24b and 3.24c to be written, after the cancellation of appropriate terms as:

$$\theta\frac{\partial C^{Cl}}{\partial t}=\frac{\partial}{\partial x}\left[\theta\wp_{Cl}(\theta)\frac{\partial C^{Cl}}{\partial x}\right]-v\frac{\partial C^{Cl}}{\partial x} \quad [3.25a]$$

$$\theta\frac{\partial C^{K}}{\partial t}+\rho\frac{\partial S^{K}}{\partial t}=\frac{\partial}{\partial x}\left[\theta\wp_{K}(\theta)\frac{\partial C^{K}}{\partial x}\right]-v\frac{\partial C^{K}}{\partial x} \quad [3.25b]$$

$$\theta\frac{\partial C^{Cf}}{\partial t}+\rho\frac{\partial S^{Cf}}{\partial t}=\frac{\partial}{\partial x}\left[\theta\wp_{Cf}(\theta)\frac{\partial C^{Cf}}{\partial x}\right]-v\frac{\partial C^{Cf}}{\partial x} \quad [3.25c]$$

Substitution of equation [3.3] into equations 3.25a, 3.25b and 3.25c result in:

$$\theta\frac{\partial C^{Cl}}{\partial t}=\frac{\partial}{\partial x}\left[\theta\wp_{Cl}(\theta)\frac{\partial C^{Cl}}{\partial x}\right]+D(\theta)\frac{d\theta}{dx}\frac{dC^{Cl}}{dx} \quad [3.26a]$$

$$\theta\frac{dC^{K}}{dt}+\rho\frac{dS^{K}}{dt}=\frac{d}{dx}\left[\theta\wp_{K}(\theta)\frac{dC^{K}}{dx}\right]+D(\theta)\frac{d\theta}{dx}\frac{dC^{K}}{dx} \quad [3.26b]$$

$$\theta\frac{dC^{Cf}}{dt}+\rho\frac{dS^{K}}{dt}=\frac{d}{dx}\left[\theta\wp_{Cf}(\theta)\frac{dC^{Cf}}{dx}\right]+D(\theta)\frac{d\theta}{dx}\frac{dC^{Cf}}{dx} \quad [3.26c]$$

In the horizontal infiltration experiment, a solution with a constant concentration of solute, was supplied to and maintained at one end of soil in a narrow horizontal semi-infinite column, having a uniform initial volumetric moisture content. This arrangement ensured that the gravitational potential was negligible and $x = 0$ at the inlet. The initial and boundary conditions with respect to the solutes were therefore,

$$C^{Cl} = C_n^{Cl}, C^K = C_n^K, C^{Cf} = C_n^{Cf}, x > 0, t = 0 \quad [3.27a]$$

$$C^{Cl} = C_0^{Cl}, C^K = C_0^K, C^{Cf} = C_0^{Cf}, x = 0, t > 0 \quad [3.27b]$$

In equation 3.27a and 3.27b, C^{Cl} is the concentration of chloride while C^K and C^{Cf} are the concentrations of potassium and chlorpyrifos respectively. It has been shown by Smiles *et al.* (1978), Laryea *et al.*, (1982) and Lagan, (2001), that equations 3.26a, 3.26b and 3.26c can be transformed by the substitution of (Boltzmann's variable) $\lambda = xt^{-½}$, on the assumption that adsorption of the potassium ion (K^+) and the chlorpyrifos to the soil colloids is instantaneous. Additionally, the substitution of the Boltzmann's variable is also based on the assumption that the dispersion coefficient ($\wp$) is dependent on water content (θ) only. Boltzman's transformation results in the following (see Appendices B and C):

$$\frac{d}{d\lambda}\left[\theta\wp_{Cl}(\theta)\frac{dC^{Cl}}{d\lambda}\right] + \frac{g(\theta)}{2}\frac{dC^{Cl}}{d\lambda} = 0 \quad [3.28a]$$

$$\frac{d}{d\lambda}\left[\theta\wp_{K}(\theta)\frac{dC^{K}}{d\lambda}\right] + \frac{g(\theta)}{2}\frac{dC^{K}}{d\lambda} + \frac{\rho\lambda}{2}\frac{dS^{K}}{d\lambda} = 0 \quad [3.28b]$$

$$\frac{d}{d\lambda}\left[\theta\wp_{Cf}(\theta)\frac{dC^{Cf}}{d\lambda}\right] + \frac{g(\theta)}{2}\frac{dC^{Cf}}{d\lambda} + \frac{\rho\lambda}{2}\frac{dS^{Cf}}{d\lambda} = 0 \quad [3.28c]$$

where $g(\theta) = \theta\lambda + 2D(\theta)\frac{d\theta}{d\lambda} = \theta\lambda - \int_{\theta_n}^{\theta}\lambda d\theta$(Smiles *et al.*,1978) [3.28d]

Equations 3.27a and 3.27b indicating the initial and boundary conditions respectively can also be transformed after substitution of the Boltzman's variable ($\lambda = xt^{-1/2}$). The sbstitutions result in the following:

$$C^{Cl} = C_n^{Cl}, C^K = C_n^K, C^F = C_n^F, \lambda = \infty \quad [3.29a]$$

$$C^{Cl} = C_0^{Cl}, C^K = C_0^K, C^F = C_0^F, \lambda = 0 \quad [3.29b]$$

Subject to the initial and boundary conditions of equations 3.29a and 3.29b, the solution for the dispersion coefficients ($\wp$) for Cl^-, K^+ and chlorpyrifos with regards to equations 3.28a, 3.28b and 3.28c results in the following equations:

$$\wp_{cl} = -\frac{1}{2\theta}\frac{d\lambda}{dC^{Cl}}\left[\int_{\lambda_{n\to\infty}}^{\lambda} g(\theta)\frac{dC^{Cl}}{d\lambda}d\lambda\right] \quad [3.30a]$$

$$\wp_k = -\frac{1}{2\theta}\frac{d\lambda}{dC^K}\left[\int_{\lambda_{n\to\infty}}^{\lambda}\left(g(\theta)\frac{dC^K}{d\lambda} + \rho\lambda\frac{dS^K}{d\lambda}\right)d\lambda\right] \quad [3.30b]$$

$$\wp_{cf} = -\frac{1}{2\theta}\frac{d\lambda}{dC^{Cf}}\left[\int_{\lambda_{n\to\infty}}^{\lambda}\left(g(\theta)\frac{dC^{Cf}}{d\lambda} + \rho\lambda\frac{dC^{Cf}}{d\lambda}\right)d\lambda\right] \quad [3.30c]$$

In the horizontal infiltration experiment, distribution of $\theta, C^{Cl}, C^K, C^{Cf}, S^K$ *and* S^{Cf} *versus* $\lambda = xt^{-1/2}$ were measured and used together with equations 3.30a, 3.30b and 3.30c to calculate the dispersion coefficients $\wp_{Cl}, \wp_K$ *and* $\wp_{Cf}$. The dispersion coefficients were then compared to enable inferences to be made.

3.3 Accounting for immobile water fraction in the case of non-interacting solute with the clay fraction of soil

It has been shown by Robin *et al.* (1983) that when the immobile water fraction is accounted for in horizontal infiltration of water into a soil column, the total water content at any value of λ is given by:

$$\theta = \theta_m + \theta_{im} \quad [3.31]$$

Where the subscripts m *and* im refer to the mobile and immobile parts of the total water content θ $(m_w^3 m_b^{-3})$, respectively. Subsequently, the average concentration of solute at any λ if the immobile water fraction is assumed to be constant is given as:

$$c = \frac{(\theta_m C_m + \theta_{im} C_{im})}{\theta_m} \quad [3.32]$$

According to the mobile immobile model proposed by Robin *et al.*, (1983), transport of a non-reactive solute takes place in the mobile water fraction. Therefore, equation 3.28a, may be re-written as:

$$\frac{d}{d\lambda}\left[\theta_m \wp_{Cl} \frac{dC_m^{Cl}}{d\lambda}\right] + \frac{g_m}{2}\frac{dC_m^{Cl}}{d\lambda} = 0 \quad [3.33a]$$

Equations 3.27a and 3.27b indicating the initial and boundary conditions respectively may also be transformed after substitution of the Boltzman's variable ($\lambda = xt^{-1/2}$), to:

$$C^{Cl} = C_{mn}^{Cl}, \quad \lambda = \infty, C = C_n \quad [3.34a]$$

$$C^{Cl} = C_{m0}^{Cl}, \lambda = 0, C = C_0 \quad [3.34b]$$

Subject to the initial and boundary conditions of equation 3.34a and 3.34b, the solution for the dispersion coefficients ($\wp$) for Cl^- with regards to equation 3.28a when the immobile water fraction is considered results in the following equation (see Appendix B):

$$\wp_{Cl} = -\frac{1}{2\theta_m}\frac{d\lambda}{dC_m^{Cl}}\int_{\lambda\to\infty}^{\lambda} g_m \frac{dC_m^{Cl}}{d\lambda}.d\lambda \quad [3.35]$$

CHAPTER FOUR

MATERIALS AND METHODS

4.1 Soil sampling and preparation

Four soil types made up of two soils from the forest-savannah transitional belt of Ghana, one from the coastal savannah zone and the other from the forest zone were used for the study. The general description and classification of the soils are given in Table 4.1. To avoid interference from antecedent agrochemical residue in the laboratory study, the soil samples were obtained from locations that had not been cultivated for more than ten years prior to sampling. The soil from the coastal savannah zone was sampled at the Kpong Agricultural Research Centre at a location that had not been cultivated for the last twenty years. The soil from the forest zone was obtained from the Ankasa forest conservation centre. The sample was taken from the native forest within the forest reserve. One of the soil samples from the forest-savannah transitional belt was obtained from Dedeso, near an abandoned small irrigation scheme in the Afram plains section of the eastern region of Ghana. The cropping history of the site indicated that the soil which was sampled had not been cultivated in more than 15 years. The other soil sample from

the forest-savannah transitional belt was obtained from a site near Foso, in the Tease District of the eastern region of Ghana. The soil was sampled from an area that had not been cultivated for over 15 years.

Each soil type was sampled within the plough depth (0 – 20 cm), transported to the laboratory and air dried. Undecomposed plant materials such as roots, sticks and other debris were removed and the remaining soil gently crushed and passed through a 2 mm sieve to obtain the fine earth fraction. The fine earth fraction was thoroughly mixed to form a composite sample and stored in plastic bags for laboratory analyses. Four undisturbed columns were also sampled within the 0 – 30 cm layers for each soil type.

Sampling of the undisturbed soil was done with a Polyvinyl chloride (PVC) pipe of 30 cm internal diameter and height of 60 cm. The weight of each PVC pipe was determined prior to sampling. To prevent leaking or boundary flow along the walls of the PVC column during the determination of saturated hydraulic conductivity and the leaching experiment, the inside of the pipes were coated with paraffin wax and allowed to stand overnight before sampling. The surface of the soil was cleared of all debris and the PVC pipe placed on top of the soil. The soil around the PVC pipe was gently shaved to form a pedestal of about 40 cm diameter.

The PVC pipe was then carefully driven into the soil to encase the soil column with the aid of a mallet. The process continued until the desired depth of 25 – 30 cm was obtained. Using a spade, the soil column in the pipe was separated about 5 cm below the penetrating depth and the sampling arrangement lifted onto a plastic plate. The soil projecting below the base of the PVC pipe was levelled off with a cutlass. The base of the pipe was then sealed with a nylon screen with mesh size 0.5 mm and firmly held in place with an elastic band. A metal strip was used to

secure the mesh and elastic band in place to prevent them from slipping. The whole arrangement was then put on a perforated plastic plate and transported to the laboratory (as shown in Figure 4.1.2). The edge of the soil at the surface of the column (where the soil comes in contact with the PVC pipe) was again sealed with quick-drying cement (as shown in Figure 4.1.3) to ensure the prevention of any leakage during determination of the saturated hydraulic conductivity.

Table 4.1 Soil types and sampling locations of the soils used in the study

Soil series	Classification	Sampling location	Vegetation zone	Annual rainfall	Texture
Akuse	Eutric Vertisol	06° 08.144' N 000° 04.305' E	Coastal Savannah	1100 – 1200 mm	Sandy Clay
Ankasa	Xanthic Ferrasol	05° 15.192' N 002° 38.420' W	Tropical rainforest	2000 – 2200 mm	Sandy Loam
Bediesie	Ferric Lixisol	06° 35.839' N 000° 10.103' W	Forest / Savannah Transitional zone	1100 – 1200 mm	Sandy Loam
Lima	Eutric Gleysol	06° 49.632'N 000° 22.067' W	Forest / Savannah Transitional zone	1100 – 1250mm	Sandy Loam

Plate 4.1.1 Sampling of an undisturbed soil column in the field.

Plate 4.1.2 **An undisturbed soil column (0 – 25 cm) ready for the determination of saturated hydraulic conductivity experiment in the laboratory.**

Plate 4.1.3 **A sample of undisturbed soil column (0 – 25 cm) after being processed and ready for determination of saturated hydraulic conductivity in the laboratory.**

4.2 Laboratory analyses for characterization of soil

4.2.1 Soil physical properties

4.2.1.1 Saturated hydraulic conductivity

Saturated hydraulic conductivity was determined on four undisturbed columns for each soil type obtained from the field by using the falling head permeameter method (Figure 4.2.1). The base of the soil column was covered with a screen to prevent the loss of soil particles during saturation and the whole column supported on a perforated plastic plate to prevent the soil from falling. A tape measure was strapped to the side of the PVC pipe containing the soil and held in place with a masking tape. The columns were then saturated overnight. A glass tube was then fitted to the top of the soil in the PVC tube and secured in place with a rubber band as indicated in the figure below. A head of water was then created on top of the soil in the column and the level of the

water noted. The drop in level of water on top of the soil column was noted with time. The saturated hydraulic conductivity was calculated from the relation:

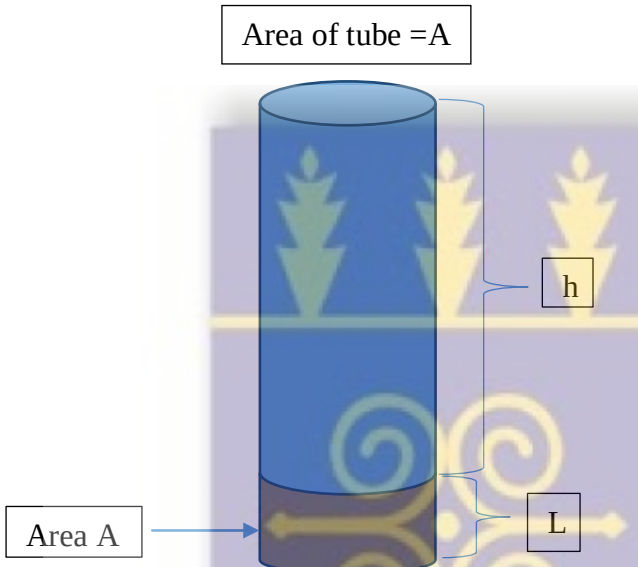

Fig. 4.2.1. **A sketch of laboratory set-up for the determination of saturated hydraulic conductivity**

$$K = l\,[\frac{\ln(h+l)/(h_1+l)}{(t-t_1)}] \qquad [4.1]$$

where,

L is the height of the soil column

h is the head of water on top of the soil column

t and t1 are the time at the beginning and end of the experiment.

4.2.1.2 Particle size distribution

The particle size distribution of composite samples of each soil was determined by the modified Bouyoucos Hydrometer method as described by Day (1965). A forty gram soil was weighed into a beaker after which 60 mL of 6% H_2O_2 was added to destroy the organic matter in the soil. One hundred millilitres of 5% calgon (sodium hexametaphosphate) solution was added. The suspension was allowed to stand for about 10 minutes and then stirred with a mechanical stirrer for 30 minutes. The tests on each soil type were done in quadruplicates.

The suspension was then transferred into a graduated sedimentation cylinder with the help of distilled water from a wash bottle and made up to the 1 litre mark with distilled water. The temperature of the suspension was recorded after equilibration. The content of the cylinder was mixed thoroughly using a plunger and hydrometer readings taken 5 minutes and 5 hours thereafter.

The suspension was then poured directly onto a 47- µm sieve and the particles retained on the sieve washed thoroughly with water and dried in an oven at 105 ^{o}C for 24 hours. The dried samples were then weighed to represent the sand fraction. Blank hydrometer readings of sodium hexametaphosphate solution at 5 minutes and 5 hours were taken. The particle size distribution was then determined using the following formulae;

$$(\text{Clay} + \text{Silt})\% = \frac{\text{5 minute hydrometer reading}}{\text{Sample mass}} \text{ x } 100 \quad [4.2]$$

$$Clay\ (\%) = \frac{5\ hour\ hydrometer\ reading}{Sample\ mass}\ x\ 100 \quad [4.3]$$

Silt (%) = (Clay + Silt) % - Clay (%)

$$Sand\ (\%) = \frac{Oven\ dry\ mass\ (g) of\ particle\ retained\ on\ 47\ \mu m\ sieve}{Sample\ mass\ (g)}\ x\ 100 \quad [4.4]$$

The textural class of the soil was then determined using the USDA textural triangle.

4.2.1.3 Particle density

The particle density of four samples of each soil type were determined using the pycnometer method (Blake and Hartge, 1986). The weight of the empty pycnometer bottle was noted. Water was de-aerated by boiling at 100 ^{o}C and allowed to cool overnight. The pycnometer bottle was filled with the de-aerated water and the weight noted. The pycnometer was emptied of de-aerated water and 10 g of soil that had been sieved through a 2 mm wire mesh was weighed and poured into the empty pycnometer and the weight noted. The de-aerated water was then added to the soil in the pycnometer. The bottle was tapped gently to get rid of all trapped air bubbles and the weight noted. Particle density was calculated as:

$$\rho_s = \frac{\rho_w(W_s - W_a)}{[(W_s - W_a) - (W_{sw} - W_w)]} \quad [4.5]$$

where ρ_w is the density of water, W_s is the weight of pycnometer and soil sample, W_a is the weight of empty pycnometer, W_{sw} is the weight of pycnometer filled with soil and water and W_w is the weight of pycnometer filled with water.

4.2.1.4 Dry bulk density

The surface of the soil was cleaned and a 5 cm diameter core sampler of known mass (M_1) and volume (V) was driven 5 cm into the soil surface. To avoid compaction, another core sampler was placed on the one in the soil such that its end was directly on that of the one in the soil and hammered. The soil around the core sampler was excavated and excess soil trimmed from its ends. The tests were done in quadruplicates for each soil type. The core sampler containing the soil was put in an oven at 105 ^{o}C for 48 hours after which it's mass (M_2) recorded. The dry bulk density (ρ_b) of each soil sample (0 – 20 cm depth) was calculated from the relation:

$$\rho_b = \frac{M_2 - M_1}{V} \qquad [4.6]$$

4.2.1.5 Soil moisture content

The volumetric soil moisture content at field capacity was determined in the laboratory according to the method of Phogat *et al.*, (1999). A 1000 g soil sample was packed into a 1.8 L cylindrical plastic pot with drainage holes underneath. For each soil type, four replicates were used. Water was added until the soil became saturated and began to drain from the bottom. The wet soil with the surface covered with plastic sheet to prevent evaporation was allowed to drain for 48 hours (until drainage ceased). The gravimetric moisture content at field capacity was then determined by taking a measured amount of soil from the pot into a moisture can (M_1). The total mass of moist soil and moisture can (M_2) was taken. The sample was then dried in an oven at

105 ^{o}C for 24 hours and reweighed to record the mass of oven-dried sample (M_3). The gravimetric moisture content was determined using the following formula:

Moisture content $\theta_g = \frac{M_2 - M_3}{M_3 - M_1}$ [4.7]

The result obtained was then multiplied by the bulk density (ρ_b) relative to the density of water (ρ_w) to obtain the volumetric moisture content (θ_v), (Phogat *et al.*, 1999):

$$\theta_v = \frac{\theta_g \, x \, \rho_b}{\rho_w} \quad [4.8]$$

4.2.1.6 Soil Moisture Characteristics

The pressure plate apparatus was used in the determination of the soil moisture characteristics. This was used for the range of 300 cm to 15000 cm of the matric potential (ψ_m). Three replicate samples were taken for each soil type. The soils were packed into metal rings of diameter 5 cm and 5 cm deep to a pre-determined bulk density. One end of the sample was covered with a nylon cloth which was held in place by an elastic band. The samples were then placed in a tray filled with distilled water to a depth just below the top of the samples and allowed to completely saturate overnight. The saturated samples were subsequently placed on a pressure plate which had been pre-saturated. The pre-saturated pressure plate together with the completely saturated soil samples were then tightly screwed into the pressure chamber. A standard commercial pressure plate apparatus (Soil moisture Equipment Corp., Santa Barbara, CA, U.S.A) was then used to apply the specific pressures of (0.3, 1, 2, 5, 7, 10, 12 and 15 bars) to the soil samples.

For each pressure indicated, the sample was allowed to drain until no further drainage occurred indicating equilibrium between the pressure and the moisture status of the soil. At this point, the pressure was stopped and the pressure chamber opened to remove the samples for weighing.

After taking the moist weight, the samples were placed in an oven at 105 ^{o}C for 48 hours, removed and re-weighed to calculate the gravimetric water content at that matric potential. Afterwards, the volume of the cylinder was determined to enable the bulk density to be estimated and subsequently used in the computation of the volumetric water content of the sample. The procedure was repeated for all the indicated pressures and for all the four soil types. The range of successive measurements of soil wetness versus pressure were taken for both desorption and sorption of the soil moisture characteristics curve for each soil type.

4.2.2 Soil chemical properties

4.2.2.1 Soil pH

Soil pH was measured at a soil to water ratio of 1:1 using a MV 88 Pracitronic pH glass electrometer. Ten grammes (10 g) of the composite sample of each soil type was weighed into a 50 mL beaker and 10 mLs of distilled water added. The soil-liquid suspension was then stirred several times for 30 minutes. The suspension was then allowed to equilibrate to room temperature. Using buffer solutions of pH 4.0 and 7.0, a Hanna H19017 microprocessor pH meter was standardized. The standardized electrode was then inserted into the supernatant of the suspension to measure the pH of the soil sample. The pH determination was replicated four times for each soil sample. The procedure was repeated using10 mL of 1M KCl added to the 10 g soil instead of water, and pH of soil in 1 M KCl measured. This was also replicated three times for each soil sample.

4.2.2.2 Electrical conductivity

Electrical conductivity (EC) of the composite soil samples were determined by weighing twenty grams of soil into a 100 mL beaker and 20 mL of distilled water added. The mixture was stirred intermittently for about 30 minutes. The mixture was allowed to settle and the EC determined

using electrical conductivity meter (PCM3, Jenway). Four replicate samples were used for each soil type.

4.2.2.3 Soil organic carbon

The wet combustion method of Walkley and Black (1934) as modified by Allison (1965) was used to determine the organic carbon content of the composite soil samples. Ten millilitres of 0.167 M potassium dichromate ($K_2Cr_2O_7$) solution and 20 mL of concentrated sulphuric acid (H_2SO_4) were added to a 0.5 g soil which had been passed through a 0.5 mm sieve in an Erlenmeyer flask. The flask was then swirled to ensure full contact of the soil with the solution after which it was allowed to stand for 30 minutes. Four replicate samples of each soil type were used for this test. The unreduced $K_2Cr_2O_7$ remaining in solution after the oxidation of the oxidizable organic material in the soil sample was titrated with 0.2 M ferrous ammonium sulphate solution after adding 10 mL of orthophosphoric acid and 2 mL of barium diphenylamine sulphonate indicator from a dirty brown colour to a bright green end point. Standardization of the $K_2Cr_2O_7$ with the ferrous ammonium sulphate was done and the amount of organic carbon calculated by subtracting the number of moles of unreduced $K_2Cr_2O_7$ from the number of moles of $K_2Cr_2O_7$ present in the standardized titration.

4.2.2.4 Total nitrogen

The Kjeldahl method (Hesse, 1971) was used to determine total nitrogen. Two grams of air-dried soil were weighed into 250 mL Kjeldahl flasks and selenium catalyst and 5 mL of concentrated sulphuric acid added. The mixture was then heated on a digestion block until the digest became clear. The digest was then allowed to cool and transferred with distilled water into a 50 mL volumetric flask and made up to volume. A 5 mL aliquot of the digest was taken into a Markham distillation apparatus and 5 mL of 40% NaOH solution added. The liberated ammonia was

collected into 5 mL of 2% boric acid to which three drops of methyl red and methylene blue indicator mixture had been added. The distillate was back titrated against 0.01 M HCl to a purplish end point. The amount of total N was then calculated from the number of moles of HCl consumed in the back titration reaction. The tests were done in quadruplicates for each soil type.

4.2.2.5 Cation exchange capacity

Ten grams of the composite sample of each soil type was weighed into an extraction bottle and 100 mL of 1M ammonium acetate solution added. The bottle with its content was shaken for 30 minutes on a mechanical shaker. The content was filtered through a No. 42 Whatman filter paper and the sample leached four times with 25 mL of methanol to wash off excess ammonium. Thereafter another 25 mL of 1M acidified potassium chloride was used to leach the soil four times. A 5 mL aliquot of the leachate was taken into a Markham distillation apparatus and 5 mL of 40% NaOH solution added to distill. The distillate was collected into 5 mL of 2% boric acid to which three drops of methyl red and methylene blue indicator mixture had been added. The distillate was back titrated against 0.01 M HCl to a purplish end point. The cation exchange capacity in $cmol_c$ /kg soil was then calculated from the number of moles of HCl consumed in the back titration reaction. The determination was done in four replicates for each soil type.

4.2.2.6 Exchangeable basic cations

Exchangeable basic cations were determined by the Ammonium Acetate method. A 5 g air-dried composite soil sample was weighed into an extraction bottle and 50 mL of ammonium acetate solution (NH_4OAc. pH7) was added. The test was repeated four times for each soil type. The suspension was shaken on a mechanical shaker for one hour and the content filtered through a Whatman No. 42 filter paper into clean centrifuge tubes. Exchangeable calcium and magnesium

in the extract were determined using the Atomic Adsorption Spectrometer (AAS). Exchangeable sodium and potassium were determined using the flame photometer.

4.2.2.7 Exchangeable acidity

Ten grams of air-dried composite soil sample was weighed into a 100 mL extraction bottle and 50 mL of 1M KCl solution was added. The suspension was shaken on a mechanical shaker for 30 minutes. The suspension was then filtered through a No. 31 Whatman filter paper into clean plastic bottle. Twenty five (25) mL aliquot was pipetted into a 100 mL conical flask and 2-3 drops of phenolphthalein indicator added. The solution was then titrated to a permanent pink end point with 0.01 M NaOH. The volume of titre was recorded as titre for H^+ and Al^{3+}. Ten (10) mL of NaF was then added to the solution at the end point and back titrated against 0.01 M HCl until colourless end point was reached. The volume of titre was then recorded as titre for Al^{3+}. The test was done for four replicate samples for each soil type.

4.2.2.8 Available phosphorus

Available phosphorus was determined by the Bray and Kurtz method (1945). The test was done on four replicates for each soil type. Four grams of composite soil sample was weighed into an extraction bottle and 40 mL of extraction solution (0.03 M NH_4F in 0.025 M HCl) was added. The suspension was put on a mechanical shaker and shaken for 5 minutes. The suspension was removed from the mechanical shaker, allowed to stand for about 30 minutes and filtered through a Whatman No. 42 filter paper. The molybdate-ascorbic acid method of Murphy and Riley (1962) was used for the colour development. Ten mL aliquot of the filtrate was pipetted into a 50 mL volumetric flask. The pH of the aliquot was adjusted by adding a few drops of p-nitro phenol indicator and a few drops of 4 M NH_4OH until the solution turned yellow. Two mL of 'reagent B', made up of 1.056 g of ascorbic acid dissolved in another reagent 'reagent A'. (Reagent A

was made up of 12 g ammonium molybdate dissolved in 250 mL distilled water plus 0.2998 g of antimony potassium tartarate dissolved in 1000 mL of 5 M H_2SO_4, mixed thoroughly and made up to 2 L with distilled water). A blank was prepared using the aforementioned procedure but, without any soil extract. A calibrating standard phosphorus solution prepared by pipetting 5 mL standard phosphorus stock solution into a 50 mL volumetric flask, followed by colour development as outlined above, was used in calibrating the spectrophotometer. The intensity of the molybdate blue colour at a wavelength of 712 nm, was measured on the spectrophotometer and recorded. The phosphorus content of the sample was calculated using the relationship:

$$P(mg/kg) = \frac{(\text{sample spectrophotometer reading} - \text{blank reading}) \times (\text{vol. of extract})}{(\text{vol. of aliquot}) \times (\text{weight of soil})} \quad [4.9]$$

4.3 Horizontal infiltration experiment

For the horizontal infiltration experiment, a perspex column of length 36.5 cm and diameter of 2.8 cm was used. The set-up and equipment are similar to those used by Elrick *et al.* (1979) for a similar set of experiments. The column was assembled from sections made up of two lengths (Figs 4.3b and 4.3c). The inlet section (Fig 4.3a) had two snout openings, one for the inflow of solution into the column and the other for the escape of air during the experiment. The first section of the column had an O-ring which served to prevent the solution from seeping out of the column. The column was assembled such that the wider sections were closer to the inlet end and the thinner ones placed towards the end of the column to facilitate an accurate determination of water content of the wetting front. To ensure even arrangement of the sections, the column was aligned using thin metal rods. The frames of the column were thereafter put in place and tightened with screws (Fig 4.3d).

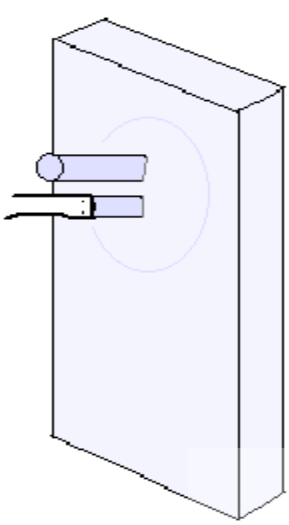

Fig. 4.3a Inlet section

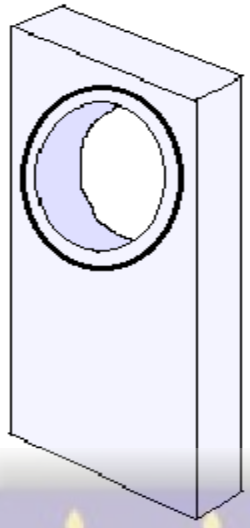

Fig. 4.3b First section with O-ring

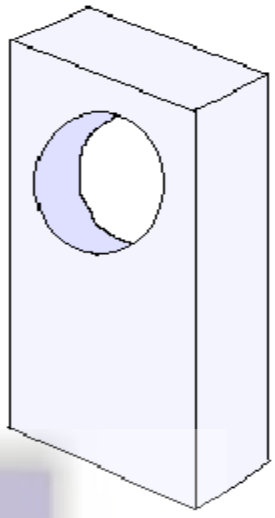

Fig. 4.3 c Wide section

Fig. 4.3 d Soil column set up for the horizontal infiltration experiment

After determining the moisture contents at field capacity for each soil type, the composite soil samples were then moistened with deionized water in order to adjust the initial moisture content to 0.1 m^3m^{-3} of the field capacity moisture content. The composite soils samples were then

packed into the column to a bulk density of 1.14 kg m^{-3}. This bulk density ensured an evenly distributed bulk density along the length of the column. Pouring the soil into the column evenly while tapping concurrently as the soil was being poured ensured that uniformity of packing the soil column was achieved. The soil was held in place by using a piece of cotton wool to hold it at the end of the column. For each soil type, three replicates were used.

The packed soil column was then connected by tubes to two 10 mL burettes placed horizontally at the level of the horizontal soil column (Slate 4.3.1). The inlet tube to the packed soil column was connected to a Marriott bottle containing a solution of either KCl or chloropyrifos and used for the required infiltration run. The burettes were filled to the zero mark at the start of the experiment. One of the two way valves connected to the burettes was then opened to allow the solution to flow into the soil column and a stop watch also started simultaneously. A port for the escape of air from the packed sol column was closed after 30 seconds.

Water was applied at the initial time t = 0 to one end of the sample (x = 0) under constant-head arrangement by means of the Marriot device. A fine plastic screen was used at both ends of the column to prevent the soil from dispersing during the experiment. The water pressure entering the column was controlled by means of valves which were connected to transparent plastic tubes linking the Marriot bottle and the burettes to the perspex column containing the packed soil. Continuous monitoring of the water entering the soil column was made possible by the Marriot-burette-plastic tube arrangement. Distance to the wetting front with time was observed visually based on obvious colour differences at the interface of wet and dry soil (Wang *et al*. 2004; Shao and Horton 1998).

Plate 4.3.1 Set-up for the horizontal infiltration experiment

The cumulative volume of solution into the packed soil column as well as the distance of the wetting front as a function of time were then recorded for each infiltration run. To ensure continuous flow of solution into the packed soil column, the burettes were regulated in such a way that when one burette ran out of solution, it was closed at the 10 mL mark, and the other burette opened immediately for flow to continue into the soil. The empty burette was then re-filled from the Marriot bottle while flow was continuing into the packed soil column from the other burette. Continuous flow of solution into the horizontal soil column was therefore ensured by this arrangement. On the assumption that adsorption is instantaneous, the infiltration runs were done up to a maximum of 60 minutes but, terminated at different elapsed times (viz. 30, 45 and 60 minutes).

4.3.1 Determination of Cl^- content in soil solution

Known weights of one-third of the wet soil subsamples from each section of the infiltration column were placed in 100 mL extraction bottles. Fifty (50) mL of deionised water were then

added to each extraction bottle and the bottles were shaken in a mechanical shaker for about 60 minutes to allow for the dissolution of the chloride. The content of the tubes were then centrifuged and the supernatant decanted for the determination of the chloride ion concentration using an ELIT 9808 ion analyser.

4.3.2 Determination of K^+ content in soil solution

Known weights of one-third of the wet subsamples from each section of the infiltration column were placed in 50 mL centrifuge tubes. Ten millilitres of 1.0 M Ammonium Acetate solution at pH 7 was then added to each tube. The tubes were then tightly covered and shaken in a mechanical shaker for 30 minutes. The suspension was then centrifuged and the supernatant solution decanted. The concentration of K^+ in the supernatant solution was determined using the flame photometer.

The concentration of K^+ represented that antecedent in the soil and that from the infiltrating solution. The concentration of K^+ adsorbed on the exchange site was estimated by subtracting the equilibrium concentration from the initial K^+ concentration of the infiltration solution.

4.3.3 Determination of Chlorpyrifos in Soil

This method is applicable for the quantitative determination of Chlorpyrifos [O, O-diethyl-O-(3,5,6-trychloro-2-pyridinyl) phosphorothioate] in soil at a validated lower level of quantification of 0.01 – 10.0 µg/g (USEPA, 1999). The principle behind the determination is that; residues of Chlorpyrifos are extracted from soil with acidic acetone. A portion of the acetone solution is concentrated, acidified water is added, and Chlorpyrifos is partitioned into a known volume of hexane. A portion of the hexane extract is analyzed by gas Chromatograph using flame photometric detection.

A known weight of soil containing chloropyrifos which had been thoroughly mixed was weighed into an extraction bottle. Twenty (20) mL of acidified acetone (98 % acetone, 1 % phosphoric acid and 1 % water) was added to the sample. The bottles were capped and put in a mechanical shaker for 30 minutes at 280 excursions per minute. The sample was then centrifuged at approximately 2500 rpm for 5 minutes. Ten mL of the supernatant was transferred into a culture test tube and evaporated to 3 mL in a water bath (set at a temperature between 40 – 45 ^{o}C) under a stream of nitrogen. Ten (10) mL of 1 % phosphoric acid was added to the concentrated acetone solution and transferred to another vial. The culture tube was rinsed with an additional 10 mL of 1 % phosphoric acid solution and combined with the prior solution.

The 20 mL solution was extracted with 2.0 mL of hexane by shaking for 15 minutes after which it was centrifuged for another 5 minutes at approximately 2500 rpm. Using a glass pipette, 1 mL of the hexane solution was transferred into an injection vial containing a vial insert after which it was sealed with a cap. The chloropyrifos content in the hexane was then determined using the gas chromatograph.

4.4 Computer Programming Method used to analyse data

Continuous Systems Modeling Programme (CSMP) (IBM, 1972) was used for the computation of the soil moisture diffusivity $D(\theta)$, the dispersion coefficients $\wp_{Cl}$, $\wp_K$ and $\wp_{Cf}$, and the notional planes of the moisture content and that of the solutes. The statements of CSMP are similar to those of FORTRAN.

The structure of the CSMP programme consists of three segments: INITIAL, DYNAMIC and TERMINAL. To run the model, data statements and calculations that are required to be performed once during a simulation process can conveniently be placed in the initial segment.

Operations that are performed repeatedly and updated for each elapsed time interval are placed in the DYNAMIC section. The DYNAMIC section is usually made up of structure statements that clearly describe a set of differential equations. In the TERMINAL section of the program control statements or calculations that should be performed at the completion of the simulation are placed. Segmenting a programme is not mandatory in CSMP. However, if a programme is not segmented, the computer automatically assumes the entire programme to be DYNAMIC.

At the terminal segment of the CSMP programme a CALL RERUN statement is placed there to perform the function of recycling the programme through additional runs with new parameters. A detailed description and explanation of the principles and procedures of CSMP have been provided by Brennan and Silberberg (1968) and Speckhart and Green (1976). Powerful and important features of CSMP which make it particularly amenable to this study are the statements which cause:

integration to be performed with time and

differentiation to be performed with respect to time.

The general forms of the statements for these mathematical operations are:

Y = INTGRL (IC, X) [4.11a]

X = DERIV (IC, Y) [4.11b]

In equation (4.11a) the output variable, Y is calculated by integrating the differential function X with the initial condition that Y at the start of the computation is equal to IC.

A METHOD statement enables a choice to be made from seven numerical integration techniques. Two of the integration techniques use a variable time step of integration while the

others use a fixed time step of integration. In equation (4.11b), the derivative output X is calculated by differentiating the integral function Y with the initial condition that X at the start of computation is equal to IC. Another feature of CSMP used frequently in this study is the calculation of definite integrals which were performed by instructing the computer to use the final time step value of the variable integration. This specification was put in the TERMINAL section.

4.4.1 Description of the computer programme for calculating the soil moisture diffusivity D (θ)

Appendix G gives the programme used to calculate the soil moisture diffusivity resulting from the horizontal infiltration experiment. The governing equations are equations [3.7] and its solution [3.9]. In the CSMP integration is performed with respect to time. Time was therefore renamed as lambda (line 3 of Appendix G) to enable integration to be performed with respect to lambda. The integral $\int_{\theta_n}^{\theta} \lambda d\theta$ in equation (3.9) was thus re-written to enable integration to be done with respect to λ instead of θ, using integration by parts.

Using integration by parts $\int_{\theta_n}^{\theta} \lambda d\theta$ in equation [3.9] becomes (see Appendix D):

$$\int_{\theta_n}^{\theta} \lambda d\theta = \theta\lambda - \theta_n\lambda_n + \int_{\lambda_n}^{\lambda} \theta d\lambda \qquad [4.12a]$$

Since integration by the computer programme necessarily commences from $t = 0$ (in this case, $\lambda = 0$), $\int_{\lambda_n}^{\lambda} \theta d\lambda$ in equation [4.12a] was re-written to enable integration to start at zero as follows:

$$\int_{0}^{\lambda_{n\to\infty}} \theta d\lambda = \int_{0}^{\lambda} \theta d\lambda + \int_{\lambda}^{\lambda_{n\to\infty}} \theta d\lambda \qquad [4.12b]$$

Therefore, equation (4.12a) becomes:

$$\int_{\theta_n}^{\theta} \lambda d\theta = \theta\lambda - \theta_n\lambda_n + \int_0^{\lambda\to\infty} \theta d\lambda - \int_0^{\lambda} \theta d\lambda \qquad [4.12c]$$

The INITIAL section (lines 2-13) of the computer programme in Appendix G, first renames time = lambda (line 3), then the moisture content at $\lambda = 0$ called THETAO was set at the initial moisture content, θ_n called THETAN and λ_n called LAMDAN were set at the final moisture content and the final time respectively. Iteration counter, J is set to zero and $\frac{d\theta}{d\lambda}]_{\lambda\to 0}$ called THLAO is given the value -40. Because the definite integral $\int_0^{\lambda\to\infty} \theta d\lambda$ is not initially known, it is designated KON2 and given the value 1.0.

After the first iteration, instruction in the TERMINAL section (KON2=C) allows the computer to use the last value of $\int_0^{\lambda} \theta d\lambda$ to replace the initial value of 1.0 assigned to it. Function THETA specifies values of λ in ascending order and their corresponding θ values.

The DYNAMIC section (lines 14 - 21) immediately follows the INITIAL section and specifies the formulation to be used and calculations to be done. The acronym THLA is a non-linear function generator (NLFGEN) to interpolate the θ and λ values given in the FUNCTION THETA in the INITIAL section. Also, DTHLA is the derivative $\left[\frac{d\theta}{d\lambda}\right]$. Here, the initial value of the $\theta(\lambda)$ slope at $\lambda = 0$ is specified as THLAO in the INITIAL section and used to start the calculations. The letter C represents the variable integral $\int_0^{\lambda} \theta d\lambda$. Lines 18 and 19 calculate $KON1(= \theta_n\lambda_n)$ and $(THLA * LAMBDA) = \theta\lambda$. Therefore, $E = (THETA * LAMBDA) - KON1$ is computed. Finally, soil moisture diffusivity is calculated with the statement in line 20, that is;

$-0.5 * (E + KON2 - C)/DTHLA.$

4.4.2 Description of computer program for calculating dispersion coefficient for Chloride ion ($\wp_{Cl}$.)

The programme used to calculate the dispersion coefficient for chloride ($\wp_{Cl}$) is shown inAppendix H. The governing differential equation is equation [3.28a] and its solution equation [3.30a]. In order for integration in CSMP to be performed with respect to lambda (the dependent variable), time was renamed lambda (line 3 of Appendix H). Two sets of functions are provided in the function statement namely, $THETA[=\theta(\lambda)$ and $SEE[=C_{Cl}(\lambda)]$. The INITIAL section (lines 2-18) of Appendix H contains the moisture and solute contents at $\lambda = 0$ called $THETA0\ and\ SEE0$respectively, the initial moisture content, called $THETAN$ (θ_n), as well as λ_n called $LAMBDAN$. The iteration counter (J) is set to zero and the differentials $\frac{d\theta}{d\lambda}]_{\lambda\to 0}$ called $THLA0$ and $\frac{dC^{Cl}}{d\lambda}]_{\lambda\to 0}$ called $SEELA0$ are assigned the respective values. Because the definite integral $\int_0^{\lambda\to\infty}\theta d\lambda$ is not initially known, it was designated as KON2 and assigned a value 1.0. After the first iteration, instructions in the TERMINAL section (KON2=C) allows the computer programme to use the last value of $\int_0^{\lambda}\theta d\lambda$ to replace the initial value of 1.0. The statements $FUNCTION\ THETA$ and $FUNCTION\ SEE$ specify values of λ in ascending order and their respective θ and Cl^- values.

Two parts make up the DYNAMIC section (lines 22-36), viz:

a. the moisture component (lines 23-28) which is similar to that in section 4.3.1 and
b. the chloride (solute) component (lines 29-36).

The moisture section calculates $D(\theta)$ as described in section 4.3.1. In order to enable the integration to start at $\lambda = 0$, the integral $\int_{\lambda_{n\to\infty}}^{\lambda} g(\theta)\frac{dC^{Cl}}{d\lambda}d\lambda$ in equation (3.30a) was re-written as follows;

$$\int_{\lambda_n\to\infty}^{\lambda} g(\theta)\frac{dC^{Cl}}{d\lambda}d\lambda = \int_0^{\lambda\to\infty} g(\theta)\frac{dC^{Cl}}{d\lambda}d\lambda - \int_0^{\lambda} g(\theta)\frac{dC^{Cl}}{d\lambda}d\lambda \quad [4.13]$$

The derivative $\frac{dC^{Cl}}{d\lambda}$is designated as Cl. The, $\frac{dC^{Cl}}{d\lambda}]_{\lambda\to 0}$ is specified as $SEELA0$ in the INITIAL section to enable calculations of the derivatives to be started. From the governing equations, $LATHH\left(=\theta\lambda + 2D(\theta)\frac{d\theta}{d\lambda}\right)$ represents $g(\theta)$ [refer to equation [3.28d] and HS is the variable integral. $(=\int_0^{\lambda} g(\theta)\frac{dC^{Cl}}{d\lambda}d\lambda)$.Lines 34 and 36 calculate $GS = C1 * LATHH$ and $HS1 = KON3 - HS$ respectively, where $KON3 = [\int_0^{\lambda\to\infty} g(\theta)\frac{dC^{Cl}}{d\lambda}d\lambda]$ is a definite integral which was not initially known and was therefore given a value 1.0. After the first iteration, instructions in the TERMINAL section making $(KON3 = HS)$ allow the computer to use the last value of $\int_0^{\lambda} g(\theta)\frac{dC^{Cl}}{d\lambda}d\lambda)$ to replace the initial value of 1.0. Finally, the dispersion coefficient of chloride, $\wp_{cl}$ is calculated with the statement $DS = THDS/THLA$ (line 33), where $THDS = (\theta\wp_{cl})$is computed in line 32, i.e. $THDS = 0.5 * HS1/C1$.

4.4.3 Description of computer program for calculating dispersion coefficient for Potassium ($\wp_{K^+}$)

The programme used to calculate the dispersion coefficients of potassium for the soils during horizontal infiltration is shown in Appendix I. The same programme was used for the calculation of the dispersion coefficients for chlopyrifos where the concentrations as functions of λ were substituted for those of K^+ in lines 13-22. The program consists of two parts, namely,

a. the moisture component (lines 24-30) which is similar to that in Appendix G and explained in section 4.6.1 and
b. the solute (insecticide/cation) component (lines 31-43).

The INITIAL section (lines 2-22 of Appendix I) contains the moisture and solute contents at $\lambda = 0$ called $THETA0$ and $SEEK0$ respectively, the initial moisture content, θ_n called $THETAN$, as well as λ_n called $LAMDAN$. Iteration counter J is set to zero and the differentials $\frac{d\theta}{d\lambda}]_{\lambda\to 0}$ called $THLA0$, $\frac{dC^K}{d\lambda}]_{\lambda\to 0}$ called $SKLA0$ and $\frac{dS^K}{d\lambda}]_{\lambda\to 0}$ called $SBKLA0$ are assigned theirrespective values. Because the definite integral $\int_0^{\lambda\to\infty}\theta d\lambda$and $\int_0^{\lambda\to\infty}\left[g(\theta)\frac{dC^K}{d\lambda}+\rho\lambda\frac{dS^K}{d\lambda}\right]d\lambda$are not initially known, they are designated as $KON2$ and $KON3$ respectively with the initial value of 1.0. After the first iteration, instructions in the TERMINAL section ($KON2 = C\ and\ KON3 = B1$) allow the computer programme to use the last values of $\int_0^{\lambda\to\infty}\theta d\lambda$ and $\int_0^{\lambda\to\infty}\left[g(\theta)\frac{dC^K}{d\lambda}+\rho\lambda\frac{dS^K}{d\lambda}\right]d\lambda$ to replace the initial value of 1.0 assigned to them. $FUNCTION\ THETA, FUNCTION\ SEEK$ and $FUNCTION\ SORBK$ specify values of λ in ascending order and their respective $\theta, C^K\ and\ S^K$values.

In the DYNAMICsection (lines 23-43) the formulas used as well as the calculations done are specified. The water flow equations which calculate $D(\lambda)$ are as explained in section 4.3.1. The governing equation for the calculation of the dispersion coefficient for potassium ($\wp_K$) in Appendix I is equation (3.28b) and its solution (3.30b). Time was renamed lambda (line 3 of Appendix I) so that integration in CSMP could be performed with respect to lambda. The integral $\int_{\lambda_{n\to\infty}}^{\lambda}\left[g(\theta)\frac{dC^K}{d\lambda}+\rho\lambda\frac{dS^K}{d\lambda}\right]d\lambda$ in equation (3.30c) was re-written as follows:

$$\int_{\lambda_{n\to\infty}}^{\lambda}\left[g(\theta)\frac{dC^K}{d\lambda}+\rho\lambda\frac{dS^K}{d\lambda}\right]d\lambda=\int_0^{\lambda\to\infty}\left[g(\theta)\frac{dC^K}{d\lambda}+\rho\lambda\frac{dS^K}{d\lambda}\right]d\lambda-\int_0^{\lambda}\left[g(\theta)\frac{dC^K}{d\lambda}+\rho\lambda\frac{dS^K}{d\lambda}\right]d\lambda$$

[4.13]

The acronyms and the algorithms for $THLA, DTHLA, C, KON1$, E, all for the computation of D in the moisture flow section are similar to that previously described in section 4.3.1 and Appendix G. For the solute (K^+) component (lines 31-43), $DSS=\left(\frac{dS^K}{d\lambda}\right)$and $DSEEK=\left(\frac{dC^K}{d\lambda}\right)$ are derivatives of $S^K(\lambda)$and$C^K(\lambda)$. The initial values of the slopes of $S^K(\lambda)\ and\ C^K(\lambda)$ at $\lambda=0$ are specified as $SBKLA0\ and\ SKLA0$ respectively in the INITIAL section. These values facilitate the commencement of the computation of the derivatives. The acronym $B1$ in line 40 of Appendix I is the variable integral $\int_0^{\lambda}\left[g(\theta)\frac{dC^K}{d\lambda}+\rho\lambda\frac{dS^K}{d\lambda}\right]d\lambda$. Lines 35 and 39 calculate $E1=LAMBDA*RHO*DSS$ and $B=(G*DSEEK)+E1$ respectively. During the infiltration experiment, the soil was packed to a uniform bulk density (ρ) of 1.14 kg m^{-3}, therefore the term RHO in the computer programme statement (line 35) assumes this constant value. Thereafter, line 41 calculates $Y=-0.5*(KON3-B1)$where $3=\int_0^{\lambda\to\infty}\left[g(\theta)\frac{dC^K}{d\lambda}+\rho\lambda\frac{dS^K}{d\lambda}\right]d\lambda$. Finally, the dispersion coefficient of chlopyrifos, ($\wp_K$) is calculated with the statement $DS=THDS/THLA$(line 43), where $THDS=(\wp_K)$ is computed in line 42 ($i.e., THDS=Y/DSEEK$).

4.4.4 Description of computer program for calculating notional planes

The notional plane about which salt dispersion occurs is defined by Smiles and Phillip (1978), Elrick *et al.* (1979) and subsequently Laryea *et al.* (1982) as:

$$\int_0^{\lambda}(C_0-C)d\lambda=\int_{\lambda}^{\infty}(C-C_n)d\lambda \qquad [4.14]$$

On the assumption that the encroaching solution perfectly displaces the antecedent solution in the soil column during horizontal infiltration, another plane $\lambda=\lambda'$ which defines the plane of

separation is described by the material balance equation defined by Smiles and Phillip (1978) and subsequently Elrick *et al.* (1979) and Laryea *et al.* (1982)as;

$$\theta\lambda^* = \int_{\theta_n}^{\theta(\lambda)^*} \lambda d\theta \qquad [4.15]$$

The programme used to calculate the notional planes for θ, Cl^-, $K^+$and chlopyrifos is shown in Appendix J. Time was renamed to equal lambda (line 3 of Appendix J) so that integration in CSMP is performed with respect to lambda. In order for integration to be done with respect to λ, as well as for it to start from time=0, integration by parts (see Appendix D) was used to recalculate equation [4.15] using:

$$\theta_n\lambda_n = \int_0^{\infty} \theta d\lambda - \int_0^{\lambda} \theta d\lambda \qquad [4.16]$$

Equation [4.14] was also re-written resulting in:

$$\int_0^{\lambda}(C_0 - C)d\lambda = \int_0^{\infty}(C - C_n)d\lambda - \int_0^{\lambda}(C - C_n)d\lambda \qquad [4.17]$$

The INITIAL section (lines 2-28 of Appendix J) contains the moisture and solute (Cl^-, K^+ or chlopyrifos) contents at λ = 0 called $THETA0$, $SEE0, SEEK0$ *and* $SEEF0$ respectively. The initial moisture content, θ_n designated$THETAN$ and λ_n called $LAMDAN$. The iteration counter J is set to zero and the differentials $\frac{d\theta}{d\lambda}]_{\lambda\to 0}$ called $THLA0$,$\frac{dC^{Cl}}{d\lambda}]_{\lambda\to 0}$ called $SEELA0$, $\frac{dC^{K}}{d\lambda}]_{\lambda\to 0}$ called $SKLA0$ are assigned their respective values accordingly. Because the definite integral $\int_0^{\lambda\to\infty} \theta d\lambda$and $\int_0^{\lambda\to\infty}(C - C_0)d\lambda$are not initially known, they are named $KON1$ *and* $KON2$for Cl^- or K^+ respectively and given the value 1.0. After the first iteration, instructions in the TERMINAL section reassigns $KON1 = C$ *and* $KON2 = B2$ so that the last values of $\int_0^{\lambda\to\infty} \theta d\lambda$and $\int_0^{\lambda\to\infty}(C - C_0)d\lambda$ are assigned to Cl^- *or* $K^+$to replace the initial value of 1.0.

FUNCTION THETA, FUNCTION SEE and FUNCTION SEEK specify values of λ in ascending order and their respective$\theta, C^{Cl}\ and\ C^{K}$values.

The DYNAMIC section (lines 29-55) specifies the formulas used and the computations done. Considering the notional plane for moisture content (lines 30-34), $THLA$, and $C = (\int_0^{\lambda} \theta d\lambda)$ are similar to those previously described in 4.3.1. The acronyms$E1 = (\theta\lambda)$, $E2 = (\theta\lambda - \theta_n\lambda_n + \int_0^{\infty} \theta d\lambda - \int_0^{\lambda} \theta d\lambda)$ and $KON1 = (\int_0^{\infty} \theta d\lambda)$ were used (lines 32-33). Finally, the notional plane for the moisture content profile is calculated with the statement $E3 = (THETAN - LAMBDAN) - KON1 + C$ (see equation 4.16). At the notional plane (λ^*), E3≈0.

The same formulae were used for the notional planes for all the solutes (i.e. Cl^-, K^+ or chlopyrifos). Considering the example for chloride (lines 35-41), $A = (\int_0^{\lambda}(C_0 - C)d\lambda$i.e. the left hand side of equation [4.17], $B2 = (\int_0^{\lambda}(C - C_n)d\lambda$and.$KON2 = (\int_0^{\infty}(C - C_n)d\lambda$. The notional plane is then calculated with the statements $B3 = KON2 - B2$ and finally, $B4 = A - B3$which should equal 0 at the notional plane. The other solutes (i.e. K^+chlopyrifos) use the same format as described for chloride.

4.5 Statistical analysis

The physico-chemical properties of the different soils, the distance to the moisture and solute fronts as well as the moisture and agrochemical concentration profiles were set in a completely randomized design with the treatments replicated three times. The combined data from each test were subjected to ANOVA and in most cases to an LSD comparison of the treatment means.

CHAPTER FIVE

RESULTS AND DISCUSSION

5.1 General Characteristics and Description of Soils

Four soil samples were used in this study. The soils were made up of a sandy loam from the tropical rain forest zone of the Western Region of Ghana and classified as Xanthic Ferrasol (Dwomo and Dedzoe, 2006). A sandy clay, sampled from the Coastal Savannah zone of the Accra plains and classified as Eutric Vertisol, Asiamah, (1995) was used in this study. Two other sandy loams, classified as a Ferric Lixisol and Eutric Gleysol by Adu and Mensah-Ansah, (1995) which were sampled from the transitional zone of the Afram plains in the Eastern Region of Ghana make up the list of the soils used in this study. Some of the physical and chemical properties of the soils are indicated in Tables 5.1.1 and 5.1.2 respectively.

The sand fractions differed significantly (P = 0.05) among the various soil samples. The Ferrasol and Lixisol have very high sand fractions (more than 70 %), indicating that they are well-drained soils. The proportion of silt in the Ferrasol and Lixisol are however low, and not very different from that of the Vertisol. Although the Gleysol has very high silt content which is more than twice the proportion in the other soils (P = 0.05), its clay content is not very different from that of the Ferrasol and Lixisol. The high sand content and the low clay fractions of these three soils which are mostly low activity clays, coupled with the prevailing temperatures suggest a fast decomposition and low retention of added organic matter. Consequently, soil organic matter and therefore organic carbon content of the soils are very low with a resultant low total nitrogen content of 0.5 and 0.8 mg/kg for the Lixisol and Gleysol respectively (Table 5.1.2).

Table 5.1.1 Some physical properties of the soils

Soil Series	Sand	Silt	Clay	Texture	θ_{fc}	θ_s	θ_r	ρ_s	ρ_b	Ks
	----------% ----------				----------g/g----------					(m/s)
Eutric Vertisol	**55.02**	9.14	**35.84**	Sandy Clay	**0.457**	0.497	**0.05**	2.76	1.28	4.70×10^{-7}
Xanthic Ferrasol	**70.94**	8.23	**20.83**	Sandy Loam	**0.272**	0.409	**0.013**	2.60	1.32	4.42×10^{-5}
Ferric Lixisol	**79.84**	4.33	**15.83**	Sandy Loam	**0.231**	0.271	**0.007**	2.63	1.42	4.71×10^{-5}
Eutric Gleysol	**61.45**	21.05	**17.50**	Sandy Loam	**0.291**	0.304	**0.008**	2.62	1.33	4.50×10^{-5}

θ_{fc} = Moisture content at field capacity; θ_s = Saturated moisture content; θ_r = Residual moisture content

ρ_s = Particle density; ρ_b = Bulk density; Ks = Saturated hydraulic conductivity

Table 5.1.2 Some chemical properties of the soils

Soil Series	pH		EC	N	OC	Avail. P	Na	K	Ca	Mg	CEC	AEC	Ex.Acid
	H_2O (1:1)	KCl (1:1)	μScm^{-1}	---------g kg^{-1}---mg kg^{-1}-----			---------- $cmol_c$ kg^{-1} ----------						
Eutric Vertisol	**6.6**	6.2	**616.7**	1.1	**12.0**	13.01	**0.45**	0.16	**19.0**	6.97	**30.48**	22.98	**1.74**
Xanthic Ferrasol	**4.1**	3.4	**200.7**	1.3	**26.3**	6.94	**0.42**	0.46	**2.64**	0.97	**9.07**	52.70	**4.93**
Ferric Lixisol	**5.9**	5.6	**308.0**	0.5	**6.8**	8.23	**0.23**	0.10	**0.27**	0.24	**3.90**	33.87	**1.41**
Eutric Gleysol	**5.8**	5.5	**601.3**	0.8	**8.9**	6.34	**0.32**	0.20	**3.53**	1.28	**7.02**	31.52	**1.35**

EC = Electrical conductivity; OC = Organic carbon; Avail. P = Available phosphorus; Ex. Acid = Exchangeable acidity

CEC = Cation exchange capacity; AEC = Anion exchange capacity; Ex. Al = Exchangeable aluminum

Table 5.1.3 Moisture content at field capacity and permanent wilting point of the soils used in the horizontal infiltration experiment

Soil	FC (g/g)	AWC (g/g)	PWP (g/g)
Eutric Vertisol	0.26	.14	0.12
Xanthic Ferrasol	0.15	.05	0.10
Ferric Lixisol	0.12	.08	0.04
Eutric Gleysol	0.17	.13	0.04

FC = Field Capacity; AWC = Available Water Capacity; PWP = Permanent Wilting Point

and therefore expected to have a high cation exchange capacity as indicated by Amatekpor and Dowuona, (1995). The CEC of 30.48 $cmol_c/kg$ coupled with organic carbon content of 12.0 g/kg ties in very well with its high clay content. Inferring from the textural triangle, the Eutric Vertisol is classified as sandy clay whilst the Xanthic Ferrasol, Ferric Lixisol and Eutric Gleysol are all classified as sandy loam soils.

Being sandy clay, the Vertisol has a high moisture content at field capacity of about 0.26 (g/g), which is respectively about 1.7 and 1.5 times that of the Ferrasol and Gleysol and more than twice that of the Lixisol. This gives an indication that the Vertisol has a higher water holding capacity than the other soils. As expected, the available water capacity expressed as the difference between the moisture content at field capacity (33kPa) and permanent wilting point

(1500 kPa) of the Vertisol was about twice that of the Ferrasol and more than one and half times more than the Lixisol, although not very different from that of the Gleysol (Table 5.1.3). The Vertisol had a saturated water content of 0.497 (g/g) which, was respectively about one and half and twice higher than that of Gleysol and Lixisol. The saturated hydraulic conductivity, which gives an indication of the soils ability to conduct water, is more than a hundred fold lower in the Vertisol relative to that of the other soils. This is an indication that the Vertisol is poorly drained which, is in conformity with the soil's high clay content. Due to its relatively high clay content, it is not surprising that the saturated hydraulic conductivity in the Vertisol is low compared to that of the other soils, which have relatively higher proportions of sand. Being a sandy clay, the saturated hydraulic conductivity of the Vertisol was larger than the range (10^{-10} – 10^{-8} m s^{-1}) indicated for most clay soils (Hillel, 2004).

The pH range of the soil samples in Table 5.1.2 indicates strongly acidic to neutral conditions for the soils (Landon, 1991). The pH in water of 4.1 for the Ferrasol, indicates that it is strongly acidic compared to that of the Lixisol and Gleysol which were slightly acidic (Landon, 1991). The Vertisol however recorded a pH within the neutral range (Landon, 1991). The strongly acidic pH of the Ferrasol may be due to the fact that it is highly weathered and located in an area of very high rainfall (Table 4.1). The high rainfall regime of the environs where the soil sample was obtained would promote leaching of bases with a consequential predominance of acidic cations Al^{3+} and H^{+} and a concomitant decrease in pH. Additionally, the Ferrasols are noted to have appreciably high levels of oxides and hydroxides of Fe and Al (Shamshuddin *et al.*, 2011). At the extremely acidic pH as indicated in the soil, the oxides of iron and aluminum will be protonated and this may in part account for the high anion exchange capacity of 52.7 $cmol_c$ kg^{-1}(P = 0.05) in the Ferrasol. The pH of the 1:1 soil to KCl ratio ranged between 6.2 for the

Vertisol to 3.4 for the Ferrasol. The difference in pH in water and KCl however suggests the presence of net negative charges at the colloidal surface of all the soil samples.

With the notable exception of the Vertisol, the sum of basic cations in most of the soils was very low. As expected, the CEC of the Vertisol was significantly high (P= 0.05) with most of the soils having CEC values less than 10 $cmol_c\ kg^{-1}$. Due to its comparatively higher clay content that are mostly montmorillonitic Dowuona (1985), the Vertisol is expected to have higher negative charges and therefore a corresponding higher capacity for exchangeable cations. It is therefore not surprising that its cation exchange capacity was more than three times higher than that of the other soils.Despite its high sand content the Ferrasol's soil organic carbon (SOC) content is more than twice that of the Vertisol. This may be attributed to the fact that the Ferrasol was sampled from a forest reserve with high litter fall.

5.2 Soil moisture and agrochemical concentration profiles from horizontal infiltration

The moisture content (θ) and concentration profiles of chloride, potassium and chlopyrifos from the horizontal infiltration experiments on the four soils are presented in Figures 5.2.1, 5.2.2, 5.2.3 and 5.2.4, respectively. The horizontal infiltration experiments were done for each moisture content and the respective solute (KCl and chlopyrifos) concentrations taken, at 30, 45 and 60 minutes in each soil sample. A scaling factor ($\lambda = xt^{-1/2}$) was used to transform the distance (x) to (λ). The curves of best fit were drawn by eye after the transformation. It was hypothesized that if equation [3.7] in the theory (Chapter 3) subject to equations [3.8a] and [3.8b] and equations [3.28a to 3.28c] subject to equations [3.29a and 3.29b] were valid, the $\theta, C^{Cl}, C^{K}, C^{Cf}$ and the corresponding amounts adsorbed per kg (S) will be unique functions of $\lambda = xt^{-1/2}$. The uniqueness of $\theta(\lambda), C^{Cl}(\lambda), C^{K}(\lambda), C^{Cf}(\lambda), S^{K}(\lambda)$ and $S^{Cf}(\lambda)$ are then used to obtain the dispersion coefficients of the ions and insecticide. The use of the Boltzmann variable (λ) in the

scaling of the moisture and agrochemical profiles to preserve similarity has been well established by Smiles *et al.* (1978), Elrick *et al.* (1979) and Laryea *et al.* (1982). It must be indicated that in the horizontal infiltration experiment, similarities in the moisture, Cl^-, K^+ and chlopyrifos profiles were preserved reasonably well as shown in Figures 5.2.1, 5.2.2, 5.2.3 and 5.2.4. Variability in packing the soil columns and problems associated with air entrapment during the infiltration experiments most likely accounted for the variability in data observed in Figs. 5.2.1 to 5.2.4.

The soil moisture content at $\lambda = 0$ during the horizontal infiltration experiments for the various soil samples is presented in Table 5.2.1. A look at the moisture content at $\lambda = 0$ in the moisture profiles indicate that the Lixisol had the lowest value. The moisture content at $\lambda = 0$ was in the order Vertisol > Ferrasol > Gleysol > Lixisol ($P = 0.05$). At the moisture content of $\lambda = 0$ the Vertisol, Ferrasol and Gleysol were respectively, 1.4, 1.3 and 1.2 times more than that of the Lixisol. This lower moisture content recorded in the Lixisol may be attributed to its high sand fraction (≈ 80%), low clay content and a very low organic carbon content of 6.8 g kg^{-1} which do not allow for greater moisture retention. Although the Ferrasol had a similar texture (sandy loam) as the Lixisol and the Gleysol, its high organic carbon content may have contributed to the high moisture content at $\lambda = 0$. The extent of infiltration, expressed as the distance to the wetting front when movement of water in the soils were measured during the horizontal infiltration experiments, was compared in the soils used in this study. Table 5.2.2 presents the average distance to the moisture and agrochemical concentration fronts in the soils during the horizontal infiltration experiments. It was observed that the chloride front moved ahead ($P = 0.05$) of the moisture front in most of the soils with the exception of the Ferrasol which, had the chloride front lagging.

Additionally, the chlopyrifos concentration front lagged behind (P = 0.05) all the other fronts although not very different from that of potassium in both the Vertisol and Lixisol. The texture of a soil and its pore size distribution are known to exert some influence on the rate and extent of infiltration (Hillel, 1998). Due to their sandy loam nature, the Lixisol, Ferrasol and the Gleysol were expected to have longer distances to the wetting front during the movement of water within the soil.

Table 5.2.1 Soil moisture content at $\lambda = 0$

Soil	Eutric Vertisol	Xanthic Ferrasol	Ferric Lixisol	Eutric Gleysol
	---------- (m^3 m^{-3}) ----------			
$\lambda = 0$	0.515a	0.459b	0.390d	0.425c

Note: Values in rows with the same letter are not significantly different at (P<0.05).

True to their nature, the Lixisol and Ferrasol recorded long distances (P = 0.05) of 2.47 x 10^{-3} and 2.18 x 10^{-3} (m $s^{-1/2}$) respectively to the moisture front during the horizontal infiltration experiment. The Gleysol being a sandy loam, notwithstanding, recorded a relatively shorter distance of 1.76 x 10^{-3} (m $s^{-1/2}$) to the moisture front which, may be attributed to the high silt content and the small pore sizes relative to the Lixisol and Ferrasol. As expected, the Vertisol with its high clay content had the shortest distance of 1.2 x 10^{-3} (m $s^{-1/2}$) to the moisture front during movement of water within the soil.

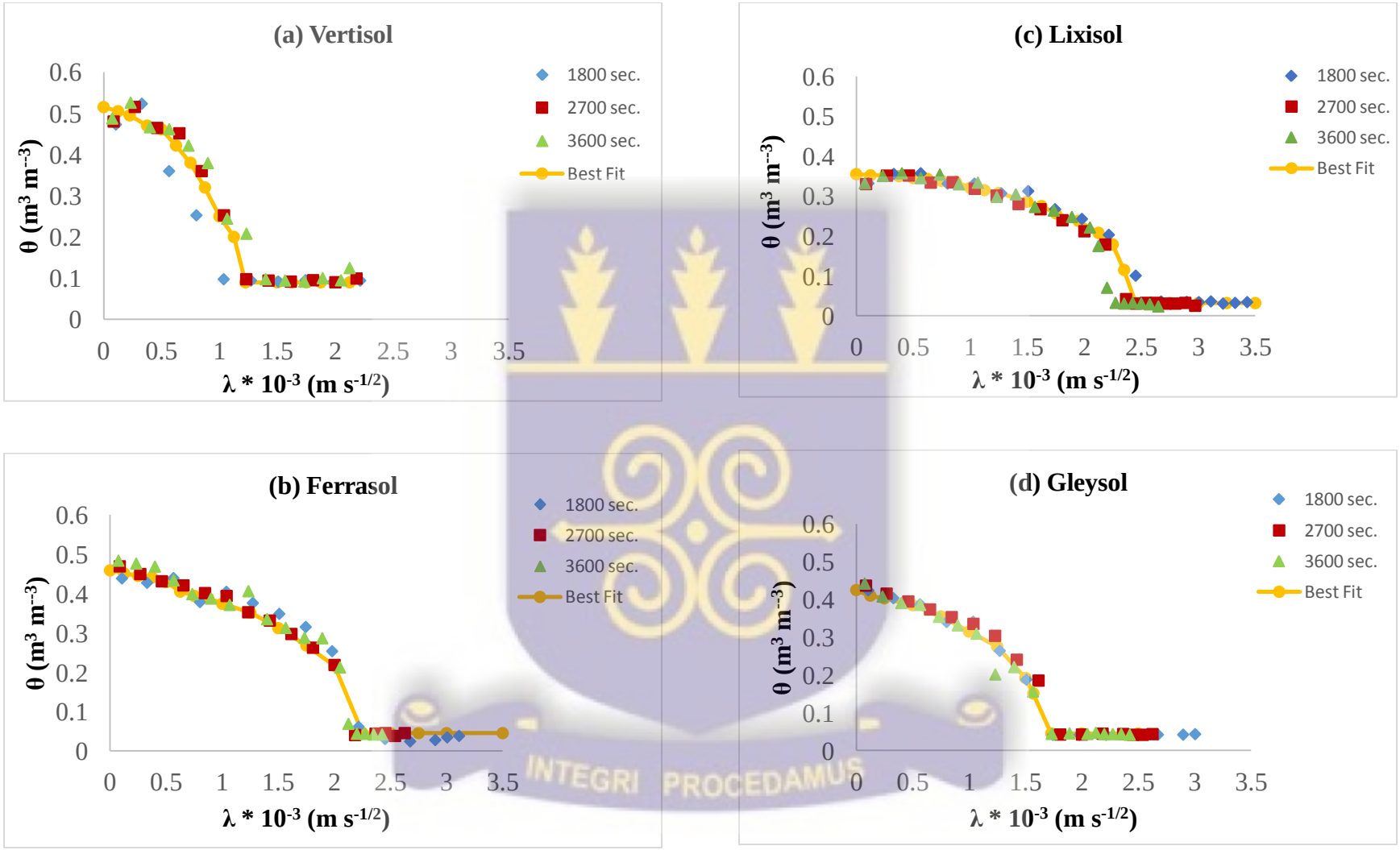

Fig. 5.2.1 Water content profiles during infiltration of water

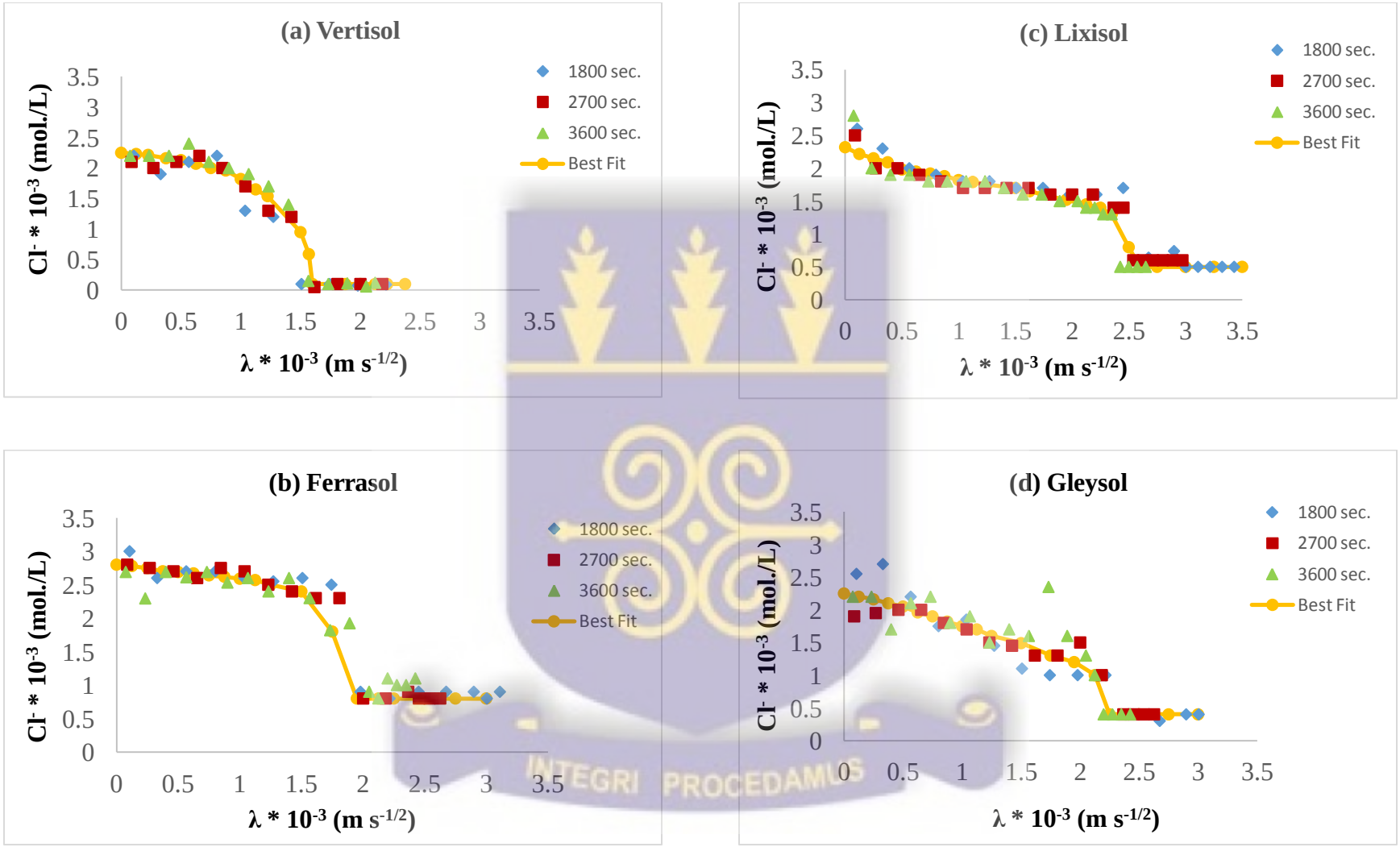

Fig. 5.2.2 Chloride profiles during infiltration of solute

Table 5.2.2 Average λ to the θ, Cl^-, K^+ and chlopyrifos concentration fronts

Soil	Eutric Vertisol	Xanthic Ferrasol	Ferric Lixisol	Eutric Gleysol
	---------- ($m\ s^{-1/2}$) ----------			
θ	1.23×10^{-3}d (f)	2.18×10^{-3}b (e)	2.47×10^{-3}a (f)	1.76×10^{-3}c (f)
Cl^-	1.56×10^{-3}c (e)	2.01×10^{-3}b (f)	2.66×10^{-3}a (e)	1.93×10^{-3}b (e)
K^+	1.13×10^{-3}d (f)	1.82×10^{-3}b (g)	2.34×10^{-3}a (g)	1.56×10^{-3}c (g)
Chf	1.06×10^{-3}d (f)	1.64×10^{-3}b (h)	2.39×10^{-3}a (g)	1.37×10^{-3}c (h)

LSD = Least Significant Difference; θ = Moisture content; Cl^- = Chloride; K^+ = Potassium; Chf = Chlopyrifos.

Note: Values in rows with the same letter (not in parenthesis) are not significantly different at $P<0.05$.

Values in columns with the same letter (in parenthesis) are not significantly different at $P<0.05$

Considering the fact that chloride is a conservative solute, the expectation was for it to be very mobile in soil during the horizontal infiltration experiment. A longer distance of 2.66×10^{-3} ($m\ s^{-1/2}$) was obtained in the Lixisol, with the Vertisol having the lowest distance of travel for the chloride ions as evidenced in table 5.2.2. The distance to the chloride front was therefore in the increasing order of Vertisol < Ferrasol = Gleysol < Lixisol. This may be attributed to the high sand fraction and the relatively high proportion of large pore size fractions of the Lixisol which may have contributed to the high mobility of the chloride ion.

With the notable exception of the Ferrasol, the chloride 'front' moved ahead of the moisture 'front' during the infiltration experiments. This trend is at variance with results from previous studies conducted by Smiles *et al*. (1978), Elrick *et al*. (1979) and Laryea *et al*. (1982). With the high CEC of the soils especially in the Vertisol, suggesting the presence of net negative charges at the colloidal surface for all the soils, the chloride front moving ahead of that of water may be attributed to anion exclusion.

It must also be noted that in the earlier studies of Smiles *et al*. (1978), Elrick *et al*. (1979) and Laryea *et al*. (1982) where the chloride front lagged behind that of the water, the soils were cation saturated prior to the horizontal infiltration of the anion. In this study however, no saturation was done which may account for the high equilibrium concentration and the distance of travel of the anion. The Ferrasol had a high AEC of 52.70 cmol kg^{-1} which was more than twice that of the Vertisol and 1.5 times more than the values recorded for the Lixisol and Gleysol. This high AEC may result from the protonation of iron and aluminum oxides which are most likely to be predominant in the Ferrasol at low pH 4.1. These may serve as sources of attraction of chloride ions during the infiltration process, leading to the chloride front lagging behind that of moisture.

The potassium concentration profile is presented in Figure 5.2.3. The potassium 'front' obtained during the horizontal infiltration experiments lagged behind that of the water and the chloride front in all the soils except the Vertisol (Table 5.2.2). This trend is expected in view of the fact that all the soils have negative charge at the colloidal surface and thus, CEC which would allow potassium ions to be held onto the exchange sites of the soil colloids. As expected, the Vertisol had the least distance to the potassium front during the experiments which, was not very different (P = 0.05) from that of the moisture front. This may be ascribed to the highest amount of clay

and the montmorillonitic nature of the clay which culminated in the highest CEC.Thus, sandy soils like the Lixisol, which has very low CEC allow the easy movement of K^+ (Sparks and Huang, 1985). Figure 5.2.4 shows the chlopyrifos concentration profile during the horizontal infiltration experiment. The concentration of the insecticide was observed to be higher in the Lixisol, with the Vertisol recording the lowest chlorpyrifos levels. It must be pointed out that the maximum chlorpyrifos concentrations recorded in the sandy loams in general far exceeds that of the Vertisol which, is a sandy clay (Table 5.2.3). Additionally, the distance to the chlorpyrifos concentration front was larger in the Lixisol ($P = 0.05$) with the Vertisol having the shortest distance. The higher levels of chlopyrifos, coupled with the larger distances to the insecticide front observed in the sandy loams may be attributed to their high sand fractions. The large pore size fractions and the low CEC of the sandy loams did not impede chlopyrifos concentration in solution and this may have accounted for the high concentrations obtained in solution. This observation is consistent with results obtained by Halimah *et al.* (2010) who reported that mobility of chlorpyrifos is greater in sandy soils because of its lower adsorption. Similar studies by Walker *et al*. (1989), Walker and Exposito (1998) and Chrisanto *et al*. (2000) have also proved that soil properties such as texture, pH and soil organic matter can influence the movement of chlopyrifos in soils. The chlopyrifos solution concentration measured in the Ferrasol during the horizontal infiltration experiment was high, although the soil had high level of soil organic matter to cause the compound to be adsorbed.

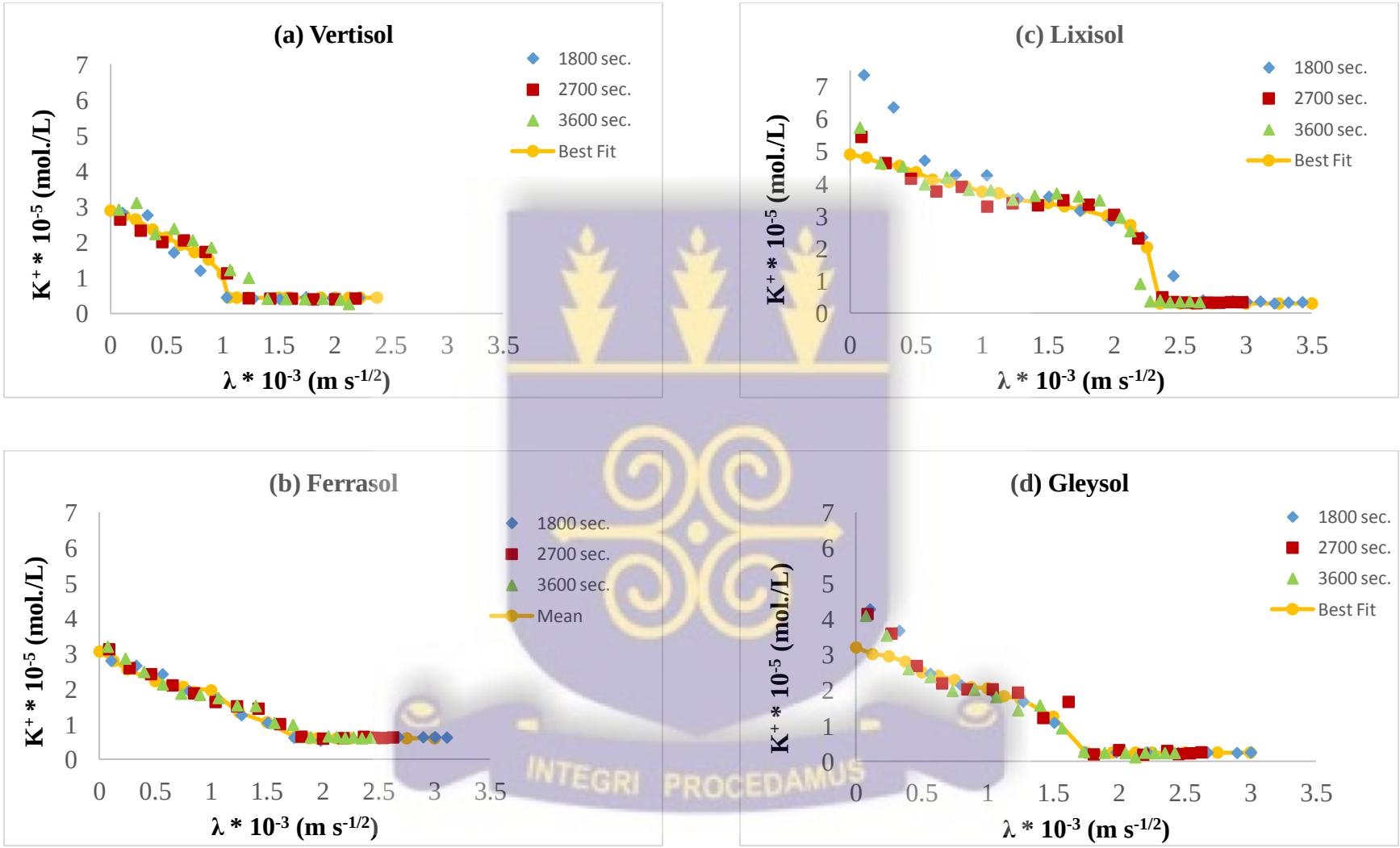

Fig. 5.2.3 K^+ profiles during horizontal infiltration of solute

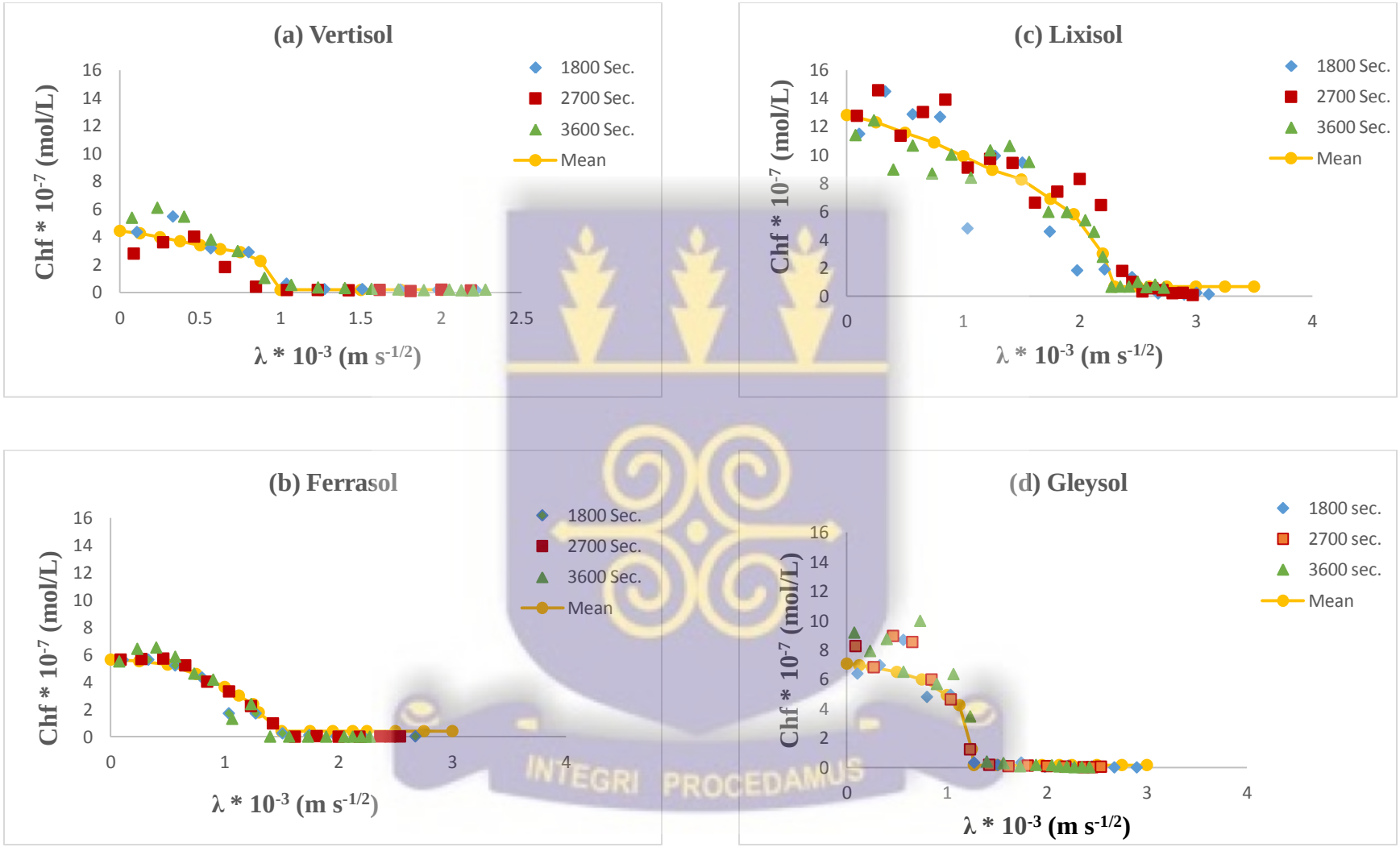

Fig. 5.2.4 **Chlopyrifos profiles during infiltration of insecticide**

Table 5.2.3 Maximum chlorpyrifos concentration in solution during infiltration experiment

Soil	Chlorpyrifos conc. (mol L^{-1})
Eutric Vertisol	4.45×10^{-7}
Xanthic Ferrasol	5.50×10^{-7}
Ferric Lixisol	12.83×10^{-7}
Eutric Gleysol	7.07×10^{-7}

At the soil's pH of 4.1 which is very close to the pKa values of acetic, citric and oxalic acids (4.2, 4.3 and 4.4, respectively) these organic acids would be dissociated for their conjugate bases, the carboxylate anion, to be adsorbed onto the sesquioxides in soil solution. With the carboxylic groups occupied by the sesquioxides of Al and Fe, the insecticide would then be free to move through the soil leading to the high concentration of the insecticide in solution.

The low solution concentration and the short distance to the chlorpyrifos front recorded in the Vertisol may be attributed to the high clay content in addition to the high soil organic carbon levels which, may have retarded the mobility of the insecticide. In the presence of organic matter, the chlorpyrifos sorption capacity of clay colloids is increased. It has been reported by van Emmerik *et al.* (2007) that the amount of chlorpyrifos sorbed onto kaolinite for instance, increased three to four folds in the presence of dissolved organic matter. With the exception of the Vertisol, the chlorpyrifos concentration front lagged behind ($P = 0.05$) that of moisture and the other solute fronts in all instances.

5.3 Infiltration adsorption isotherms of potassium and chlopyrifos

Figure 5.3.1 and 5.3.2 present the adsorption isotherms determined from the horizontal infiltration experiments for potassium and chlorpyrifos, respectively. In all instances, the adsorption isotherms appear curvilinear in shape for concentrations of adsorbed K^+ versus that remaining in solution at equilibrium for all the soil types. The trend in peak amount of K^+ adsorbed when the different soil types are considered is in the order Vertisol > Ferrasol > Gleysol > Lixisol. The amount of adsorbed K^+ as a fraction of CEC is presented in Table 5.3.1. When the amount of K^+ adsorbed as a fraction of the CEC of the soil at the equilibrating solution was considered, it was observed that less than 4% of the exchange sites of the various soil types were occupied by the K^+. Although the amount of K^+ adsorbed by the Lixisol was lower than that of the other soils, it occupied about 3.5 % of the exchange site available for cation adsorption. Also, the amount of K^+ adsorbed by the Vertisol was relatively high but, it occupied only 0.64 % of the exchange sites for CEC. This is expected in view of the higher CEC of the Vertisol due to its higher clay and soil organic carbon content.

Similar to that of K^+ in all the soils, the adsorption isotherm of chlopyrifos appear to be curvilinear in shape conforming to the Langmuir type. It must be stated however that the isotherm for the Ferrasol appear almost linear. The rate of adsorption of chlopyrifos as indicated by the curves appears to favour the Vertisol with a higher value. The Vertisol and Ferrasol also had higher amounts of adsorbed chlopyrifos which, indicates that soil organic carbon content has a significant influence on the adsorption of the insecticide compound.

Table 5.3.1 Amount of K^+ adsorbed as a fraction of cation exchange capacity during infiltration experiment

Soil	K^+ adsorbed (mol kg^{-1})	Fraction of CEC (%)
Eutric Vertisol	0.196	0.64
Xanthic Ferrasol	0.180	1.98
Ferric Lixisol	0.139	3.56
Eutric Gleysol	0.170	2.42

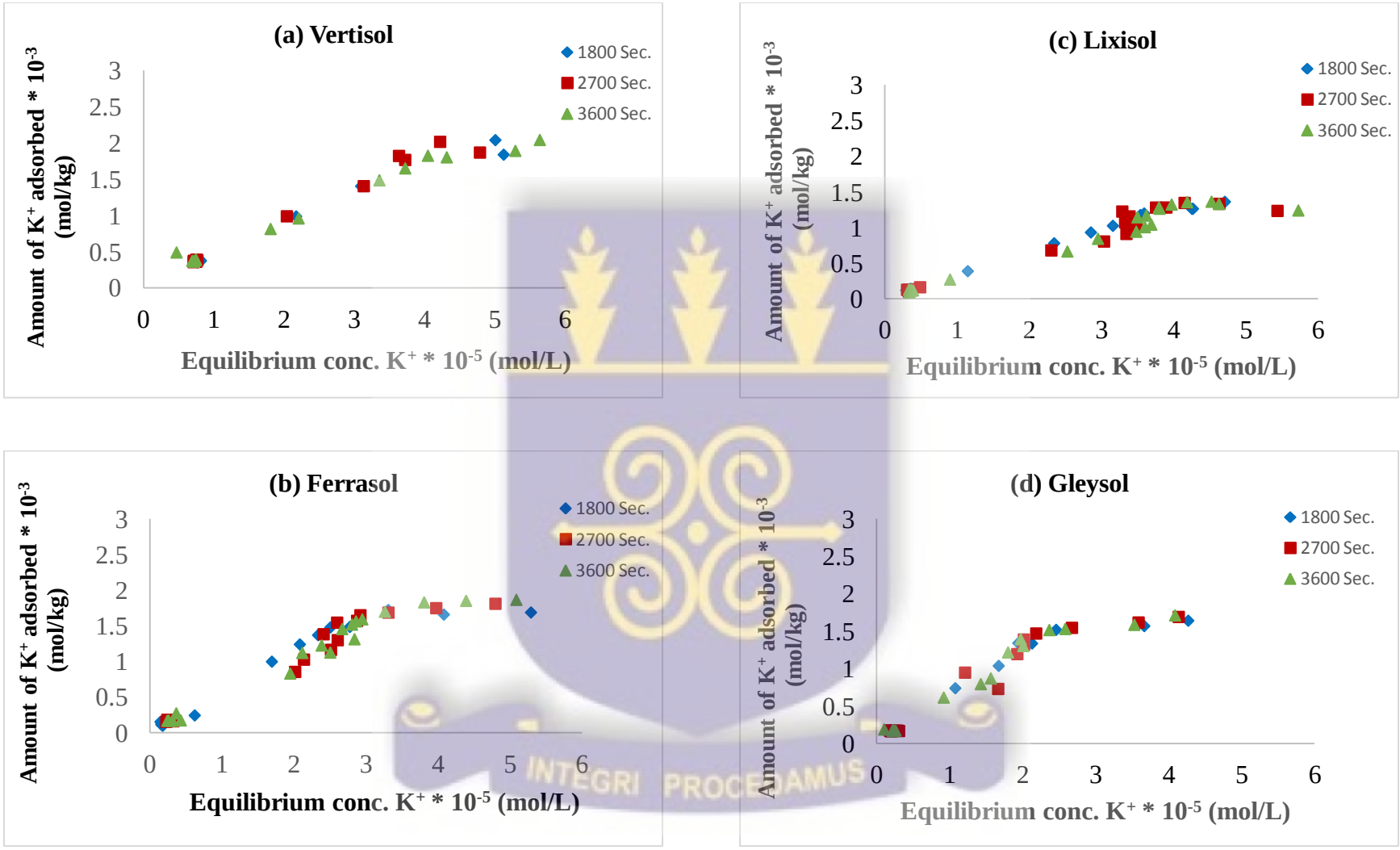

Fig. 5.3.1 Infiltration adsorption isotherms for K^+

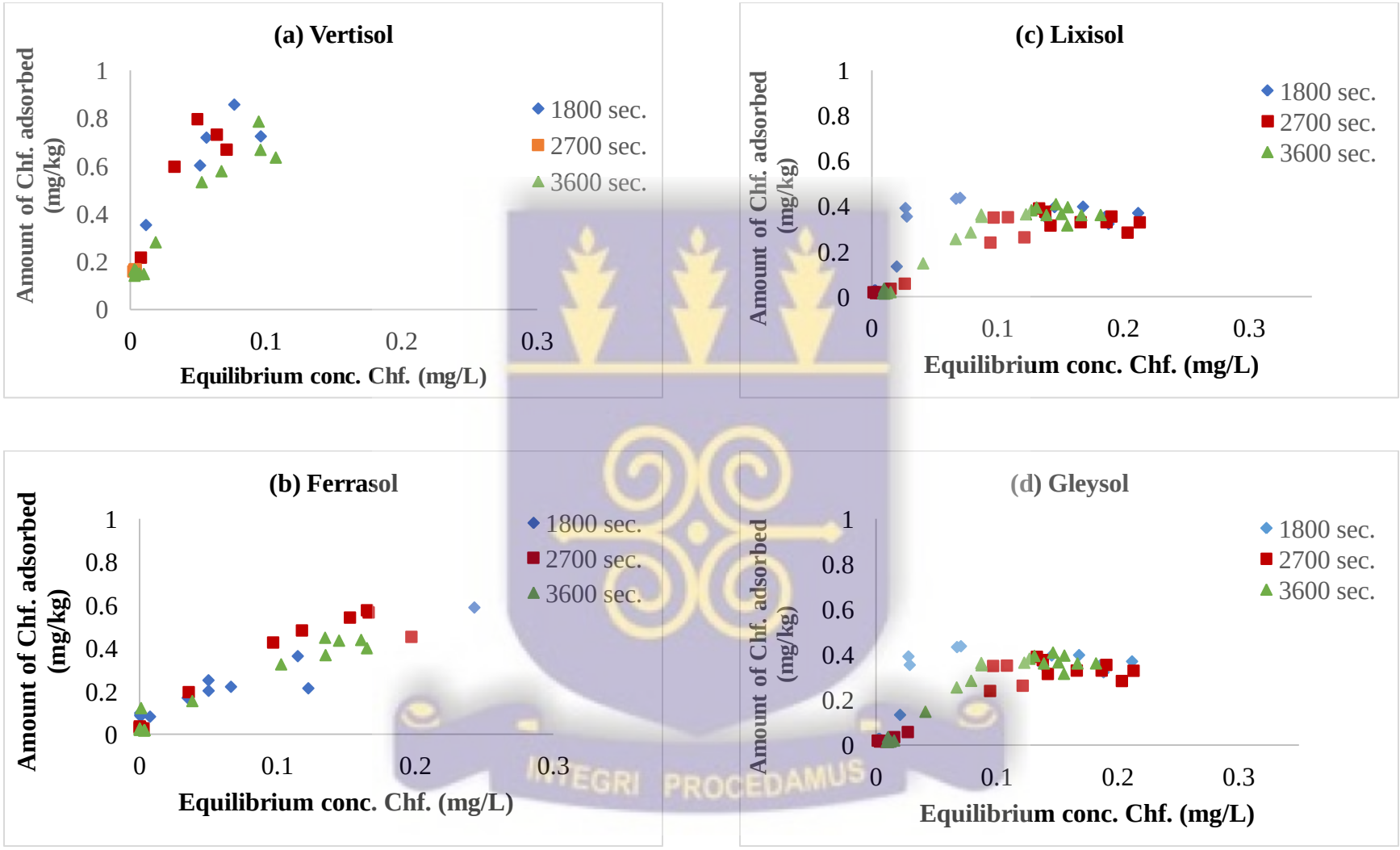

Fig. 5.3.2 Infiltration adsorption isotherms for chlopyrifos

5.4 Derived data from the infiltration experiments

5.4.1 Soil water diffusivity

Figure 5.4.1 presents the soil water diffusivity function D(θ) for the soils during the horizontal infiltration experiment. These are plots of soil water diffusivity (D) and the moisture content of the soils (θ), determined during the horizontal infiltration experiments. The D(θ) values were obtained from the θ(λ) relationships and calculated with the CSMP program. In all instances, diffusivity increased sharply with increase in soil water content. The increase in soil water diffusivity with water content has been explained on the basis of the gradual increase in the radii of water conducting pores and consequently a decrease in tortuosity of the actual flow path when the water content increases towards saturation (Aoda and Younan, 2010; Aoda *et al*. 1993).

At the maximum moisture content in each soil the maximum diffusivity function observed was in the decreasing order Lixisol > Ferrasol > Gleysol > Vertisol (Table 5.4.1). The trend gives the indication that the sand fraction of the soil played an important role in moisture diffusivity during the infiltration experiment. The coarse textured nature of the Lixisol that may have given rise to the predominance of larger pore sizes within the soil, together with the very low level of soil organic carbon may have allowed the rapid movement of moisture and thus contributed to the higher values of D (θ) observed. Conversely, the Vertisol with relatively high clay content had the lowest D(θ) values. The low moisture diffusivity values obtained in the Vertisol is probably a reflection of possible presence of charges on the clay surfaces. The high clay content and comparatively high cation exchange capacity as well as the relatively high soil organic matter of the Vertisol (although lower than that of the Ferrasol), are mostly responsible for the high level of negative charges on the surfaces of the soil colloids. The effects of these charges in retarding the movement of water in the soil can thus not be ignored.

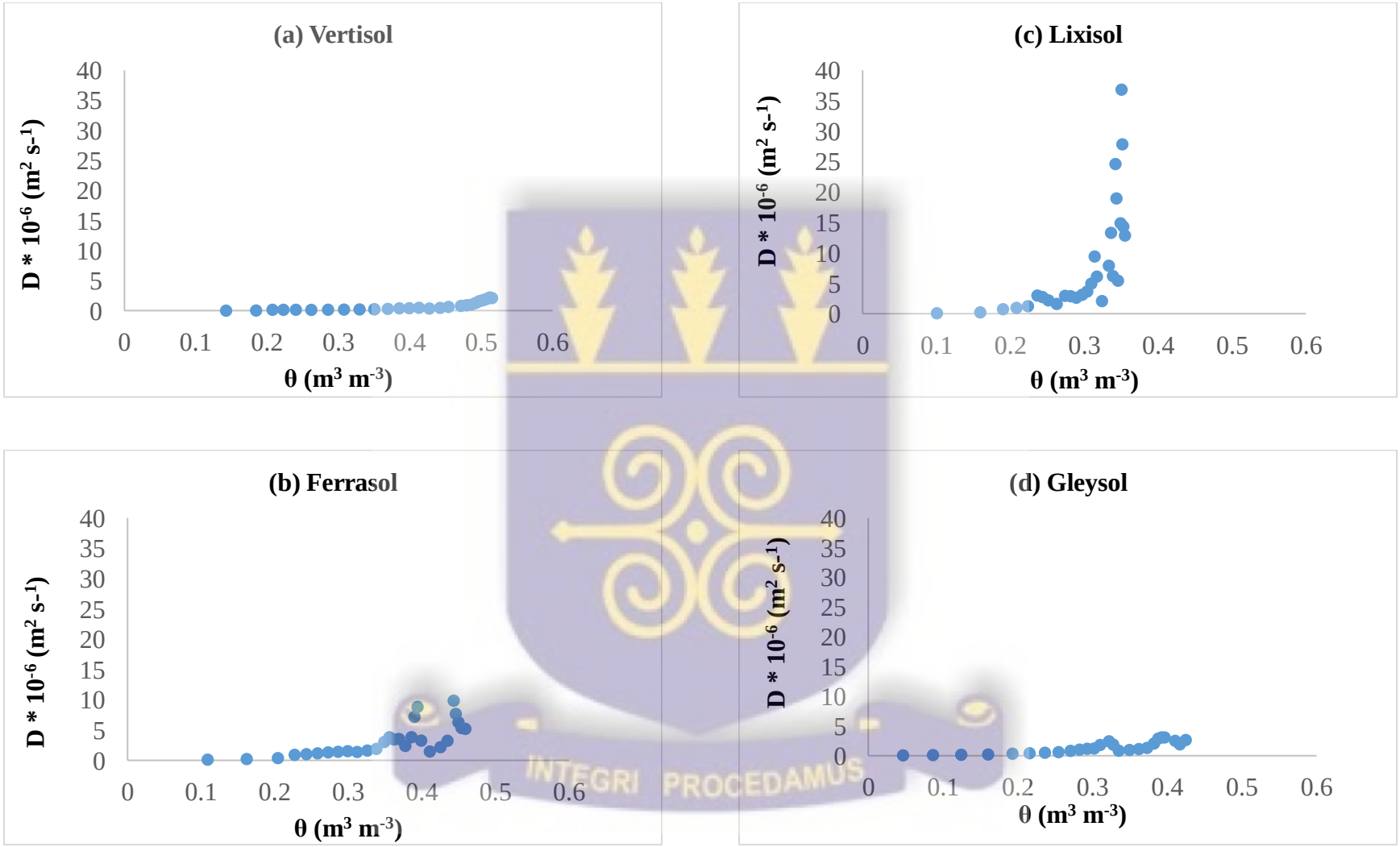

Fig. 5.4.1 **Moisture Diffusivity function during horizontal infiltration**

Table 5.4.1 Maximum water diffusivity values and corresponding moisture and clay content of soil

Soil	Moisture content ($m^3\ m^{-3}$)	Moisture diffusivity ($m^2 s^{-1}$)	Clay content (%)
Eutric Vertisol	0.515	2.11×10^{-6}	35.84
Xanthic Ferrasol	0.459	9.83×10^{-6}	20.83
Ferric Lixisol	0.390	3.68×10^{-5}	15.83
Eutric Gleysol	0.425	3.02×10^{-6}	17.50

Although the Ferrasol had high clay and soil organic carbon content relative to that of the Gleysol, the higher percentage of sand which may have possibly contributed to a higher proportion of large pore sizes possibly accounted for the high D (θ) values obtained.

5.4.2 Dispersion coefficient of chloride in soil

The dispersion coefficient of chloride, $\wp_{cl}(\theta)$ when solution of KCl was used in the horizontal infiltration into the soil columns are shown in Figs. 5.4.2 (a, b, c and d). The $\wp_{cl}(\theta)$ values were obtained from calculations carried out with the CSMP program using the $C_{Cl}(\lambda)$ data obtained from the horizontal infiltration experiments. The dispersion coefficient values were larger at points corresponding to the wet end of the soil column and decreased to a minimum towards the dry end in all the soils. Examination of the values of θ when the dispersion coefficient was lowest in the soils suggests that soil texture exerted some influence on the trend. The trend of the values of θ at which the dispersion coefficient was lowest was in the order, Vertisol > Gleysol = Ferrasol > Lixisol, thus relating to the amount of clay present. With very high proportions of sand, the Lixisol and Ferrasol soils were expected to have the least θ values at which the dispersion coefficients were lowest. As expected, this trend was observed with the two soils having very low θ values at the lowest dispersion coefficients of chloride. The Vertisol with high levels of clay, had $\theta = 0.09$ m^3 m^{-3} ($P < 0.05$), compared to ($\theta = 0.045$, $\theta = 0.045$ and $\theta = 0.032$) m^3 m^{-3} in the Gleysol, Ferrasol and Lixisol respectively. Although the texture of Lixisol is sandy loam and therefore had a corresponding lower θ value, it also recorded the lowest level of clay. This relationship is consistent with the fact that the clay content increases water retention in soils.

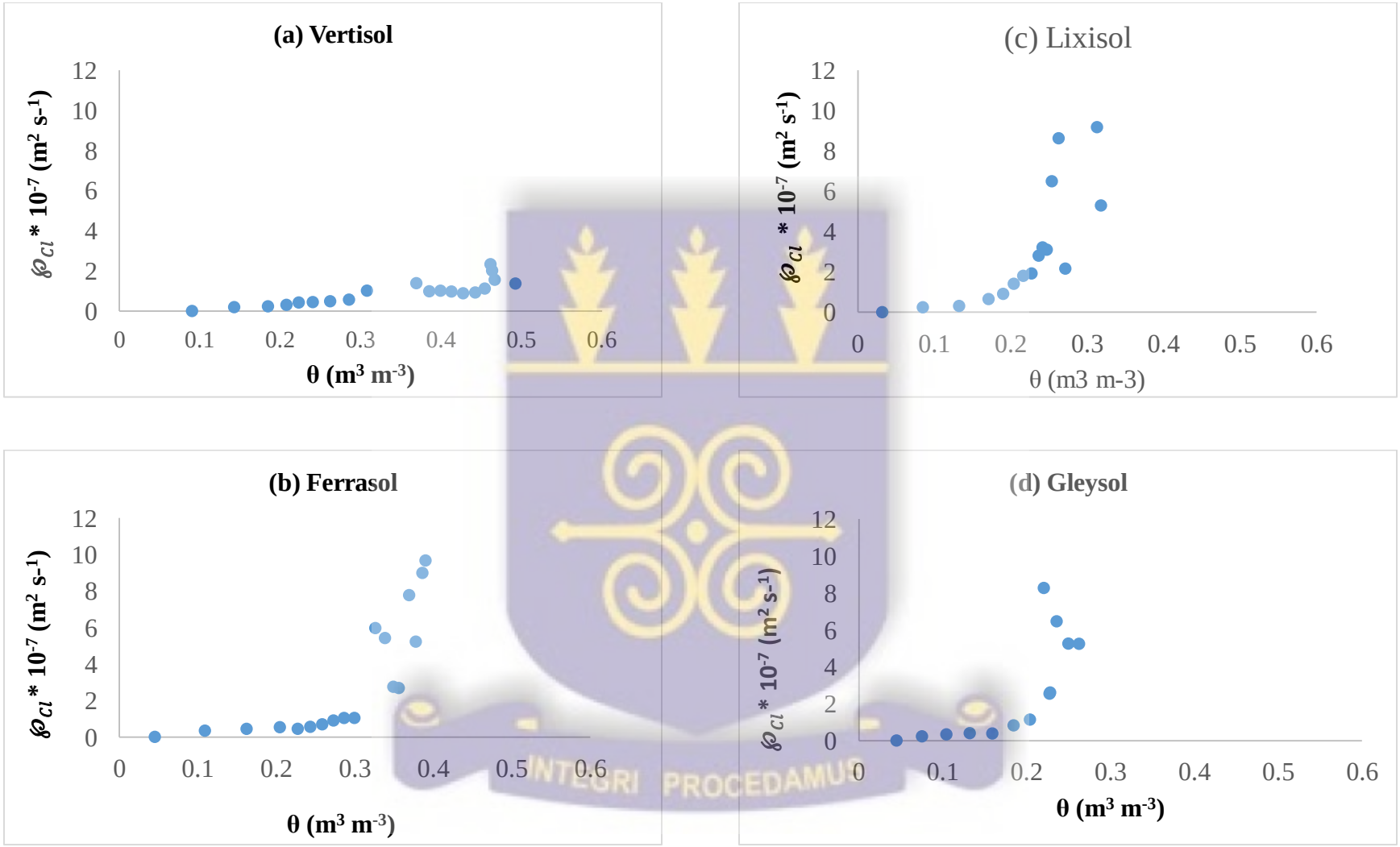

Fig. 5.4.2 **Dispersion coefficients for Cl^- during horizontal infiltration**

Table 5.4.2 Moisture content at which dispersion coefficient ($\wp_{Cl}$) of chloride was minimum

Soil	Dispersion coefficient (m^2 s^{-1})	θ (m^3 m^{-3})
Eutric Vertisol	0	0.090a
Xanthic Ferrasol	0	0.045b
Ferric Lixisol	0	0.032b
Eutric Gleysol	0	0.045b

Table 5.4.3 Maximum dispersion coefficient of chloride ($\wp_{Cl}$) and the corresponding moisture content

Soil	Dispersion coefficient (m^2 s^{-1})	θ (m^3 m^{-3})
Eutric Vertisol	2.33×10^{-7}	0.46
Xanthic Ferrasol	9.66×10^{-7}	0.39
Ferric Lixisol	9.17×10^{-7}	0.31
Eutric Gleysol	5.23×10^{-7}	0.26

It was also observed that dispersion of chloride was greater in the soils with relatively high fractions of sand. In soils with a coarse texture, the fraction of larger pore sizes and hydraulic conductivity of the soil matrix are much higher, leading to greater mixing. This trend is consistent with observations made by Vanderborght *et al*. (2000) and Vereecken *et al*. (1990). Thus, the Ferrasol and Lixisol had higher values than that of the Gleysol which in tend was greater than the Vertisol. The trend in the maximum dispersion coefficient of chloride was in the order Ferrasol > Lixisol > Gleysol > Vertisol. The maximum dispersion coefficient value observed for the Ferrasol at $\theta = 0.39$ m^3 $m^{-3}$and Lixisol at $\theta = 0.31$ m^3 m^{-3} (both with similar levels of sand) for instance, were more than three folds greater than that of the Vertisol at $\theta = 0.46$ m^3 m^{-3} (Table 5.4.3). It must also be noted that with the exception of the Ferrasol, which had a relatively higher clay content, the moisture content at which the peak dispersion coefficients of chloride were recorded in the sandy loams were similar and lower than that of the Vertisol. It could be inferred from the values obtained that the influence of the sand fraction reflected on the extent of mixing of Cl^- in the soils. The large pore size fraction that may have resulted in faster flow rates probably contributed to greater mixing of the Cl^- in the Lixisol and Ferrasol.

5.4.3 Dispersion coefficient of K^+ and chlopyrifos in soil

The dispersion coefficients of K^+ versus moisture content, $\wp_K(\theta)$ for all the soil samples used in the study are shown in Figure 5.4.3. The trend was similar to that of the chloride for the relationships with a decrease from large values corresponding to the wet end of the column to the minimum value of zero for Vertisol, Ferrasol, Lixisol and Gleysol respectively (Table 5.4.4). The moisture content and corresponding dispersion coefficient at the maximum and minimum values

of dispersion are shown in Table 5.4.4. The influence of soil texture on the maximum dispersion coefficients in the various soils are reflected here.

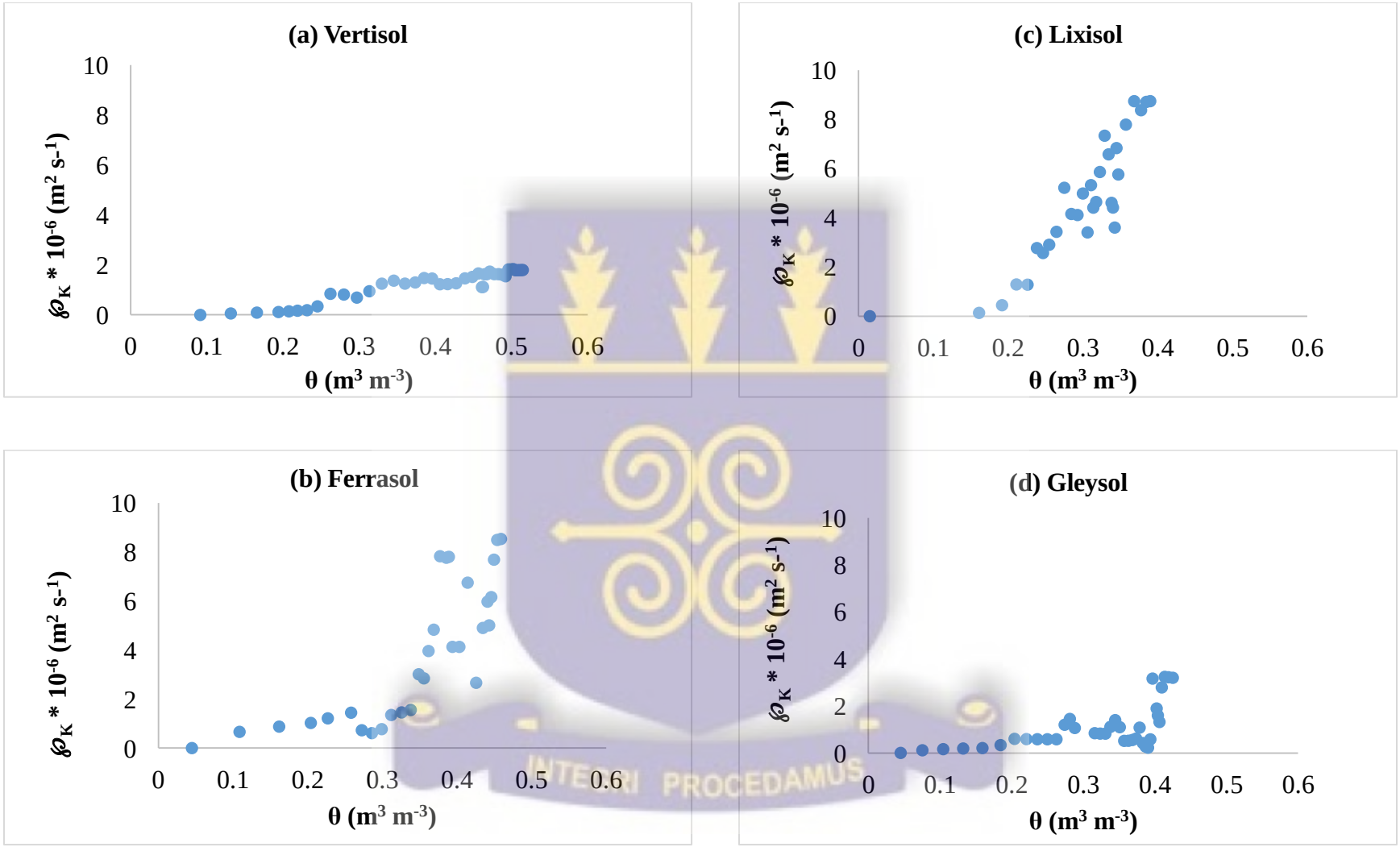

Fig. 5.4.3 **Dispersion coefficients for K^+ during horizontal infiltration**

Table 5. 4.4 Maximum and minimum values of dispersion coefficient of potassium ($\wp_K$) and chlopyrifos ($\wp_{Chf}$) and corresponding moisture content (θ)

	Max. $\wp_K$ (m^2 s^{-1})	θ at Max. $\wp_K$ (m^3 m^{-3})	Min. $\wp_K$ (m^2 s^{-1})	θ at Min. $\wp_K$ (m^3 m^{-3})	Max. $\wp_{Chf}$ (m^2 s^{-1})	θ at Max. $\wp_{Chf}$ (m^3 m^{-3})	Min. $\wp_{Chf}$ (m^2 s^{-1})	θ at Min. $\wp_{Chf}$ (m^3 m^{-3})
Soil								
Eutric Vertisol	1.80×10^{-6}	0.520	0	0.090	2.30×10^{-7}	0.413	0	0.09
Xanthic Ferrasol	8.52×10^{-6}	0.459	0	0.045	3.11×10^{-7}	0.415	0	0.09
Ferric Lixisol	8.74×10^{-6}	0.390	0	0.010	8.82×10^{-7}	0.390	0	0.10
Eutric Gleysol	3.20×10^{-6}	0.426	0	0.050	6.57×10^{-7}	0.411	0	0.08

Max. $\wp_K$ = Maximum value of dispersion coefficient of potassium; Min. $\wp_K$ = Minimum value of dispersion coefficient of potassium

Max. $\wp_{Chf}$ = Maximum value of dispersion coefficient of chlopyrifos; Min. $\wp_{Chf}$ = Minimum value of dispersion coefficient of chlopyrifos

θ at Max. $\wp_K$ = Moisture content at maximum value of dispersion coefficient of potassium

θ at Min. $\wp_K$ = moisture content at minimum value of dispersion coefficient of potassium

θ at Max. $\wp_{Chf}$ = Moisture content at maximum value of dispersion coefficient of potassium;

θ at Min. $\wp_{Chf}$ = moisture content at minimum value of dispersion coefficient of potassium

The maximum dispersion coefficients ($\wp_K$) of the sandy loams exceed that of the sandy clay. This could be explained in terms of the sandy loams having larger pose sizes and thus allowing greater mixing of the K^+. The Lixisol had the largest value of 8.74 x 10^{-6} (m^2 s^{-1}) which was not very different from that of the Ferrasol but over 4.5 and 2.5 times more than the corresponding values obtained by the Vertisol and the Gleysol respectively. In all instances, it is worth noting that the maximum dispersion coefficient values were larger for the K^+ than the Cl^-.

The dispersion coefficients of chlopyrifos versus moisture content determined from the horizontal infiltration of experiments are presented in Figure 5.4.4. As expected, the trend is similar to that of the chloride and the potassium in all the soils with the $\wp_{Chf}$ (θ) relationship decreasing from large values corresponding to the wet end of the column to a minimum value corresponding to the relatively dry end of the column. However, maximum values of dispersion coefficients obtained for chlorpyrifos in soil were smaller than the corresponding values for potassium in all instances (Table 5.4.4). As indicated earlier (section 5.2), soil properties exert a significant influence on the transport of chlopyrifos in soils. The apparent differences in the maximum values of dispersion coefficient observed in the different soils is not surprising. It must also be pointed out that the notable influence of soil organic matter on the dispersion of the insecticide compound in soils as exhibited by the Vertisol and Ferrasol cannot be overlooked. The maximum dispersion values are in the increasing order of Vertisol< Ferrasol < Gleysol < Lixisol. The Ferrasol which has similar fraction of sand as the Lixisol is expected to have the insecticide compound more dispersed. With a high soil organic carbon content, the relatively low maximum dispersion value exhibited by the Ferrasol suggest that the level of soil organic matter coupled with that of clay content may have influenced the dispersion of the insecticide compound in the soils used in this study. This is reflected by the

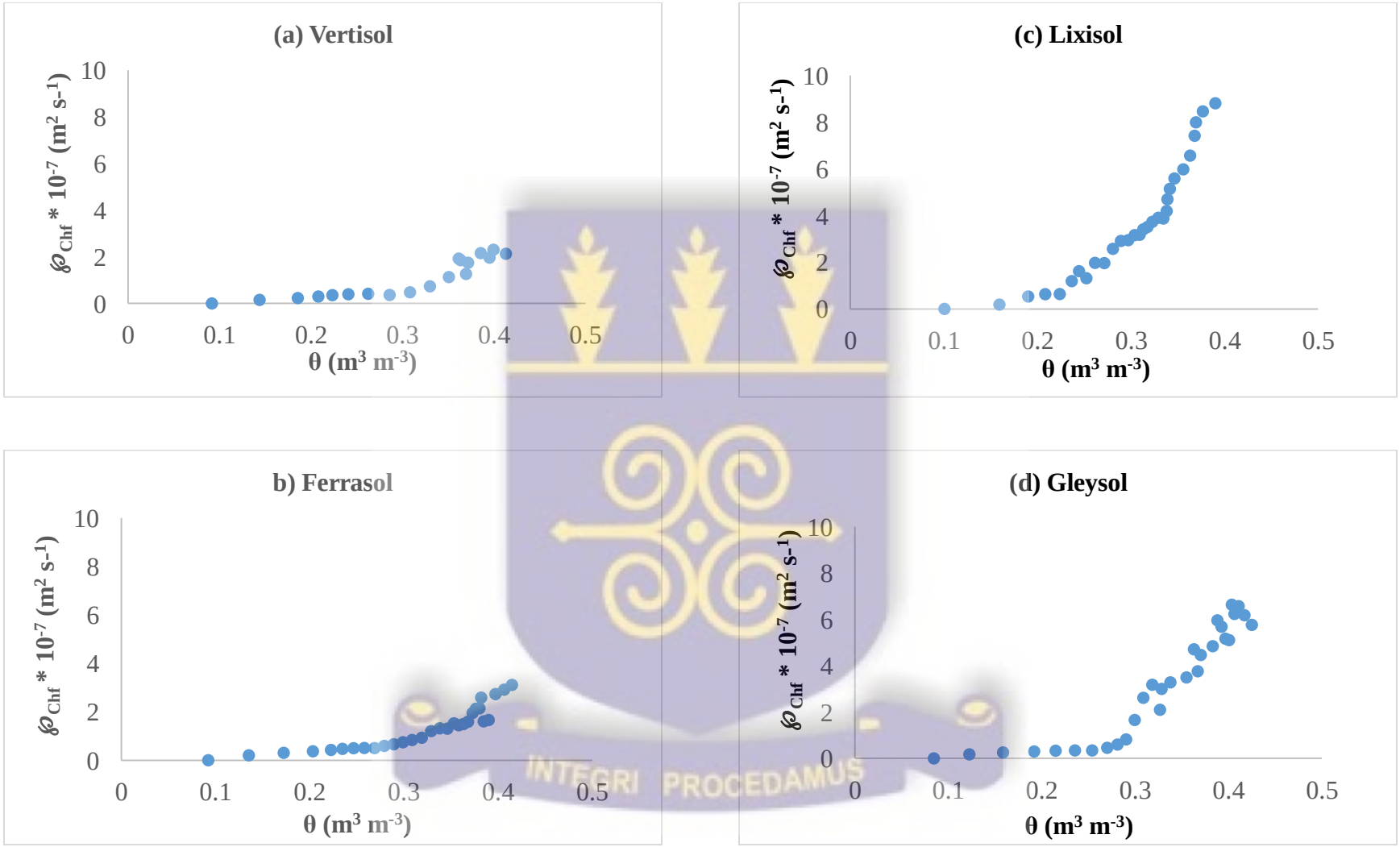

Fig. 5.4.4 Dispersion coefficients for Chlopyrifos during horizontal infiltration

very low dispersion values observed in the Vertisol due to the high levels of soil organic matter and clay.

5.4.4 Notional plane and immobile water fraction

From the moisture profiles, a plane of separation, which establishes the front of the invading water (when it is assumed that the water initially in the soil column is perfectly displaced by the infiltrating solution) could be identified during horizontal infiltration of solution into soil column. According Smiles and Philip (1978), Elrick *et al.* (1979), Laryea *et al.* (1982) and Robin *et al* (1983), the plane about which this separation occurs is described by the material balance equation $\theta\lambda^* = \int_{\theta_n}^{\theta(\lambda)^*} \lambda d\theta$ (i.e equation 4.15). This plane is identified as the notional plane for water. Another plane about which salt dispersion occurs is defined as $\int_0^{\lambda}(C_0 - C)d\lambda = \int_{\lambda}^{\infty}(C - C_n)d\lambda$ (i.e. equation 4.14). The assumption underlying this concept is that, if flow in the soil column is to assume a piston-like manner, then it could be best described by the notional plane. Since the salt is in solution and thus will be moving with the infiltrating water in soil, the plane or moving front of the solute and solvent should be the same (i.e. $\lambda^* = \lambda'$). For the chloride, differences in the water and salt plane may be ascribed to the presence of immobile and inaccessible water close to the negatively charged surfaces of the soil colloid.

Figure 5.5.1 presents the notional planes for chloride and water during infiltration of solute in soil columns for the different soil types. In the Vertisol and Gleysol the notional plane for the chloride salt (λ'_{cl}) lies ahead of the water plane (λ^*). The corresponding difference in moisture content at the two notional planes indicate the size of the immobile water fraction in soils. The difference in the two planes was larger in the sandy clay than to the Gleysol, suggesting that the size of the immobile water fraction is smaller in the latter.

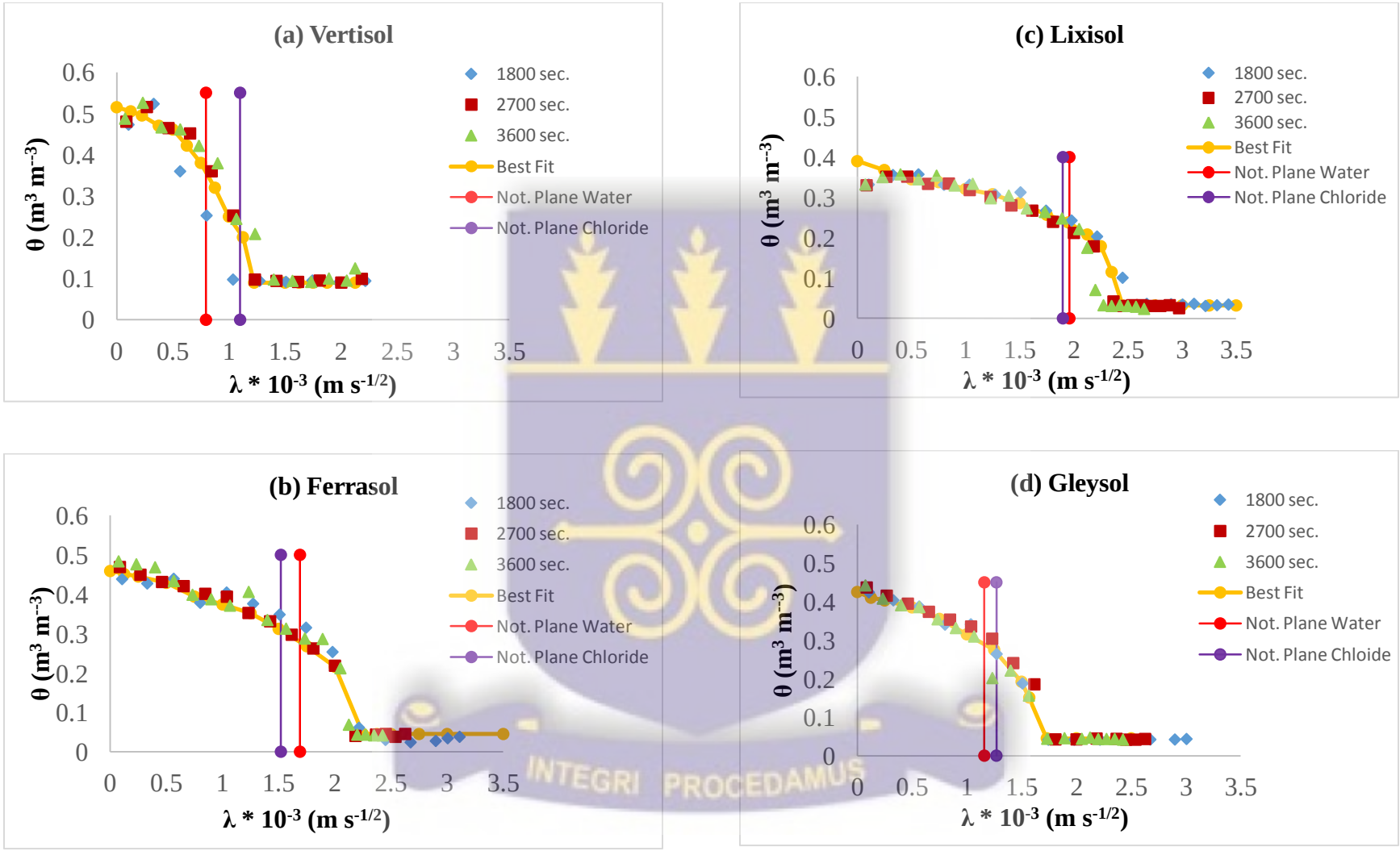

Figure 5.5.1 Notional planes for chloride and water during horizontal infiltration of solute

The size of the immobile water fraction (θ_{im}) was estimated as (8.94 x 10^{-5} m^3 m^{-3}) in the Eutric Vertisol and (3.14 x 10^{-5} m^3 m^{-3}) for the Eutric Gleysol. This is not surprising since the Vertisol has high levels of clay and soil organic matter, thus a higher CEC and therefore expected to have a larger θ_{im}. The estimated values of θ_{im} obtained for the Vertisol and Gleysol ties in well with immobile water ranges of 5.31 to 14.28 % of soil moisture content reported by Tabarzad *et al.* (2011) in repacked soils in laboratory experiments and up to 21.3 % of soil moisture content estimated by Alletto *et al.* (2006) in field soils of different textures. Additionally, it was reported that the size of θ_{im} is related to the clay content and the structure of the soil.

In the Xanthic Ferrasol and Ferric Lixisol however, it was observed that the chloride plane (λ'_{cl}) lagged behind that of the water (λ^*) although the difference between the two planes was relatively small in the Ferric Lixisol. With chloride being a non-interacting solute, the expectation was for the plane of dispersion of the salt to move ahead of the water plane (just like the trend that was observed in the Vertisol and Gleysol). The fact that it lagged behind that of the water suggests some form of retardation, possibly as a result of adsorption. This phenomenon may be ascribed to the possible presence of oxides and hydroxides of iron and aluminium which are predominant in Oxisols such as the Ferrasol, especially at the low pH of 4.1. Since the chloride which, is noted as a non-interacting solute exhibited some form of retardation during the horizontal infiltration experiment in this soil sample, the concept of differences in notional planes as the basis for the establishment of θ_{im} in these soils will not be valid. Thus, the immobile water domain could not be established in the Xanthic Ferrasol and Ferric Lixisol.

Table 5.5.1 Notional planes λ' and λ^* for the horizontal infiltration experiments

Soil	λ'_{cl}	λ'_{K}	λ'_{Chf}	λ^*
Eutric Vertisol	1.10×10^{-3}	6.12×10^{-4}	5.81×10^{-4}	7.96×10^{-4}
Xanthic Ferrasol	1.52×10^{-3}	9.00×10^{-4}	8.44×10^{-4}	1.69×10^{-3}
Ferric Lixisol	1.90×10^{-3}	1.59×10^{-3}	1.59×10^{-3}	1.96×10^{-3}
Eutric Gleysol	1.27×10^{-3}	1.13×10^{-3}	1.08×10^{-3}	1.16×10^{-3}

Table 5.5.1 presents the estimation of the notional planes λ' and λ^* for the horizontal infiltration experiments described in section 4.3 under materials and methods. It is noted that in the Vertisol and Gleysol, the chloride plane moved ahead of all the other planes. For these two soils, the notional planes were in the order $\lambda'_{cl}>\lambda^*>\lambda'_K>\lambda'_{Chf}$ indicating that the mobility of the insecticide and potassium were the most affected. Although the trend was similar to that of the Gleysol, the extent of dispersion of the solutes was much smaller in the Vertisol. This may be due to the high clay and organic carbon content of the sandy clay which reflected on the extent of retardation of these two agrochemicals. The other two sandy loams exhibited trends that were slightly different with notional plane for water moving ahead of all the other planes. For the Ferrasol, the notional planes were in the order $\lambda^*>\lambda'_{cl}>\lambda'_K>\lambda'_{Chf}$. The Lixisol on the other hand exhibited a similar trend to that of the Ferrasol except that the notional planes of Potassium and Chlopyrifos were equal i.e. $\lambda^*>\lambda'_{cl}>\lambda'_K=\lambda'_{Chf}$. It must be indicated however that the influence of soil organic matter and clay content reflected on the mobility of agrochemicals in the soils.

5.4.5 Dispersion of chloride in soils after accounting for immobile water fraction

Figure 5.6.1 presents the dispersion coefficients of chloride versus moisture content after accounting for the fraction of the immobile water content for the Vertisol and Gleysol. As expected, the relations decrease from large values corresponding to the wet end of the soil column to minimum values that correspond to the relatively dry end of the column. The peak dispersion coefficient ($\wp_{Clm}$) values observed were relatively smaller when immobile water content was accounted for in the two soils. For the Vertisol, the peak dispersion coefficient value obtained for chloride when total moisture content is considered was more than three times the peak value obtained when the immobile water fraction was accounted for. The corresponding difference in moisture content associated with the peak dispersion coefficient values are however very low

(Table 5.6). This suggests that a small difference in moisture content will have a marked influence on the dispersion of chloride in the sandy loam. This seems to support the assumption by Smiles *et al.*,(1978) that the dispersion coefficient ($\wp$) should be considered a function of moisture content (θ) only.

Similar to the observation made in the Vertisol, the dispersion coefficient recorded in the Gleysol when immobile water content is not taken into account is more than 8 times the value obtained when θ_{im} was considered in the estimation of the dispersion coefficient. Unlike the observation made in the Vertisol however, the difference in corresponding moisture content at the peak dispersion coefficient was about one and half folds in favour of dispersion coefficient when immobile water content is accounted for. This still supports the assumption by Smiles *et al.* (1978) that the dispersion coefficient ($\wp$) should be considered a function of moisture content (θ) only.

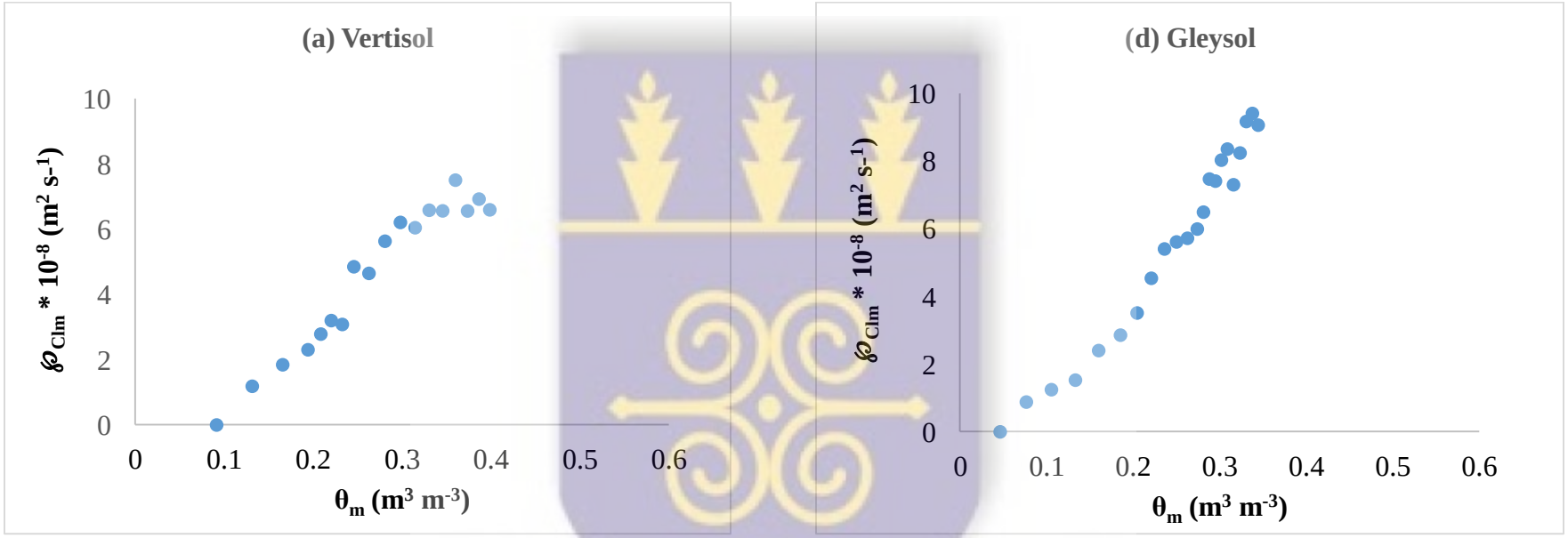

Fig. 5.6.1 **Dispersion coefficient of Cl_m^- during horizontal infiltration in soil**

Table 5. 6. 1 Dispersion coefficient for chloride ($\wp_{Cl}$) with θ_{im} and without θ_{im} and corresponding θ in two soils during infiltration experiment

Soil	($\wp_{Clm}$) with (m^2 s^{-1})	($\wp_{Cl}$) without θ_{im} (m^2 s^{-1})
Eutric Vertisol	7.51×10^{-8}	2.33×10^{-7}
θ (m^3 m^{-3})	***0.36***	***0.46***
Eutric Gleysol	1.05×10^{-6}	1.55×10^{-6}
θ (m^3 m^{-3})	***0.26***	***0.37***

CHAPTER SIX

CONCLUSIONS AND RECOMMENDATIONS

6.1 Conclusions

A horizontal flow study using potassium chloride (KCl) and chlorpyrifos as infiltration solutions was conducted in columns of repacked soil in the laboratory. Based on the results obtained, the following conclusions are noted.

6.1.1 Infiltration profiles of moisture and solutes

The study concludes that similarity was preserved in the water content, agrochemical profile relationship with regards to the variable $\lambda = xt^{-1/2}$. Therefore, it could be concluded that soil water diffusivity and the dispersion coefficients in the respective flow equations may be considered to be functions of water content only. In all instances the chloride front moved ahead of the water front during the infiltration process except in the Ferrasol where the chloride concentration front lagged behind that of the water. Also, the concentration front for the insecticide and K^+ were similar in the Lixisol. The Vertisol had the insecticide concentration profile moving behind that of the other agrochemical compounds. It is therefore concluded that agrochemical transport is generally faster in the sandy loams than the sandy clays.

6.1.2 Soil moisture diffusivity

It was observed in the study that higher soil moisture diffusivity function was recorded in the sandy loams as against the sandy clay soil. Probably due to the relatively large number of small pore sizes, the Vertisol had lower moisture diffusivity function in all instances. It is therefore concluded that soil texture and by extension the pore size distribution has a dominant influence on the process of infiltration in soils.

6.1.3 Infiltration adsorption isotherms

The results from the infiltration experiments showed that adsorption isotherms obtained during the horizontal infiltration experiments were curvilinear, thus conforming to the Langmuir type. Also, the high CEC of the Vertisol led to higher amounts of adsorption of the interacting solutes. It is concluded that the clay content, the type of clay as well as the organic matter content of the soil exert considerable influence on the mobility of agrochemical compounds in soils.

6.1.4 Dispersion of agrochemicals in soil

The notional plane for the insecticide lagged behind that of water and all the other agrochemical compounds in most of the soils used in the infiltration study except, the Ferric Lixisol where it was similar to the plane of Potassium. While the plane of the chloride moved ahead of the water as a result of anion exclusion and the presence of immobile water in the Eutric Vertisol and Eutric Gleysol, it lagged behind the notional plane of water in the Xanthic Ferrasol due to the presence of oxides of iron and aluminum. Additionally, the agrochemical concentration fronts were predominantly larger in all the sandy loams relative to the sandy clay. Within the sandy loams, there were marked differences in agrochemical movement due to differences in soil properties. It is thus concluded that mobility of agrochemical compounds is not the same in the soils used for the study.

6.1.5 Establishment of immobile water content

Differences between the plane of separation of the encroaching and antecedent water and the plane of dispersion of the non-interacting solute is ascribed to the presence of immobile water content. The difference between the two planes was found to be larger in the Vertisol. It may be concluded that the size of the immobile water content in soil is affected by the texture of soil as well as the pore size distribution.

6.2 Recommendation

- The KCl concentration front in the Vertisol during the horizontal infiltration was 1.56 x 10^{-3} (m $s^{-1/2}$) indicating that should a farmer be using the fertilizer on Akuse series near the Volta Lake, a minimum buffer zone of 68 metres from the shore-line should be allowed, to minimize pollution of the water body with chloride.
- For the application of KCl on a Ferrasol near a water body, a buffer zone of not less than 95 metres from the bank should be considered.
- Farmers using muriate of potash on Bediesie series within the Afram plains are to create a buffer zone of not less than 116 metres from the banks of the Volta Lake.
- Similarly, farmers are advised to leave a buffer zone of not less than 84 metres from the bank of the Volta Lake when using muriate of potash on Lima series.

Recommendation for further research

- Simultaneous horizontal and vertical infiltration of fertilizer material and pesticide compound should be considered in future research.

REFERENCES

Abdul A. S. and Gibson T. L. 1986. Equilibrium batch experiments with six polycyclic aromatic hydrocarbons and two aquifer materials. *Hazardous Waste and Hazardous Materials* 3, 125-137.

Acquaah, S. O. 1997. Lindane and Endosulfan Residues in Water and Fish in the Ashanti Region of Ghana. *Proceedings of Symposium on Environmental Behaviour of Crop Protection Chemicals by the IAEA/FAO*, IAEA, Vienna, 1-5 July, 1997.

Addiscott, T. M. and Wagenet, R. J. (1985). Concepts of Solute Leaching in Soils: a Review of Modeling Approaches. J. Soil Sci. 36: 411 – 424.

Adiku, S.K. 1982. Movement of salt and water near crystalline salt in relatively dry soils: The effect of relative sizes of salt crystals and soil aggregates. BSc. Dissertation, University of Ghana, Ghana.

Adu, S. V. and Mensah-Ansah, J. A. 1995. *Soils of the Afram Plains Basin, Ghana*. Memoir No. 11. CSIR-Soil Research Institute, Kwadaso, Kumasi.

Allison, L. E. (1965) Organic Carbon, Walkley – Black method. In: C. A. Black, D. D. Evans, J. L. White, L. E. Ensminger and F. E. Clark (eds). *Methods of soil analysis. Part 2, Chemical and Microbiological properties*. American Society of Agronomy Inc. Madison, Wisconsin. pp. 1372-1376.

Amatekpor, J.K. and Dowuona, G.N.N. 1995. Site characterization. IBSRAM Vertisol Project. Department of Soil Science, University of Ghana, Legon. 42pp.

Aoda, M. I., Nedawi, D. R. and Abdel-Rassul, I. A. 1993. Salts effects on water transport functions in an unsaturated soil. Iraqi J. Agric. Sci. 24(1):20-29.

Aoda, M.I. and Younan, T.F. 2010. Calculation of soil water diffusivity using a model for soil moisture profile under different salinity conditions. Journal of Engineering 1 (16): 4569 – 4579.

Armah, A. K., Dapaah, G. A. and Wiafi, G. 1999. Water Quality Studies on Two Irrigation Associated Rivers in Southern Ghana. *Journal of Ghana Science Association*, Vol. 1, 2: 100-109.

Arthur, B. K. 2010. Simultaneous Movement of Ammonium and Potassium during Unsaturated Transient Water Flow in Soil. M. Phil Thesis, University of Ghana. Ghana.

Asiamah, R. D. 1995. *Soils of the Ho-Keta Plains, Volta Region, Ghana*. Memoir No. 10. CSIR-Soil Research Institute, Kwadaso, Kumasi.

Attila, K. and Diana, V. 2009. Photostability and photodegradation pathways of distinctive pesticides. Journal of Environmental Quality. 38(1):157–163.

Barbash, J. E. and Resek, E. A. 1996. Pesticides in Ground Water: Distribution, Trends, and Governing Factors. *Pesticides in the Hydrologic System* series 2, Ann Arbor Press, Chelsea, Michigan, 590 p.

Biggar, J. W. and Nielsen, D. R. (1962). Miscible Displacement: II. Behaviour of Tracers. Soil Sci. Soc. Am. Proc., 26: 125 – 128.

Blake, G.R. and K.H. Hartge. 1986. Particle density. Pages 377-382. In A. Klute (Ed.), Methods of Soil Analysis. Part 1- Physical and Mineralogical methods. Second Edition. Agronomy No.

9. Part 1. America Society of Agronomy and Soil Science Society of America, Madison, Wisconsin, USA.

Blonquist, J. M., Jones, S. B., Lebron, I. and Robinson, D. A. 2006. Microstructural and phase configurational effects determining water content: Dielectric relationships of aggregated porous media. Water Resources Research, vol. 42, W05424, doi:10.1029/2005WR004418.

Braids, O.C. 1981. *Seminar on the Fundamentals of Groundwater Quality Protection*, Geraghty and Miller Inc. and Am. Ecology Services Inc., Oct. 5-6.

Brand, E.W. and Philipson, H.B. 1985. Review of international practice for the sampling and testing of residual soils, in Brand, E.W. and Philipson, H.B. (eds) Sampling and Testing of Residual soils: A Review of International Practices. Technical Committee on Sampling and Testing of Residual Soils, International Society for Soil Mechanics and Foundation Engineering, 7–22.

Bray, R.H. and Kurtz, L.T. 1945. Determination of total organic and available forms of phosphorus in soils. Soil Science, 59, 39 – 45.

Brennan, R.D. and Silberberg, M.Y. 1968. The system 360 Continuous System Modeling Program. Simulation 11: 301-308.

Calamari, D. and Naeve, H. 1994. *Review of Pollution in the African Aquatic Environment.* Committee for Inland Fisheries of Africa (CIFA) Technical Paper No. 25. FAO, Rome.

Carslaw, J.S. and Jaeger, J.C. 1959. Conduction of Heat in Solids. Oxford Univ. Press (Clarendon). London and New York. pp. 59.

Carvalho, F.P. 2006. Agriculture, pesticides, food security and food safety. *Environmental Science & Policy* 9:685-692.

Cerejeira, M.J., Viana, P., Batista, S., Pereira, T., Silva, E., Valerio, M.J., Silva, A., Ferreira, M., and Silva-Fernandes, A.M. 2003. Pesticides in Portuguese surface and ground waters. *Water Research* 37:1055-1063.

Chapman, R. A., and Cole, C. M. 1982a. Observations on the influence of water and soil pH on the persistence of insecticides. Journal of Environmental Science and Health, Part B 15:39–46.

Chapman, R.R. and Cole, C.M., 1982b. Observations on the influence of water and soil pH on the persistence of insecticides: Journal of Environmental Science and Health. vol. B (17), no. 5, p. 487-504.

Chen, Y. X., Chen, H. L., Xu, Y. T. and Shen, M. W. 2004. Irreversible sorption of pentachlorophenol to sediments: experimental observation. Environ Int. 30:31- 37.

Chiou, C. T., Kile D. E., and Malcolm R. L. 1988. Sorption of vapors of some organic liquids on soil humic acid and its relation to partitioning of compounds in soil organic matter. *Environ. Sci. Technol.* **22**, 298-303.

Chiou, C. T., Porter, P. E. and Schmedding, D. W. 1983. Partitioning equilibria of nonionic compounds between soil organic matter and water. Environ Sci. Technol. 17:227-231.

Chrisanto, T., Sanchez-Martin, M.J. and Sanchez-Camazano, M. 2000. Mobility of pesticides in soils: Influence of soil properties and pesticide structure. Toxicol. Environ. Chem., 47: 97 – 104.

Coats, K.H., and Smith, B. D. 1964. Dead-end pore volume and dispersion in porous media. SPE Journal 46:73-84.

Cooper, J. and Dobson, H. 2007. The benefits of pesticides to mankind and the environment. Crop Protection 26(9):1337–1348.

Dabrowski, J. M., Peall. S. K. C., Reinecke, A. J., Liess, M. and Schulz, R. 2002. Runoff-related pesticide input into the Lourens River, South Africa: basic data for exposure assessment and risk mitigation at the catchment scale. Water, Air, Soil Pollution 135 (1–4):265–283.

Darko, G. and Acquaah, S. O. 2008. Levels of Organochlorine Pesticide Residues in Diary Products in Kumasi, Ghana. *Chemosphere*, Vol. 71, No. 2: 294-298. doi:10.1016/j.chemosphere.2007.09.005.

Davey, R. B., Meisch, M. V. and Carter, F. L. 1976. Toxicity of five rice field pesticides to the mosquitofish, Gambusia affinis and green sunfish, Lepomis cyanellus, under laboratory and field conditions in Arkansas. Environ Entomol. 5(6):1053–1056.

Day, P.R. 1965. Particle fractionation and particle-size analysis. In: Black, C.A., Evans, D.D., White, J.L., Ensminger, L.E. and Clark, F.E. (Eds.), Methods of soil analysis, Part 1. Physical and mineralogical properties, including statistics of measurement and sampling. American Society of Agronomy, Inc. pp. 545-567.

Dinham, B. 2003. Growing vegetables in developing countries for local urban populations and export markets: problems confronting small-scale producers. *Pest Management Science* 59:575-582. doi:10.1002/ps.654.

Đurović, R., Gajić-Umiljendić, J., and Đorđević, T. 2009. Effects of Organic Matter and Clay Content in Soil on Pesticide Adsorption Processes. Pesticides Phytomedicine (Belgrade) 24, 51-57.

Dowuona, G.N.N. 1985. Correlation of Ghanaian system of soil classification with other international systems. M.Sc. Soil Sci. Thesis. University of Ghana, Legon, Accra. 220 pp.

Dwomo, O. and Dedzoe, C. D. 2006. Oxisol (Ferrasol) Development in two Agro-Ecological Zones of Ghana; A Preliminary Evaluation of Some Profiles. Technical Report No. 582. CSIR-Soil Research Institute, Kwadaso, Kumasi.

Eaton, D. L., Daroff, R. B., Autrup, H., Bridges, J., Buffler, P., Costa, L. G., Coyle, J., McKhann, G., Mobley, W. C., Nadel, L., Neubert, D., Schulte-Hermann, R. and Spencer, P. S. 2008. Review of the toxicology of chlorpyrifos with an emphasis on human exposure and neurodevelopment. Critical Review of Toxicology. 2:1–125.

Eddleston, M., Karalliedde, L., Buckley, N., Fernando, R., Hutchinson, G,, Isbister, G., Konradsen, F., Murray, D., Piola, J. C., Senanayake, N., Sheriff, R., Singh, S., Siwach, S. B. and Smit, L. 2002. Pesticide poisoning in the developing world – a minimum pesticides list. Lancet 360(9340):1163–1167.

Elrick, D.E., Laryea, K.B. and Groenevelt, P.H. 1979. Hydrodynamic dispersion during Infiltration of water in soil. Soil Sci. Soc. Am. J. 43:856-865.

Essumang, D. K Togoh, G. K. and Chokky, L. 2009. Pesticide Residues in the Water and Fish (Lagoon Tilapia) Samples from Lagoons in Ghana. *Bulletin of the Chemical Society of Ethiopia*, Vol. 23, 1: 19-27.

FAO/WHO (2000) *Pesticide residues in food — 1999 evaluations. Part II — Toxicological*. Geneva, World Health Organization, Joint FAO/WHO Meeting on Pesticide Residues (WHO/PCS/00.4).

Fianko, J. R., Donkor, A., Lowor, S. T. and Yeboah, P. O. 2011. Agrochemicals and the Ghanaian Environment, a review. Journal of Environmental Protection. 2: 221-230.

unda, C. T., Sonay, S. O., and Sabine, G. 2014. Specific Surface Area Effect on Adsorption of Chlorpyrifos and TCP by Soils and Modelling. Soil and Sediment Contamination: An International Journal. DOI:=10.1080/15320383.2014.912610.

Gebremariam, S. Y. and Beutel, M. W. 2010. Effects of drain-fill cycling on chlorpyrifos mineralization in wetland sediment-water microcosms. Chemosphere 78(11):1337–1341.

Gebremariam, S. Y., Beutel, M. W., Yonge, D. R., Flury, M. and Harsh, J. B. 2012. Adsorption and Desorption of Chlorpyrifos to Soils and Sediments. In D.M. Whitacre (ed.), *Reviews of Environmental Contamination and Toxicology*. DOI 10.1007/978-1-4614-1463-6_3, Springer Science and Business Media, LLC. p 124 - 161

Getzin, L. W. 1985. Factors influencing the persistence and effectiveness of chlorpyrifos in soil. Journ. Econ. Entomol 78:412–418.

Halimah, M., Tan, Y. A., Ismail, S. and Nashriyah, M. 2010. Downward movement of chloropyrifos in the soil of an oil palm plantation in Sepang, Selangor, Malaysia. Journal of Oil Palm Research. Vol. 22 p 721 – 728.

Hillel, D. 1998. Environmental Soil Physics. Academic Press, New York, USA, 771p

Hillel, D. 2004. Introduction to Environmental Soil Physics. Kindle Edition. Elsevier Academic Press. http://www.academicpress.com

Hesse, P. R. (1971) *A textbook of soil chemical analysis*. John Muray Publishers Ltd. New York

Huang, X and Lee, L. S. 2001. Effect of dissolved organic matter from animal waste effluent on chlorpyrifos sorption on soil. Journal of Environmental Quality 30: 1258 – 1265.

Huber, A., Bach, M., Frede, H.G. 2000. Pollution of surface waters with pesticides in Germany: modeling non-point source inputs. *Agriculture Ecosystems and Environment* 80:191-204.

IBM Corporation. 1972. System/360 Continuous System Modeling Program. User's Manual, 5th Edition, GH20-0367-4. Data Processing Division, IBM, White Plains, USA.

Karanth, S. and Pope, C. 2000. Carbosylesterase and A-Esterase Activities during Maturation and Aging: Relationship to the toxicity of Chlorpyrifos and Parathion in Rats. *Toxicol. Sci.* 58, 282-289.

Kidd, H. and James, D. R. 1991. The Agrochemicals Handbook. A 0791/Aug. 91. Third edition. Unwin Brothers Ltd. Old Working, Surney. p 3 – 11.

Kidd, K.A., Bootsma, H.A. and Hesslein, R.H. 2001. Biomagnification of DDT through the benthic and pelagic food webs of Lake Malawi, East Africa: Importance of trophic level and carbon source. Environmental Science and Technology 35:14-20.

Konda, L. N., Czinkota, I., Fuleky, G., Morovjan, G. (2002). Modeling of single-step and multistep adsorption isotherms of organic pesticides on soil. Journal of Agricultural and Food Chemistry, 50:7326-7331.

Laabs, V. and Amelung, W. 2005. Sorption and aging corn and soybean pesticides in tropical soils in Brasil. J Agric Food Chem 53, 7184-7194.

Lal, R and Shukla, M. K. 2002. Principles of Soil Physics. Marcel Dekker Inc. New York. pp 355 – 379.

Landon, J.R. (Ed.), 1991. Booker tropical soil manual: A Handbook for Soil Survey and Agricultural Land Evaluation in the Tropics and Subtropics., New York. 474p.

Larson, S. J., Capel, P. D., Goolsby, D. A., Zaugg, S. D. and Sandstrom, M. W. 1995. Relations between pesticide use and riverine flux in the Mississippi River Basin. Chemosphere 31:3305–3321.

Laryea, K.B. 1979. Solute dispersion in soil. Ph.D Thesis. University of Guelph, Canada.

Laryea, K.B., Elrick, D.E. and Robin M.J.L. 1982. Hydrodynamic dispersion involving cationic adsorption during unsaturated, transient water flow in soil. Soil Sci. Soc. Am. J. 46: 666-671.

Lewis, R. A. 1998. *Lewis' Dictionary of Toxicology*; Lewis Publishers: New York. pp 681 - 1030.

McCarthy J. F. and Jiminez B. D. (1985) Interactions between polycyclic aromatic hydrocarbons and dissolved humic material; binding and dissociation. *Environ. Sci. Technol.* **19**, 1072-1076.

Merrington, G., Winder, L., Parkinson, R. and Redman, M. 2002. Agricultural Pollution. Spon Press, London, UK. 243 pp.

(MOFA) Ministry of Food and Agriculture, 2003. Agriculture in Ghana: Facts and Figures," Produced by the Statistics, Research and Information Directorate, Accra.

Ministry of Food and Agriculture (MOFA), 2014. Agriculture in Ghana: Facts and Figures," Produced by the Statistics, Research and Information Directorate, Accra.

Moldrup P., Poulsen T. G., Rolston D. E., Yamaguchi T., and Hansen J. A. 1994. Integrated flux model for unsteady transport of trace organic chemicals in soils. *Soil Science* **157**, 137-152.

Morrill, L.G., Mahilum, B.C. and Mohiuddin, S.H. 1982. Organic compounds in Soils: Sorption, Degradation and Persistence. Ann Arbor Science, 326p.

Murphy, J. and Riley, J.P. 1962. A modified single solution method for the determination for the determination of phosphate in natural waters. Anal. Chim. Acta 27: 31 – 36.

Murray, R. T., von Stein, C., Kennedy, I. R., and Sanchez-Bayo, F. 2001. Stability of chlorpyrifos for termiticidal control in six Australian soils. Journ. Agric Food Chem 49(6):2844–2847.

Nair, A. S. and Pradeep, T. 2007. Extraction of Chlorpyrifos and Malathion from Water by Metal Nanoparticles. Journal of Nanoscience and Nanotechnology 7, 1–7.

Nielsen, D.R. and Biggar, J.W. 1961. Miscible displacement in soils: Experimental information. Soil Sci. Soc. Am.Proc. 25, 1– 5.

Nielsen, D.R., Biggar, J.W. and Davidson, J.M., 1962. Experimental consideration of diffusion analysis in unsaturated flow problem. Soil Sci. Soc. Am. Proc. 26, 107–111.

Nielson, D. R., van Genuchten M. Th., and Bigger, J. W. 1986. Water flow and solute transport processes in the unsaturated zone. Water Resour. Res., 22(9): 89S-108S.

Ntow, J. W. 2007. Pesticide Residues in Volta Lake, Ghana," *Lakes and Reservoirs*: *Research and Management*, Vol. 10, 4: 243-248. doi:10.1111/j.1440-1770.2005.00278.

Ntow, W. J. 2001. Organochlorine Pesticides in Water, Sediments, Crops and Human Fluids in a Farming Community in Ghana. *Environmental Contamination and Toxicology*, Vol. 40, No. 4: 557-563. doi:10.1007/s002440010210 .

Ntow, W. J. 1998. Pesticide Misuse at Akumadan to be tackled. *NARP Newsletter*, Vol. 3, No. 3.

OECD Guidelines for the Testing of Chemicals (1997) Test No. 106: Adsorption - desorption using a batch equilibrium method. OECD Organization for Economic Co-Operation and Development. p 25 - 57

Oerke, E. C. 2006. Crop loses to pest. Journal of Agricultural Science 144:31–43.

Phogat, V.K., Agrawal, R.P., Oswal, M.C. and Kuhad, M.S. 1999.Laboratory Manual for Soil Physical Analysis. Dept. of Soil Science, CCS Haryana Agricultural University, India. pp. 13 – 18.

Pimentel, D. 1995. Amounts of pesticides reaching target pests: environmental impacts and ethics. Journal of Agriculture and Environ. Ethic 8:17–29.

Racke, K. D. 1993. Environmental fate of chlorpyrifos. Reviews of Environmental Contamination and Toxicology. 13:1–150.

Racke, K. D., Fontaine, D. D., Yoder, R. N. and Miller, J. R. 1994. Chlorpyrifos degradation in soil at termiticidal application rates. Pesticide Science. 42(1):43–51.

Radcliffe, D. E. and Rasmussen, T. C. 2002. Soil Water Movement. In A. W. Warrick (ed.), Soil

Roberts, T. R. and Hutson, D. H. 1999. *Metabolic Pathways of Agrochemicals - Part 2: Insecticides and Fungicides*. The Royal Society of Chemistry: Cambridge, UK. pp 235-242.

Robin, M.J.L., Laryea, K.B. and Elrick, D.E. 1983. Hydrodynamic dispersion during absorption of water by soil. 2 Immobile water. Journal of Hydrology, 65: 333-348.

Roh, J. Y. and Choi, J. 2008. Ecotoxicological evaluation of chlorpyrifos exposure on the Nematode Caenorhabditis elegans. Ecotoxicol Environ Saf. 71(2):483–489.

Sanchez, P. A. and Logan, T.J. 1992. Myths and science about the chemistry and fertility of soils in the tropics. *In* R. Lal and P. A. Sanchez. Myths and science of soils of the tropics. Soil Science Society of America special Publication no. 29. p 35 – 46.

Sattler, C., Kächele, H., and Verch, G. 2006. Assessing the intensity of pesticide use in agriculture. Agriculture, Ecosystems and Environment doi:10.1016/j.agee.2006.07.017.

Schimmel, S. C., Garnas, R. L., Patrick, J. M. Jr, and Moore, J. C. 1983. Acute toxicity, bioconcentration and persistence of AC 222,705, benthiocarb, chlorpyrifos, fenvalerate, methyl parathion and permethrin in the estuarine environment. J. Agric. Food Chem. 312 (1): 104 – 113.

Schwarzenbach R. P. and Westall J. (1981) Transport of nonpolar organic compounds from surface water to groundwater; laboratory sorption studies. *Environ. Sci. Technol.* **15**, 1360-1367. methyl parathion, and permethrin in the estuarine environment. Journal of Agriculture, Food and Chemistry. 31(1):104–113.

Shamshuddin, J., Fauziah, C. I., Anda, M., Kapok, J. and Shazana,M. A. R. S. 2011. Using Ground Basalt and/or Organic Fertilizer to Enhance Productivity of Acid Soils in Malaysia for Crop Production. Malaysian Journal of Soil Science, vol. 15: 127 – 146.

Shao, M. and Horton. R. 1998. Integral method for estimating soil and hydraulic properties. Soil Sci. Soc. Am. J. 62:585-592.

Singh, B.R, and Steinnes, E. 1994. Soil and water contamination by heavy metals. In: Lal R, Stewart A, editors. Soil processes and water quality. Advances in soil science. Boca Raton, Florida: Lewis Publishers: 233 - 271.

Site, A. D. 2001. Factors Affecting Sorption of Organic Compounds in Natural Sorbent/Water Systems and Sorption Coefficients for Selected Pollutants. A Review. Journ. Phys. Chem. Vol. 30, No. 1.

Smegal, D. C. 2000. *Human Health Risk Assessment Chlorpyrifos*; U.S. Environmental Protection Agency, Office of Prevention, Pesticides and Toxic Substances, Office of Pesticide Programs, Health Effects Division, U.S. Government Printing Office: Washington, DC. pp 1-131.

Smiles, D.E., Phillip, J.R. Knight, J.H. and Elrick, D.E. 1978. Hydrodynamic dispersion during absorption of water by soil. Soil Sci. Soc. Am. J. 42:229-234.

Smiles, D.E. and Phillip, J.R. 1978. Solute transport during unsteady unsaturated water flow in a clay soil. Soil Sci. Soc. Am. J. 46:9-14.

Solomon, K.R., Matthies, M. and Vighi, M. 2013. Assessment of PBTs in the EU: a critical assessment of the proposed evaluation scheme with reference to plant protection products. Environ Sci. EU 25:1–25.

Sparks, D.L. and Huang, P.M. 1985. Physical chemistry of soil potassium.. In R.D. Munson (ed.) Potassium in agriculture. American Societyof Agronomy, Madison, WI. p. .201-276

Speckhart, F.H. and Green, W.L. 1976. A guide to using CSMP-The Continuous System Modeling Program. A program for simulating physical systems. Prentice-Hall Inc., Englewood Cliffs, New Jersey. 325 pp.

Tabarzad, A., A. R. Sepaskhah, and T. Farnud. 2011. Determination of chemical transport properties for different textures of undistributed soils. *Archives of Agronomy and Soil Science* 57(8): 915–930.

Tagatz, M. E., Gregory, N. R. and Plaia, G. R. 1982. Effects of chlorpyrifos on fi eld- and laboratory-developed estuarine benthic communities. J Toxicol. Environ Health 10:411–421.

Thrasher, J. D., Gunnar, H. and Broughton, A. 2002. Immunological Abnormalities in Humans Chronically Exposed to Chlorpyrifos, Archives of Environmental Health, 57:181–187.

Tomlin, C. D. S. 2006. *The Pesticide Manual, A World Compendium*. 14th ed.; British Crop Protection Council: Alton, Hampshire, UK. pp 186-187.

U. S. Environmental Protection Agency 1986. Ambient water quality criteria for chlorpyrifos-1986. Report No EPA-440/5-86-005. U.S. EPA, Washington, DC.

United States Environmental Protection Agency. 1999. *Reregistration Eligibility Science Chapter for Chlorpyrifos, Fate and Environmental Risk Assessment.* Environmental Chemistry Laboratory, Office of Prevention, Pesticides and Toxic Substances, Office of Pesticide Programs, Environmental Fate and Effects Division, U.S. Government Printing Office: Washington, DC.

United States Department of Health and Human Services. 1997. *Toxicological Profile for Chlorpyrifos*. Agency for Toxic Substances and Disease Registry, Public Health Service: Atlanta.

United States Environmental Protection Agency. 1999. Reregistration Eligibility Science Chapter for Chlorpyrifos, Fate and Environmental Risk Assessment. Office of Prevention, Pesticides and Toxic Substances, Office of Pesticide Programs, Environmental Fate and Effects Division, U.S. Government Printing Office: Washington, DC.

U. S. Environmental Protection Agency. 2006. *Reregistration Eligibility Decision (RED) for Chlorpyrifos*; Office of Prevention, Pesticides and Toxic Substances, Office of Pesticide Programs, U.S. Government Printing Office: Washington, DC.

Van Emmerik, T.J., Angove, M.J., Johnson, B.B. and Wells, J.D. 2007. Sorption of chlorpyrifos to selected minerals and the effect of humic acid. *J. Agric. Food Chem*. 55: 7527-7533.

van Genuchten, M.T., and. Wierenga. P.J. 1976. Mass-Transfer Studies in Sorbing Porous-Media .1. Analytical Solutions. Soil Sci. Soc. Am. J. 40:473-480.

Vanderborght, J., Jacques, D. and Feyen. J. 2000. Deriving transport parameters from transient flow leaching experiments by approximate steady-state flow convection dispersion models. Soil Sci. Soc. Am. J. 64:1317-1327.

Vereecken, H., J. Maes, and J. Feyen. 1990. Estimating Unsaturated Hydraulic Conductivity from Easily Measured Soil Properties. Soil Sci. 149:1-12.

Wang, Q., Shao, M. and Horton. R. 2004. A simple method for estimating water diffusivity of unsaturated soils. Soil Sci. Soc. Am. J. 68: 713-718.

Wang, T.C. and Hoffman, M.E., 1991, Degradation of organophosphorus pesticides in coastal water: Journal of the Association of Official Analytical Chemists, vol. 74, no. 5, p. 883-886.

Walker, A., Cotterill, E.G and Welch, S.J. 1989. Adsorption and degradation of chlorsulfuron and metsulfuron-methyl and triasulfuron in soils from different depths. Weed Sci. 29: 281 – 287.

Walker, A. and Exposito, M.J. 1998. Adsorption of isoproturon, diuron and metsulfuron methyl in two soils at high soil-solution ratio. Weed Res., 38:229 – 238.

Walkley, A. and I.A. Black. 1934. An examination of the Degtjareff method for determining soil organic matter, and a proposed modification of the chronic acid titration method. Soil Sci. 34: 29-38.

Wauchope R. D., Yeh S., Linders J. B. H. J., Kloskowski R., Tanaka K., Rubin B., Katayama A., Kördel W., Gerstl Z., Lane M., Unsworth J. B. 2002. Pesticide soil sorption parameters: theory, measurement, uses, limitations and reliability. Pestici. Manag. Sci. 58:419-445.

Wesseling, C., Corriols, M. and Bravo, V. 2005. Acute pesticide poisoning and pesticide registration in Central America. Toxicol. Appl. Pharmacol. 207:S697–S705.

Weber, W. J., McGinley, P. M. and Katz, L. E. 1991. Sorption phenomena in subsurface system: concepts, models and effects on contaminant fate and transport. Water Res; 25:499-528.

White, R. E., Heng, L.K. and Edis, R. B. 1998. Transfer function approached to modelling solute transport in soils. In: H. M. Selim and L. Ma (eds.), physical non-equilibrium in soils. Ann Arbor Press, Michigan, pp 311-346.

Wild, A. 2006. Soils and the Environment. Cambridge University Press, Cambridge. UK. pp 89 – 106.

Yeboah, F. A., Mensah, F. O. and Afreh, A. K. 2004. The Probable Toxic Effects of Aerosol Pesticides on Hepatic Function among Farmers at Akomadan/Afrancho Traditional Area of Ghana. *Journal of Ghana Science Association*. Vol. 6, 2: 39-43.

Zepp, R. G. and P. F. Schlotzhauer. 1983. Influence of algae on photolysis rates of chemicals in water. *Environmental Science and Technology* 17:462-468.

APPENDIX A

Recall equations [3.7], [3.8a] and [3.8b] which are respectively

$$-\frac{\lambda}{2}\frac{d\theta}{d\lambda} = \frac{d}{d\lambda}\left[D(\theta)\frac{d\theta}{d\lambda}\right] \quad [A1]$$

$$\lambda = \infty, \theta = \theta_n \quad [A2a]$$

$$\lambda = 0, \theta = \theta_o \quad [A2b]$$

Multiplying equation [A1] through by $d\lambda$ gives,

$$-\frac{\lambda}{2}\frac{d\theta}{d\lambda}d\lambda = \frac{d}{d\lambda}\left[D(\theta)\frac{d\theta}{d\lambda}\right]d\lambda \quad [A3]$$

Which upon integration using equation [A2a] and [A2b] as limits yield,

$$-\int_{\theta_n}^{\theta}\frac{\lambda}{2}d\theta = \int_{\lambda_\infty}^{\lambda}\frac{d}{d\lambda}\left[D(\theta)\frac{d\theta}{d\lambda}\right]d\lambda \quad [A4]$$

$$-\frac{1}{2}\int_{\theta_n}^{\theta}\lambda d\theta = D(\theta)\frac{d\theta}{d\lambda}\downarrow_{\lambda} - D(\theta)\frac{d\theta}{d\lambda}\downarrow_{\infty} \quad [A5]$$

But, $D(\theta)\frac{d\theta}{d\lambda}\downarrow_{\infty} = 0$

Therefore, $D(\theta)\frac{d\theta}{d\lambda} = -\frac{1}{2}\int_{\theta_n}^{\theta}\lambda d\theta$ [A6]

$$D(\theta) = -\frac{1}{2}\frac{d\lambda}{d\theta}\int_{\theta_n}^{\theta}\lambda d\theta \quad [A7]$$

APPENDIX: B

Solution for soil dispersion coefficient D (θ) for the transport of a non-interacting solute under horizontal transient state conditions.

The combined flux of solute $= \begin{bmatrix} Convective \\ Flux \end{bmatrix} + \begin{bmatrix} Flux\ due \\ to\ diffusion \end{bmatrix} + \begin{bmatrix} Flux\ due\ to \\ hydrodynamic \\ dispersion \end{bmatrix}$

This may be represented mathematically as:

$$J_c = v\theta c - \theta D_{sh}\frac{dC}{dx} \quad [B1]$$

where, $J_c = flux\ of\ solute, v = pore\ water\ velocity, c = solute\ concentration,$

$\theta = volumetric\ water\ content, D_{sh} = hydrodynamic\ dispersion\ coefficient\ and$

$\frac{dc}{dx} = solute\ concentration\ gradient.$

In solute flow under horizontal transient state conditions, the flow velocity is so slow that the dispersion coefficient is considered a function of water content only. The flow of non-interacting solute through soil with time may thus be represented by recalling equation [3.25a], which is,

$$\frac{\partial(\theta C)}{\partial t} = -\frac{\partial(vC)}{\partial x} + \frac{\partial}{\partial x}\left[\theta D_s(\theta)\frac{\partial C}{\partial x}\right] \quad [B2]$$

Equation [B2] may be re-written as:

$$\frac{\partial(\theta C)}{\partial t} = \frac{\partial}{\partial x}\left[\theta D_s(\theta)\frac{\partial C}{\partial x}\right] - v\frac{\partial C}{\partial x} - C\frac{\partial v}{\partial x} \quad [B3]$$

From the continuity equation for water flow;

$$\frac{\partial \theta}{\partial t} = -\frac{\partial v}{\partial x} \quad [B4]$$

Using the chain rule, substitution of equation [B4] into the RHS of [B3] results in:

$$\theta\frac{\partial C}{\partial t} + C\frac{\partial \theta}{\partial t} = \frac{\partial}{\partial x}\left[\theta D_s(\theta)\frac{\partial C}{\partial x}\right] - v\frac{\partial C}{\partial x} + C\frac{\partial \theta}{\partial t} \quad [B5]$$

Equation [B5] may be re-written after cancellation of appropriate terms as:

$$\theta\frac{\partial C}{\partial t} = \frac{\partial}{\partial x}\left[\theta D_s(\theta)\frac{\partial C}{\partial x}\right] - v\frac{\partial C}{\partial x} \quad [B6]$$

From equation [3.4] under section 3.1:

$v = -D(\theta)\frac{\partial \theta}{\partial x}$. Therefore, equation [B6] may be written as:

$$\theta\frac{\partial C}{\partial t} = \frac{\partial}{\partial x}\left[\theta D_s(\theta)\frac{\partial C}{\partial x}\right] + D(\theta)\frac{\partial \theta}{\partial x}\frac{\partial C}{\partial x} \quad [B7]$$

The Boltzmann's variable $\lambda = xt^{-1/2}$ was then used for the transformation of the equation into an ordinary differential one.

$$\frac{\partial \lambda}{\partial x} = t^{-1/2} \quad [B8]$$

$$\frac{\partial \lambda}{\partial t} = -\frac{1}{2} x t^{-\frac{3}{2}}; \qquad \frac{\partial \lambda}{\partial t} = -\frac{1}{2} \lambda t^{-1} \quad [B9]$$

Equation [B7] may be written as:

$$\theta \frac{\partial C}{\partial \lambda} \frac{\partial \lambda}{\partial t} = \frac{\partial}{\partial \lambda} \left[\theta D_s(\theta) \frac{\partial C}{\partial \lambda} \frac{\partial \lambda}{\partial x} \right] \frac{\partial \lambda}{\partial x} + D(\theta) \frac{\partial \theta}{\partial \lambda} \frac{\partial \lambda}{\partial x} \frac{\partial C}{\partial \lambda} \frac{\partial \lambda}{\partial x} \quad [B10]$$

Cancellation of the appropriate terms and the application of the Boltzmann's transformation results in:

$$-\frac{\theta \lambda}{2} \frac{\partial C}{\partial \lambda} t^{-1} = t^{-\frac{1}{2}} \frac{\partial}{\partial \lambda} \left[\theta D_s(\theta) \frac{\partial C}{\partial \lambda} t^{-\frac{1}{2}} \right] + t^{-\frac{1}{2}} D(\theta) \frac{\partial \theta}{\partial \lambda} \frac{\partial C}{\partial \lambda} \quad [B11]$$

$$-\frac{\theta \lambda}{2} \frac{dC}{d\lambda} = \frac{d}{d\lambda} \left[\theta D_s(\theta) \frac{dC}{d\lambda} \right] + D(\theta) \frac{d\theta}{d\lambda} \frac{dC}{d\lambda} \quad [B12]$$

Equation [B12] may be re-arranged as:

$$-\frac{\theta \lambda}{2} \frac{dC}{\partial \lambda} - D(\theta) \frac{d\theta}{\partial \lambda} \frac{dC}{\partial \lambda} = \frac{d}{d\theta} \left[\theta D_s(\theta) \frac{dC}{d\lambda} \right] \quad [B13]$$

$$-\frac{dC}{d\lambda} \left(\frac{\theta \lambda}{2} + D(\theta) \frac{d\theta}{d\lambda} \right) = \frac{d}{d\lambda} \left[\theta D_s(\theta) \frac{dC}{d\lambda} \right] \quad [B14]$$

from equation [3.10] under section 3.1,

$D(\theta) = -\frac{1}{2} \frac{d\lambda}{d\theta} \int_{\theta_n}^{\theta} \lambda d\theta$, which upon substitution into equation [B14] results in:

$$-\frac{dC}{d\lambda} \left(\frac{\theta \lambda}{2} - \frac{1}{2} \int_{\theta_n}^{\theta} \lambda d\theta \right) = \frac{d}{d\lambda} \left[\theta D_s(\theta) \frac{dC}{d\lambda} \right] \quad [B15]$$

$$-\frac{1}{2} \frac{dC}{d\lambda} \left[\theta \lambda - \int_{\theta_n}^{\theta} \lambda d\theta \right] = \frac{d}{d\lambda} \left[\theta D_s(\theta) \frac{dC}{d\lambda} \right] \quad [B16]$$

Let $[\theta\lambda - \int_{\theta_n}^{\theta} \lambda d\theta] = g(\theta)$:

$$\frac{d}{d\lambda}\left[\theta D_s(\theta)\frac{dC}{d\lambda}\right] + \frac{g(\theta)}{2}\frac{dC}{d\lambda} = 0 \quad [B17]$$

$$\frac{d}{d\lambda}\left[\theta D_s(\theta)\frac{dc}{d\lambda}\right] = -\frac{g(\theta)}{2}\frac{dc}{d\lambda} \quad [B18]$$

Multiply through by $d\lambda$ and integrate from λ to $\lambda_{\to\infty}$

$$\int_{\lambda\to\infty}^{\lambda} \frac{d}{d\lambda}\left[\theta D_s(\theta)\frac{dc}{d\lambda}\right] d\lambda = -\frac{g(\theta)}{2}\frac{dc}{d\lambda}d\lambda \quad [B19]$$

$$\theta D_s(\theta)\frac{dC}{d\lambda}\downarrow_{\lambda} - \theta D(\theta)\frac{dC}{d\lambda}\downarrow_{\lambda\to\infty} = -\frac{1}{2}\int_{\lambda\to\infty}^{\lambda} g(\theta)\frac{dc}{d\lambda}d\lambda \quad [B20]$$

but, $\theta D(\theta)\frac{dC}{d\lambda}\downarrow_{\lambda\to\infty} = 0$

$$\theta D_s(\theta)\frac{dC}{d\lambda} = -\frac{1}{2}\int_{\lambda\to\infty}^{\lambda} g(\theta)\frac{dc}{d\lambda}d\lambda \quad [B21]$$

Accounting for immobile water content

According to Robin *et al.* (1983), total water content at any value of λ when immobile water content is considered is given by:

$$\theta = \theta_m + \theta_{im} \quad [B22]$$

Subsequently, the average concentration of solute at any λ is given as:

$$c = \frac{(\theta_m C_m + \theta_{im} C_{im})}{\theta} \quad [B23]$$

If the immobile water fraction is assumed to be constant, equation 3.31 may be written as:

$$c = \frac{\theta_m C_m + \theta_{im} C_{im}}{\theta_m} \quad [B24]$$

$$\frac{dC}{d\lambda} = \frac{d}{d\lambda}\left(\frac{\theta_m C_m}{\theta_m} + \frac{\theta_{im} C_{im}}{\theta_m}\right) \quad [B25]$$

$$\frac{dC}{d\lambda} = \frac{d}{d\lambda}\left(\frac{\theta_m C_m}{\theta_m}\right) + \frac{d}{d\lambda}\left(\frac{\theta_{im} C_{im}}{\theta_m}\right) \quad [B26]$$

But, $\frac{d}{d\lambda}\left(\frac{\theta_{im} C_{im}}{\theta_m}\right) = 0$, if we assume the immobile water fraction to be constant. Therefore,

$$\frac{dC}{d\lambda} = \frac{d}{d\lambda}\left(\frac{\theta_m C_m}{\theta_m}\right) \quad [B27]$$

Equation [C23] may be re-written after cancellation of appropriate terms as:

$$\frac{dC}{d\lambda} = \frac{d}{d\lambda}(C_m) \quad [B28]$$

According to the mobile-immobile model proposed by Robin *et al.* (1983), transport of a non-reactive solute takes place in the mobile water fraction. Therefore for chloride, equation [B17] may be written as:

$$\frac{d}{d\lambda}\left[\theta_m D_s \frac{dC_m^{Cl}}{d\lambda}\right] + \frac{g_m}{2}\frac{dC_m^{Cl}}{d\lambda} = 0 \quad [B29]$$

$$\frac{d}{d\lambda}\left[\theta_m D_s \frac{dC_m^{Cl}}{d\lambda}\right] = -\frac{g_m}{2}\frac{dC_m^{Cl}}{d\lambda} \quad [B30]$$

Multiply through by $d\lambda$,

$$d\left[\theta_m D_s \frac{dC_m^{Cl}}{d\lambda}\right] = -\frac{g_m}{2}\frac{dC_m^{Cl}}{d\lambda}_m . d\lambda \quad [B31]$$

Integrate both sides,

$$\theta_m D_s \frac{dC_m^{Cl}}{d\lambda} = -\frac{1}{2}\int_{\lambda\to\infty}^{\lambda} g_m \frac{dC_m^{Cl}}{d\lambda} . d\lambda \quad [B33]$$

Divide through by θ_m

$$D_s \frac{dC_m^{Cl}}{d\lambda} = -\frac{1}{2\theta_m}\int_{\lambda\to\infty}^{\lambda} g_m \frac{dC_m^{Cl}}{d\lambda}.d\lambda \qquad [B34]$$

Divide through by $\frac{dC_m^{Cl}}{d\lambda}$

$$D_s = -\frac{1}{2\theta_m}\frac{d\lambda}{dC_m^{Cl}}\int_{\lambda\to\infty}^{\lambda} g_m \frac{dC_m^{Cl}}{d\lambda}.d\lambda \qquad [B35]$$

APPENDIX: C

Solution for hydrodynamic dispersion coefficientD_s (θ) for the transport of an adsorbing solute under horizontal transient state conditions.

The flow of an adsorbing solute through soil with time may thus be represented mathematically as:

$$\frac{\partial(\theta C)}{\partial t} + \frac{\partial}{\partial t}(\rho S) = -\frac{\partial(vC)}{\partial x} + \frac{\partial}{\partial x}\left[\theta D_s(\theta)\frac{\partial C}{\partial x}\right] \qquad [C1]$$

Equation [C1] may be re-written as;

$$\frac{\partial(\theta C)}{\partial t} + \frac{\partial}{\partial t}(\rho S) = \frac{\partial}{\partial x}\left[\theta D_s(\theta)\frac{\partial C}{\partial x}\right] - \frac{\partial(vC)}{\partial x} \qquad [C2]$$

From the continuity equation for water flow;

$$\frac{\partial\theta}{\partial t} = -\frac{\partial v}{\partial x} \qquad [C3]$$

Substitution of equation [C3] into [C2] using the chain rule results in;

$$C\frac{\partial v}{\partial x} + \theta\frac{\partial C}{\partial t} + \rho\frac{\partial S}{\partial t} = \frac{\partial}{\partial x}\left[\theta D_s(\theta)\frac{\partial C}{\partial x}\right] - v\frac{\partial C}{\partial x} - C\frac{\partial v}{\partial x} \qquad [C4]$$

After cancellation of appropriate terms, equation [C4] may be re-written as;

$$\theta \frac{\partial C}{\partial t} + \rho \frac{\partial S}{\partial t} = \frac{\partial}{\partial x}\left[\theta D_s(\theta) \frac{\partial C}{\partial x}\right] - v \frac{\partial C}{\partial x} \quad [C5]$$

From equation [3.4] under section 3.1;

$v = -D(\theta) \frac{\partial \theta}{\partial x}$. Therefore, equation [C5] may be written as:

$$\theta \frac{\partial C}{\partial t} + \rho \frac{\partial S}{\partial t} = \frac{\partial}{\partial x}\left[\theta D_s(\theta) \frac{\partial C}{\partial x}\right] + D(\theta) \frac{\partial \theta}{\partial x} . \frac{\partial C}{\partial x} \quad [C6]$$

The Boltzmann's variable $\lambda = xt^{1/2}$ was then used for the transformation of the equation into an ordinary differential one.

$$\frac{\partial \lambda}{\partial x} = t^{-1/2} \quad [C7]$$

$$\frac{\partial \lambda}{\partial t} = -\frac{1}{2} x t^{-\frac{3}{2}}; \qquad \frac{\partial \lambda}{\partial t} = -\frac{1}{2} \lambda t^{-1} \quad [C8]$$

Equation [C6] may be re-written as:

$$\theta \frac{\partial C}{\partial \lambda} \frac{\partial \lambda}{\partial t} + \rho \frac{\partial S}{\partial \lambda} \frac{d\lambda}{dt} = \frac{\partial}{\partial \lambda}\left[\theta D_s(\theta) \frac{\partial C}{\partial \lambda} \frac{\partial \lambda}{\partial x}\right] \frac{\partial \lambda}{\partial x} + D(\theta) \frac{\partial \theta}{\partial \lambda} \frac{\partial \lambda}{\partial x} \frac{\partial C}{\partial \lambda} \frac{\partial \lambda}{\partial x} \quad [C9]$$

$$\theta \frac{\partial C}{\partial \lambda}\left(-\frac{1}{2} \lambda t^{-1}\right) - \rho \frac{\partial S}{\partial \lambda}\left(\frac{1}{2} \lambda t^{-1}\right) = \frac{\partial}{\partial \lambda}\left[\theta D_s(\theta) \frac{\partial C}{\partial \lambda}\left(t^{-\frac{1}{2}}\right)\right]\left(t^{-\frac{1}{2}}\right) + D(\theta) \frac{\partial \theta}{\partial \lambda} \frac{\partial C}{\partial \lambda}(t^{-1}) \quad [C10]$$

After cancellation of appropriate terms, equation [C10] may be written as:

$$-\frac{\theta \lambda}{2} \frac{dC}{d\lambda} - \frac{\lambda}{2} \rho \frac{dS}{d\lambda} = \frac{d}{d\lambda}\left[\theta D_s(\theta) \frac{dC}{d\lambda}\right] + D(\theta) \frac{d\theta}{d\lambda} \frac{dC}{d\lambda} \quad [C11]$$

$$\frac{d}{d\lambda}\left[\theta D_s(\theta) \frac{dC}{d\lambda}\right] + \frac{\lambda}{2} \frac{dC}{d\lambda} + \frac{\lambda}{2} \rho \frac{dS}{d\lambda} + D(\theta) \frac{d\theta}{d\lambda} \frac{dC}{d\lambda} = 0 \quad [C12]$$

$$\frac{d}{d\lambda}\left[\theta D_s(\theta) \frac{dC}{d\lambda}\right] + \frac{\lambda}{2} \frac{dC}{d\lambda} + \frac{\lambda}{2} D(\theta) \frac{d\theta}{d\lambda} \frac{dC}{d\lambda} + \frac{\lambda}{2} \rho \frac{dS}{d\lambda} = 0 \quad [C13]$$

$$\frac{d}{d\lambda}\left[\theta D_s(\theta)\frac{dC}{d\lambda}\right]+\frac{1}{2}\left(\lambda+2D(\theta)\frac{d\theta}{d\lambda}\right)\frac{dC}{d\lambda}+\frac{\lambda}{2}\rho\frac{dS}{d\lambda}=0 \quad [C14]$$

$$Let\ \left(\lambda+2D(\theta)\frac{d\theta}{d\lambda}\right)=g$$

$$\frac{d}{d\lambda}\left[\theta D_s(\theta)\frac{dC}{d\lambda}\right]+\frac{1}{2}g(\theta)\frac{dC}{d\lambda}+\frac{\lambda}{2}\rho\frac{dS}{d\lambda}=0 \quad [C15]$$

$$\frac{d}{d\lambda}\left[\theta D_s(\theta)\frac{dC}{d\lambda}\right]d\lambda=-\frac{1}{2}\left[g(\theta)\frac{dC}{d\lambda}+\lambda\rho\frac{dS}{d\lambda}\right] \quad [C16]$$

Multiply through by $d\lambda$ and integrate between the limits λ and $\lambda_{\to\infty}$

$$\theta D_s(\theta)\frac{dC}{d\lambda}\downarrow_{\lambda}-\theta D_s(\theta)\frac{dC}{d\lambda}\downarrow_{\lambda\to\infty}$$

but, $\left[\theta D_s(\theta)\frac{dC}{d\lambda}\downarrow_{\lambda\to\infty}\right]=0$ because, $\frac{dC}{d\lambda}$ is constant at $\lambda_{\to\infty}$

$$\int_{\lambda\to\infty}^{\lambda}\frac{d}{d\lambda}\left[\theta D_s(\theta)\frac{dC}{d\lambda}\right]d\lambda=-\frac{1}{2}\int_{\lambda\to\infty}^{\lambda}\left[g(\theta)\frac{dC}{d\lambda}+\lambda\rho\frac{dS}{d\lambda}\right]d\lambda \quad [C17]$$

Therefore,

$$\theta D_s(\theta)\frac{dC}{d\lambda}=-\frac{1}{2}\int_{\lambda\to\infty}^{\lambda}\left[g(\theta)\frac{dC}{d\lambda}+\lambda\rho\frac{dS}{d\lambda}\right]d\lambda \quad [C18]$$

Divide through by $\theta\frac{dC}{d\lambda}$

$$D_s(\theta)=-\frac{1}{2\theta}\frac{d\lambda}{dC}\int_{\lambda\to\infty}^{\lambda}\left[g(\theta)\frac{dC}{d\lambda}+\lambda\rho\frac{dS}{d\lambda}\right]d\lambda \quad [C19]$$

APPENDIX D

Integration by parts

$u = \lambda,$ $du = d\lambda$

$dv = d\theta,$ $v = \theta$

$\int_{\theta_n}^{\theta} \lambda d\theta = uv - \int v\, du$

$$\int_{\theta_n}^{\theta} \lambda d\theta = \theta\lambda\Big|_{\theta_n}^{\theta} - \int_{\lambda_n}^{\lambda} \theta d\lambda$$

Integration by parts, accounting for immobile water fraction

$$\boldsymbol{\theta_m \lambda - \int_{\theta_{mn}}^{\theta_m} \lambda(\theta_m) d\theta_m}$$

$u = \lambda,$ $du = d\lambda$

$dv = d\theta,$ $v = \theta$

$$\int_{\theta_n}^{\theta} \lambda d\theta = uv - \int v\, du$$

$$\theta_m \lambda]_{\theta_n}^{\theta} - \int_{\lambda_n}^{\lambda} \theta_m d\lambda$$

$$\theta_m\lambda - \theta_{mn}\lambda_n - \int_{\lambda_n}^{\lambda} \theta_m d\lambda$$

$$\theta_m\lambda - [\theta_m\lambda - \theta_{mn}\lambda_n - \int_{\lambda_n}^{\lambda} \theta_m d\lambda]$$

$$[\theta_m\lambda - \theta_m\lambda] + \theta_{mn}\lambda_n + \int_{\lambda_n}^{\lambda} \theta_m d\lambda$$

$$\theta_{mn}\lambda_n - \int_{\lambda}^{\lambda_n} \theta_m d\lambda$$

$$\theta_{mn}\lambda_n - [\int_0^{\lambda_n} \theta_m d\lambda - \int_0^{\lambda} \theta_m d\lambda\,]$$

$$\theta_{mn}\lambda_n - \int_0^{\lambda_n} \theta_m d\lambda + \int_0^{\lambda} \theta_m d\lambda$$

APPENDIX E

Calculations for Particle size distribution

Temperature of the suspension = 28 ℃

The hydrometer is calibrated at a suspension temperature of 19.4 ℃. For every degree difference above or below 19.4 ℃, the hydrometer reading of the suspension must be corrected by adding or subtracting 0.4 respectively. However, since it is impossible to take hydrometer readings more accurately than 0.5 g/L, corrections may be rationalized as follows (see Table B1 below):

Table B1 Correction factors for hydrometer readings in Bouyoucos method for particle size analysis.

Temperature (°C)	Correction to hydrometer reading
15.5	-1.5
16.0 - 17.0	-1.0
18.0 - 18.5	-0.5
19.0 - 20.0	0
20.5 - 21.0	+0.5
21.5 - 23.0	+1.0
23.5 - 24.0	+1.5

(Keen, 1931; Piper, 1944; Bouyoucos, 1951; Day, 1965; Baver et al, 1972)

$$\%\ Clay\ and\ Silt = \frac{(5\ minutes\ reading - correction\ for\ temperature)}{weight\ of\ sample} X100 \quad [B1]$$

$$\%\ Clay = \frac{(5\ hour reading - correction for temperature)}{weight of sample}\ X\ 100 \quad [B2]$$

$$\%\ Silt = \%(Clay and Silt) - \%\ Clay \quad [B3]$$

$$\%\ Sand = \frac{(ovendry weight of particles retained on the\ 47\ \mu m seive)}{weight of sample}\ X\ 100 \quad [B4]$$

APPENDIX F

Measurement of Saturated Hydraulic Conductivity.

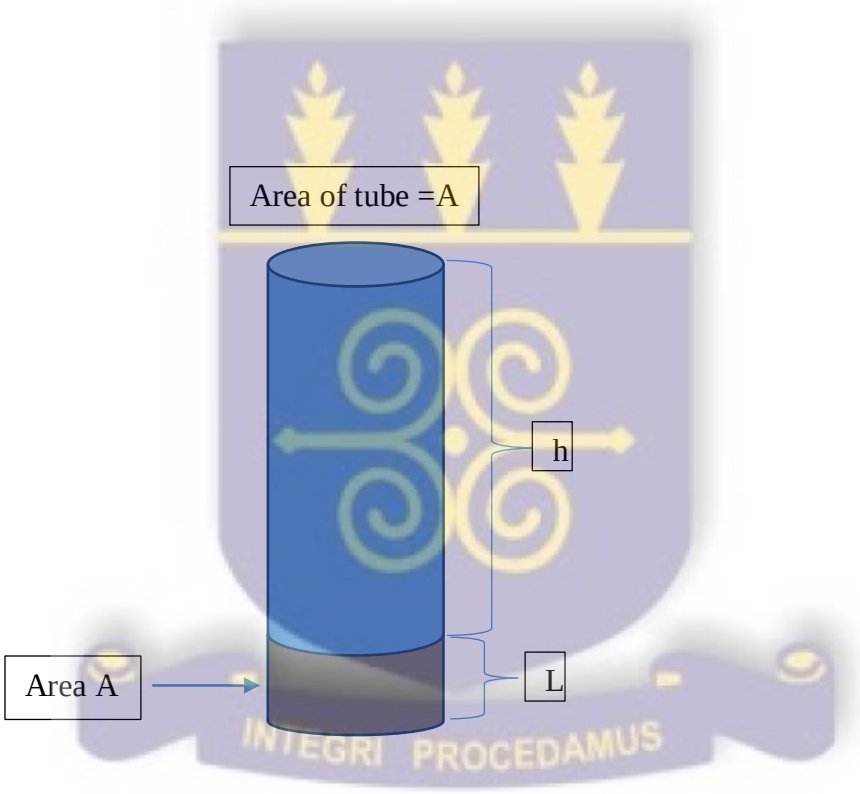

In this determination, Darcy's law is equated with the expression for flux density derived from the rate of decrease of ponding. The resulting expression is then integrated to derive a relationship for the saturated hydraulic conductivity (K_{sat}).

$$\frac{dQ}{dt} = \frac{KA\Delta\psi_h}{L} \quad [E1]$$

$$dQ = \frac{KA\Delta\psi_h}{L} dt \quad [E2]$$

Let $\Delta\psi_h = h + L \; and \; dQ = Adh$

$$Adh = \frac{KAh+L}{L} \quad [E3]$$

$$AdhL = KAh + L$$

$$K = \frac{AdhL}{Ah+L} \quad \rightarrow \quad K = \frac{dhL}{h+L} \quad [E4]$$

$$\int_{h_1}^{h} \frac{L}{h+L} dh = \int_{t_1}^{t} K \; ` \quad [E5]$$

$$at \; t = t_1, h = h_1$$

$$at \; t = t, h = h$$

$$Lln(h+L)]_{h_1}^{h} = Kt]_{t_1}^{t} \quad [E6]$$

$$Lln(h+L)]_{h_1}^{h} = K(t - t_1) \quad [E7]$$

$$L\ln(h+L) - L(h_1+L) = K(t - t_1)$$

$$L[\ln (h+L)/(h_1+L) = K(t - t_1) \quad [E8]$$

$$K = \frac{L[\ln (h+L)/(h_1+L)]}{(t-t_1)} \qquad [E9]$$

APPENDIX: G

CSMP Programme for calculating soil water diffusivity

```
TITLE CALCULATION OF SOIL WATER DIFFUSIVITY (AKUSE)

 INITIAL
  RENAME TIME = LAMDA
    INCON THETAO = 0.515, THETAN = 0.085, LAMDAN=2.1E-03, J=0
    PARAMETER DTHLAO=-40.0,KON2=1.0
    FUNCTION TBTHLA=(0.0,.515),(2.5E-04,.505),(5.0E-04,.495),...
    (7.5E-04,.47),(1.0E-03,.461),(1.25E-03,.422),(1.5E-03,.38),...
    (1.75E-03,.32),(1.875E-03,.25),(1.95E-03,.20),(2.0E-03,.09),...
    (2.1E-03,.085)
 DYNAMIC
      THLA = NLFGEN(TBTHLA,LAMDA)
      DTHLA = DERIV(DTHLAO,THLA)
      THETA1 = INTGRL(THETAO,DTHLA)
      C = INTGRL(0.0,THLA)
      KON1=THETAN*LAMDAN
      E=(THLA*LAMDA)-KON1
      D=-0.5*(E+KON2-C)/DTHLA
 TERMINAL
      PRINT D,E,THETA1,THLA,C,DTHLA
      TIMER FINTIM = 2.10E-03, PRDEL = 6.83E-05
      J = J+1
      KON2=C
   100 FORMAT(///'D,THLA,THETA1 = ',5E15.6)
    20 IF (J.GT.3) STOP
      CALL RERUN
```

```
    PAGE WIDTH=80
  END
  STOP
  ENDJOB
```

APPENDIX: H

CSMP programme for dispersion coefficient of chloride

```
TITLE CALCULATION OF DISPERSION COEFFICIENT FOR CHLORIDE (AKUSE)

  INITIAL
    RENAME TIME = LAMDA
      INCON THETAO=0.515,THETAN=0.085,LAMDAN=2.1E-03,J=0,...
      SEE0=2.25E-03,SEEN=1.0E-04
      PARAMETER THLAO=-40,KON2=1.0,SEELAO=-8.0E-02,KON3=1.0
      FUNCTION THETA=(0.0,.515),(2.5E-04,.505),(5.0E-04,.495),...
      (7.5E-04,.47),(1.0E-03,.461),(1.25E-03,.422),(1.5E-03,.38),...
      (1.75E-03,.32),(1.875E-03,.25),(1.95E-03,.20),(2.0E-03,.09),...
      (2.1E-03,.085)
      FUNCTION SEE=(0.0, 2.25E-03),(2.50E-04,2.23E-03),...
      (5.0E-04,2.22E-03),(6.25E-04,2.21E-03),(7.5E-04,2.205E-03),...
      (1.0E-03,2.2E-03),(1.25E-03,2.17E-03),(1.5E-03,2.08E-03),...
      (1.75E-03,2.0E-03),(1.875E-03,1.90E-03),(2.1E-03,1.8E-03),...
      (2.3E-03,1.6E-03),(2.5E-03,1.4E-03),(2.7E-03,1.0E-03),...
      (2.85E-03,1.0E-04)
  DYNAMIC
       THLA=NLFGEN(THETA,LAMDA)
       DTHLA=DERIV(THLAO,THLA)
       C=INTGRL(0.0,THLA)
       KON1=THETAN*LAMDAN
       E=(THLA*LAMDA)-KON1
       D=-0.5*(E+KON2-C)/DTHLA
       SEELA=NLFGEN(SEE,LAMDA)
       C1=DERIV(SEELAO,SEELA)
       LATHH=(THLA*LAMDA)+(2.0*D*DTHLA)
```

```
      GS=C1*LATHH
      HS=INTGRL(0.0,GS)
      HS1=KON3-HS
      THDS=(0.5*HS1)/C1
      DS=THDS/THLA
TERMINAL
      TIMER FINTIM=2.10E-03, PRDEL=6.83E-05
      PRINT D,LATHH,DS,SEELA,THLA
      J=J+1
      KON2=C
      KON3=HS
  100 FORMAT(///'D,DS,SEELA = ',3E15.6)
   20 IF (J.GT.5)STOP
      CALL RERUN
     PAGE WIDTH=80
END
STOP
END JOB
```

APPENDIX: I

CSMP programme for dispersion coefficient of potassium

```
TITLE CALCULATION OF DISPERSION COEFFICIENT FOR POTASSIUM (AKUSE)

 INITIAL
  RENAME TIME = LAMDA
   INCON THETAO=0.515,THETAN=0.085,LAMDAN=2.1E-03,J=0,...
   SEEK0=5.3E-05,SEEKN=9.0E-06
   PARAMETER THLAO=-40,KON2=1.0,SKLAO=-4.0E-03,KON3=1.0,...
   KON1=1.0,RHO=1.14
   FUNCTION THETA=(0.0,.515),(2.5E-04,.505),(5.0E-04,.495),...
   (7.5E-04,.47),(1.0E-03,.461),(1.25E-03,.422),(1.5E-03,.38),...
   (1.75E-03,.32),(1.875E-03,.25),(1.95E-03,.20),(2.0E-03,.09),...
   (2.1E-03,.085)
   FUNCTION SEEK=(0.0, 5.3E-05),(2.50E-04,5.2E-05),...
   (5.0E-04,4.8E-05),(7.5E-04,4.5E-05),(1.0E-03,4.0E-05),...
   (1.25E-03,3.6E-05),(1.5E-03,3.15E-05),(1.75E-03,2.5E-05),...
   (1.8E-03,2.2E-05),(1.85E-03,1.7E-05),(1.9E-03,9.0E-06)
   FUNCTION SORBK=(0.0,1.96E-03),(2.5E-04,1.9E-03),...
   (5.0E-04,1.85E-03),(7.5E-04,1.79E-03),(1.0E-03,1.45E-03),...
   (1.25E-03,1.65E-03),(1.5E-03,1.45E-03),(1.75E-03,1.2E-03),...
   (1.96E-03,9.0E-04),(2.0E-03,3.8E-04)
 DYNAMIC
     THLA=NLFGEN(THETA,LAMDA)
     DTHLA=DERIV(THLAO,THLA)
     THETA1=INTGRL(THETAO,DTHLA)
     C=INTGRL(0.0,THLA)
     KON1=THETAN*LAMDAN
     E=(THLA*LAMDA)-KON1
     D=-0.5*(E+KON2-C)/DTHLA
```

```
      SEEKLA=AFGEN(SEEK,LAMDA)
      ADSK=AFGEN(SORBK,SEEKLA)
      DSS=DERIV(SBKLAO,ADSK)
      DSEEK=DERIV(SKLAO,SEEKLA)
      E1=LAMDA*RHO*DSS
      LATHH=(THLA*LAMDA)+(2.0*D*DTHLA)
      NOSORT
      IF(DSEEK.EQ.0) DSEEK=-1.0E-20
      B=(LATHH*DSEEK)+E1
      B1=INTGRL(0.0,B)
      Y=-0.5*(KON3-B1)
      THDS=Y/DSEEK
      DS=THDS/THLA
  TERMINAL
      TIMER FINTIM=2.10E-03, PRDEL=7.0E-05
      PRINT D,DS,THLA,DSEEK,SEEKLA
      J=J+1
      KON2=C
      KON3=B1
      WRITE(6,100)D,DS,THLA,DSEEK,SEEKLA
  100 FORMAT(///'D,DS,THLA,DSEEK,SEEKLA = ',5E15.6)
   20 IF (J.GT.5)STOP
      CALL RERUN

     PAGE WIDTH=80
  END
  STOP
ENDJOB
```

APPENDIX: J

CSMP programme for the calculation of notional planes

```
TITLE INTERPOLATED DATA FOR THE CALCULATION OF NOTIONAL PLANE
(AKUSE)

 INITIAL
  RENAME TIME = LAMDA
    INCON THETAO=.515,THETAN=.085,LAMDAN=2.1E-03,J=0,...
    SEEO=2.25E-03,SEEN=1.0E-04,SEEKO=5.3E-05,SEEK=9.0E-06
    PARAMETER THLAO=-80.0,SEELAO=-40.0,SKLAO=-4.0E-03,...
    KON1=1.0,KON2=1.0,KON3=1.0
    FUNCTION TBTHLA=(0,.515),(2.5E-04,.50),(5.0E-04,.495),...
    (7.5E-04,.47),(1.0E-03,.461),(1.25E-03,.422),(1.5E-03,.38),...
    (1.75E-03,.32),(1.875E-03,.25),(1.95E-03,.20),(2.0E-03,.09),...
    (2.1E-03,.085)
    FUNCTION SEE=(0, 2.25E-03),(2.5E-04,2.23E-03),...
    (5.0E-04,2.22E-03),(6.25E-04,2.21E-03),(1.0E-03,2.2E-03),...
    (1.25E-03,2.17E-03),(1.5E-03,2.08E-03),(1.75E-03,2.0E-03),...
    (1.875E-03,1.9E-03),(2.1E-03,1.8E-03),(2.3E-03,1.6E-03),...
    (2.5E-03,1.4E-03),(2.7E-03,1.0E-03),(2.85E-03,1.0E-04)
    FUNCTION SEEK=(0,5.3E-05),(2.5E-04,5.2E-05),(5.0E-04,4.8E-05),...
    (7.5E-04,4.5E-05),(1.0E-03,4.0E-05),(1.25E-03,3.6E-05),...
    (1.5E-03,3.15E-05),(1.75E-03,2.5E-05),(1.8E-03,2.2E-05),...
    (1.85E-03,1.7E-05),(1.9E-03,9.0E-06)
 DYNAMIC
      THLA=NLFGEN(TBTHLA,LAMDA)
      C=INTGRL(0.0,THLA)
      E1=THLA*LAMDA
      E2=E1-(THETAN*LAMDAN)+KON1-C
      SEELA=NLFGEN(SEE,LAMDA)
```

```
      A1=SEEO-SEELA
      A=INTGRL(0.0,A1)
      B1=SEELA-SEEN
      B2=INTGRL(0.0,B1)
      B3=KON2-B2
      B4=A-B3
      SEEKLA=NLFGEN(SEEK,LAMDA)
      H1=SEEKO-SEEKLA
      H=INTGRL(0.0,H1)
      K1=SEEKLA-SEEKN
      K2=INTGRL(0.0,K1)
      K3=KON3-K2
      K4=H-K3
TERMINAL
      TIMER FINTIM = 2.10E-03, PRDEL = 7.0E-05
      PRINT E1,E2,B4,K4
      J=J+1
      KON1=C
      KON2=B2
      KON3=K2
      WRITE(6,100) E1,E2,B4,K4
  100 FORMAT(///'E1,E2,B4,K4 = ',4E15.6)
   20 IF (J.GT.5) STOP
      CALL RERUN

     PAGE WIDTH=80
END
STOP
ENDJOB
```

APPENDIX: K

CSMP programme for dispersion coefficient of chloride

```
TITLE CALCULATION OF DISPERSION COEFFICIENT FOR CHLORIDE
TAKING INTO ACCOUNT THE IMMOBILE WATER CONTENT (AKUSE)
 INITIAL
  RENAME TIME = LAMDA
     INCON THETAO=0.515,THETAN=0.085,LAMDAN=2.1E-03,J=0,...
     THETAI=0.0053,SEE0=2.25E-03,SEEN=1.0E-04,SEEIM=2.50E-04
     PARAMETER THLAO=-40,SEELAO=-8.0E-02,KON1=1.0,KON2=1.0
     FUNCTION THETA=(0.0,.515),(2.5E-04,.505),(5.0E-04,.495),...
     (7.5E-04,.470),(1.0E-03,.461),(1.25E-03,.422),(1.5E-03,.38),...
     (1.75E-03,.32),(1.875E-03,.25),(1.95E-03,.20),(2.0E-03,.09),...
     (2.10E-03,.085)
     FUNCTION SEE=(0.0,2.25E-03),(2.50E-04,2.23E-03),...
     (5.0E-04,2.22E-03),(6.25E-04,2.21E-03),(7.5E-04,2.205E-03),...
     (1.0E-03,2.2E-03),(1.25E-03,2.17E-03),(1.5E-03,2.08E-03),...
     (1.75E-03,2.0E-03),(1.875E-03,1.90E-03),(2.1E-03,1.8E-03),...
     (2.3E-03,1.6E-03),(2.5E-03,1.4E-03),(2.7E-03,1.0E-03),...
     (2.85E-03,1.0E-04)
 DYNAMIC
     THLA=NLFGEN(THETA,LAMDA)
     MTHLA=(THLA-THETAI)
     TETAMN=(THETAN-THETAI)
     KON3=TETAMN*LAMDAN
     SEELA=AFGEN(SEE,LAMDA)
     SEEMLA=(THLA*SEELA-THETAI*SEEIM)/MTHLA
     DSEMLA=DERIV(SEELAO,SEEMLA)
     A=(2*MTHLA*DSEMLA)
     GM=KON3-KON2+A1
     B1=GM*DSEMLA
     A1=INTGRL(0.0,MTHLA)
```

```
      B2=INTGRL(0.0,B1)
      DSCL=(KON1-B2)/A
  TERMINAL
      TIMER FINTIM=2.10E-03, PRDEL=7.0E-05
      PRINT DSCL,GM,MTHLA,SEEMLA,A1,B2
      J=J+1
      KON2=A1
      KON1=B2
      WRITE(6,100) DSCL,GM,MTHLA,SEEMLA,A1,B2
    100 FORMAT(///'DSCL,GM,MTHLA,SEEMLA,A1,B2= ',6E15.6)
     20 IF (J.GT.4) STOP
      CALL RERUN
      PAGE WIDTH=80
  END
  STOP
```

APPENDIX L1: Analysis of variance (ANOVA) for sand fractions of soil samples used in horizontal infiltration experiments

Source of variation	d.f.	s.s.	m.s.	v.r.	F. pr
Rep. stratum	2	14.020	7.010	1.27	
Soil	3	1022.095	340.698	61.60	<.001
Residual	6	33.187	5.531		
Total	11	1069.301			

df = degrees of freedom; ss = sum of squares; ms = mean square; vr = variance ratio;
F pr. = F probability

APPENDIX L2: Analysis of variance (ANOVA) for silt fractions of soil samples used in horizontal infiltration experiments

Source of variation	d.f.	s.s.	m.s.	v.r.	F. pr
Rep. stratum	2	1.082	0.541	0.23	

Soil	3	447.837	149.279	64.34	<.001
Residual	6	13.920	2.320		
Total	11	462.840			

df = degrees of freedom; ss = sum of squares; ms = mean square; vr = variance ratio;
F pr. = F probability

APPENDIX L3: Analysis of variance (ANOVA) for clay content of soil samples used in horizontal infiltration experiments

Source of variation	d.f.	s.s.	m.s.	v.r.	F. pr
Rep. stratum	2	9.375	4.688	1.80	
Soil	3	750.000	250.000	96.00	<.001
Residual	6	15.625	2.604		
Total	11	775.000			

df = degrees of freedom; ss = sum of squares; ms = mean square; vr = variance ratio;
F pr. = F probability

APPENDIX L4: Analysis of variance (ANOVA) for saturation water content of soil sample used in horizontal infiltration experiments

Source of variation	d.f.	s.s.	m.s.	v.r.	F. pr
Rep. stratum	2	0.001976	0.000988	0.58	

Soil	3	0.106036	0.035345	20.67	<.001
Residual	6	0.010257	0.001710		
Total	11	0.118269			

df = degrees of freedom; ss = sum of squares; ms = mean square; vr = variance ratio;
F pr. = F probability

APPENDIX L5: Analysis of variance (ANOVA) for organic carbon content of soil samples used in horizontal infiltration experiments

Source of variation	d.f.	s.s.	m.s.	v.r.	F. pr
Rep. stratum	2	0.0022167	0.0011083	1.82	
Soil	3	7.0474250	2.3491417	3861.60	<.001
Residual	6	0.0036500	0.0006083		
Total	11	7.0532917			

df = degrees of freedom; ss = sum of squares; ms = mean square; vr = variance ratio;
F pr. = F probability

APPENDIX L6: Analysis of variance (ANOVA) for CEC of soil samples used in horizontal infiltration experiments

Source of variation	d.f.	s.s.	m.s.	v.r.	F. pr
Rep. stratum	2	0.3872	0.1936	1.72	

Soil	3	1317.0534	439.0178	3900.07	<.001
Residual	6	0.6754	0.1126		
Total	11	1318.1160			

df = degrees of freedom; ss = sum of squares; ms = mean square; vr = variance ratio;
F pr. = F probability

APPENDIX L7: Analysis of variance (ANOVA) for Exch. Acidity of soil samples used in horizontal infiltration experiments

Source of variation	d.f.	s.s.	m.s.	v.r.	F. pr
Rep. stratum	2	0.0002667	0.0001333	0.27	
Soil	3	26.6830667	8.8943556	18193.00	<.001
Residual	6	0.0029333	0.0004889		
Total	11	26.6862667			

df = degrees of freedom; ss = sum of squares; ms = mean square; vr = variance ratio;
F pr. = F probability

APPENDIX L8: Analysis of variance (ANOVA) for AEC of soil samples used in horizontal infiltration experiments

Source of variation	d.f.	s.s.	m.s.	v.r.	F. pr
Rep. stratum	2	1.967	0.984	0.59	

Soil	3	1375.478	458.493	273.24	<.001
Residual	6	10.068	1.678		
Total	11	1387.513			

df = degrees of freedom; ss = sum of squares; ms = mean square; vr = variance ratio;
F pr. = F probability

APPENDIX L9: Analysis of variance (ANOVA) for initial and final moisture contents during horizontal infiltration experiments

Source of variation	**d.f.**	**s.s.**	**m.s.**	**v.r.**	**F pr.**
Rep stratum	**2**	**0.0003323**	**0.0001662**	**1.41**	
Rep.*Units* stratum					
Soil_Type	**3**	**0.0486611**	**0.0162204**	**137.82**	**<.001**
Moist	**1**	**0.8629834**	**0.8629834**	**7332.65**	**<.001**
Soil_Type.Moist	**3**	**0.0080725**	**0.0026908**	**22.86**	**<.001**
Residual	**14**	**0.0016477**	**0.0001177**		
Total	**23**	**0.9216970**			

Tables of means

Variate: Resp

Grand mean 0.2437

Soil_Type	**Ferrasol**	**Gleysol**	**Lixisol**	**Vertisol**
	0.2460	**0.2255**	**0.1898**	**0.3135**

Moist	**Final**	**initial**
	0.0541	**0.4333**

Soil_Type	Moist	Final	initial
Ferrasol		0.0410	0.4510
Gleysol		0.0423	0.4087
Lixisol		0.0273	0.3523
Vertisol		0.1057	0.5213

Least significant differences of means (5% level)

Table	Soil_Type	Moist	Soil_Type Moist
rep.	6	12	3
d.f.	14	14	14
l.s.d.	0.01343	0.00950	0.01900